Earth Syst. Sci. Data, 18, 1405–1462, 2026
https://doi.org/10.5194/essd-18-1405-2026

Open Access Earth System Science Data

Synthesis of data products for ocean carbonate chemistry

Li-Qing Jiang[1,2,59], Amanda Fay[3], Jens Daniel Müller[4,5], Luke Gregor[4,6], Alizée Roobaert[7], Lydia Keppler[8], Dustin Carroll[9,10], Siv K. Lauvset[11], Tim DeVries[12], Judith Hauck[13,14], Christian Rödenbeck[15], Nicolas Metzl[16], Andrea J. Fassbender[17], Jean-Pierre Gattuso[18,19], Peter Landschützer[7], Rik Wanninkhof[20], Christopher Sabine[21], Simone R. Alin[17], Mario Hoppema[13], Are Olsen[22], Matthew P. Humphreys[23], Kunal Chakraborty[24], Ana C. Franco[25,26], Kumiko Azetsu-Scott[27], Dorothee C. E. Bakker[28], Leticia Barbero[20,29], Nicholas R. Bates[30,31], Nicole Besemer[20], Henry C. Bittig[32], Albert E. Boyd[20,29], Daniel Broullón[33], Wei-Jun Cai[34], Brendan R. Carter[35,17], Thi-Tuyet-Trang Chau[36,37], Chen-Tung Arthur Chen[38], Frédéric Cyr[39,40], John E. Dore[41], Ian Enochs[20], Richard A. Feely[17], Hernan E. Garcia[2], Marion Gehlen[36], Prasanna Kanti Ghoshal[24], Lucas Gloege[3], Melchor González-Dávila[42], Nicolas Gruber[4], Debby Ianson[43], Yosuke Iida[44], Masao Ishii[45], Apurva Padamnabh Joshi[24], Esther Kennedy[46], Alex Kozyr[1,2], Nico Lange[11], Claire Lo Monaco[16], Derek P. Manzello[47], Galen A. McKinley[3], Natalie M. Monacci[48], Xose A. Padin[33], Ana M. Palacio-Castro[20,29], Fiz F. Pérez[33], J. Magdalena Santana-Casiano[42], Jonathan Sharp[35,17], Adrienne Sutton[17], Jim Swift[49], Toste Tanhua[50], Maciej Telszewski[51], Jens Terhaar[52,53], Ruben van Hooidonk[54], Anton Velo[33], Andrew J. Watson[55], Angelicque E. White[21], Zelun Wu[34], Liang Xue[56], Hyelim Yoo[1,2], Jiye Zeng[57], and Guorong Zhong[58]

[1]Cooperative Institute for Satellite Earth System Studies, Earth System Science Interdisciplinary Center, University of Maryland, College Park, Maryland 20740, United States
[2]NOAA/NESDIS National Centers for Environmental Information, Silver Spring, Maryland 20910, United States
[3]Columbia University and Lamont-Doherty Earth Observatory, Palisades, New York 10964, United States
[4]Environmental Physics, Institute of Biogeochemistry and Pollutant Dynamics, ETH Zürich, Zurich, Switzerland
[5]Carbon to Sea Initiative, Washington, D.C., United States
[6]Swiss Data Science Center, ETH Zurich and EPFL, Zurich, Switzerland
[7]Flanders Marine Institute (VLIZ), Jacobsenstraat 1, 8400 Ostend, Belgium
[8]Vycarb Inc., Brooklyn, New York, United States
[9]Moss Landing Marine Laboratories, San José State University, Moss Landing, California, United States
[10]Jet Propulsion Laboratory, California Institute of Technology, Pasadena, California, United States
[11]NORCE Research AS, Bjerknes Centre for Climate Research, Bergen, Norway
[12]Department of Geography and Earth Research Institute, University of California, Santa Barbara, California, United States
[13]Alfred Wegener Institute Helmholtz Centre for Polar and Marine Research, Bremerhaven, Germany
[14]Department 02 Biology/Chemistry, University of Bremen, Bremen, Germany
[15]Max Planck Institute for Biogeochemistry, Jena, Germany
[16]Laboratoire LOCEAN/IPSL, Sorbonne Université – CNRS-IRD-MNHN, 75005 Paris, France
[17]NOAA/OAR Pacific Marine Environmental Laboratory, Seattle, Washington 98115, United States
[18]Sorbonne Université, CNRS, Laboratoire d'Océanographie de Villefranche, 06230 Villefranche-sur-Mer, France
[19]Institute for Sustainable Development and International Relations, Paris, France
[20]NOAA/OAR Atlantic Oceanographic and Meteorological Laboratory, Miami, Florida 33149, United States

Published by Copernicus Publications.

[21]Department of Oceanography, University of Hawaii at Mānoa,
1000 Pope Rd., Honolulu, Hawaii 96822, United States
[22]Geophysical Institute, University of Bergen and Bjerknes Centre for Climate Research, Bergen, Norway
[23]Department of Ocean Systems, NIOZ Royal Netherlands Institute for Sea Research, Texel, the Netherlands
[24]Indian National Centre for Ocean Information Services, Ministry of Earth Sciences, Hyderabad, India
[25]Department of Earth, Ocean and Atmospheric Sciences,
University of British Columbia, Vancouver, BC, Canada
[26]Current affiliation: Earth Sciences Department, Barcelona Supercomputing Center, Barcelona, Spain
[27]Fisheries and Oceans, Canada, Bedford Institute of Oceanography, Dartmouth, Nova Scotia, Canada
[28]Centre for Ocean and Atmospheric Sciences, School of Environmental Sciences,
University of East Anglia, Norwich, NR4 7TJ, United Kingdom
[29]Cooperative Institute for Marine and Atmospheric Studies, Rosenstiel School of Marine
and Atmospheric Science, University of Miami, Miami, Florida 33149, United States
[30]Bermuda Institute of Ocean Sciences, ASU-BIOS, 17 Biological Lane, St. Georges, GEO1, Bermuda
[31]School of Ocean Futures, Arizona State University, Tempe, Arizona 85281, United States
[32]Leibniz Institute for Baltic Sea Research Warnemünde (IOW), Rostock, Germany
[33]Instituto de Investigacións Mariñas, IIM – CSIC, Vigo, Spain
[34]School of Marine Science and Policy, University of Delaware, Newark, Delaware 19716, United States
[35]Cooperative Institute for Climate, Ocean, and Ecosystem Studies,
University of Washington, Seattle, Washington, United States
[36]Laboratoire des Sciences du Climat et de l'Environnement, LSCE-IPSL, CEA-CNRS-UVSQ,
Université Paris-Saclay, 91191 Gif-sur-Yvette, France
[37]Laboratoire Interdisciplinaire des Sciences du Numérique (LISN), Centre de recherches INRIA,
Université Paris–Saclay, René Thom, 91190 Gif-sur-Yvette, France
[38]Department of Oceanography, National Sun Yat-Sen University, Kaohsiung, Taiwan
[39]Northwest Atlantic Fisheries Centre, Fisheries and Oceans Canada,
St. John's, Newfoundland and Labrador, Canada
[40]Current affiliation: Centre for Fisheries Ecosystems Research, Fisheries and
Marine Institute of Memorial University of Newfoundland, St. John's, Canada
[41]Department of Land Resources and Environmental Sciences,
Montana State University, Bozeman, Montana, United States
[42]Instituto de Oceanografía Cambio Global, IOCAG, Universidad de Las Palmas de Gran Canaria,
35017 Las Palmas de Gran Canaria, Spain
[43]Institute of Ocean Sciences, Fisheries and Oceans Canada, Sidney, British Columbia, Canada
[44]Atmosphere and Ocean Department, Japan Meteorological Agency,
3-6-9 Toranomon, Minato City, Tokyo, Japan
[45]Meteorological Research Institute, Japan Meteorological Agency, Tsukuba, Japan
[46]Bodea Marine Laboratory, University of California Davis, Davis, California, United States
[47]Coral Reef Watch, US National Oceanic and Atmospheric Administration,
College Park, Maryland, United States
[48]College of Fisheries and Ocean Sciences, University of Alaska Fairbanks, Fairbanks, Alaska, United States
[49]Scripps Institution of Oceanography, La Jolla, California, United States
[50]GEOMAR Helmholtz Centre for Ocean Research Kiel, Kiel, Germany
[51]International Ocean Carbon Coordination Project, Institute of Oceanology of Polish Academy of Sciences,
Sopot, Poland
[52]Climate and Environmental Physics, Physics Institute, University of Bern, Bern, Switzerland
[53]Oeschger Centre for Climate Change Research, University of Bern, Bern, Switzerland
[54]Science for Climate Change Resilience, Boulder, Colorado 80302, United States
[55]Global Systems Institute, University of Exeter, Exeter, United Kingdom
[56]First Institute of Oceanography, and Key Laboratory of Marine Science and Numerical Modeling,
Ministry of Natural Resources, Qingdao, China
[57]National Institute for Environmental Studies, Tsukuba, Japan
[58]Institute of Oceanology, Chinese Academy of Sciences, Qingdao, China
[59]Geosciences Research Division, Scripps Institution of Oceanography, University of California at San Diego,
La Jolla, CA 92037, United States

Correspondence: Li-Qing Jiang (liqing.jiang@noaa.gov)

Received: 1 May 2025 – Discussion started: 15 May 2025
Revised: 19 November 2025 – Accepted: 25 November 2025 – Published: 24 February 2026

Abstract. As the largest active carbon reservoir on Earth, the ocean is a cornerstone of the global carbon cycle, playing a pivotal role in modulating ocean health and the Earth's climate system. Understanding these crucial roles requires access to a broad array of data products documenting the changing chemistry of the global ocean as a vast and interconnected system. This review article provides an overview of 68 existing ocean carbonate chemistry data products and data product sets, encompassing compilations of cruise datasets, derived gap-filled data products, model simulations, and compilations thereof. It is intended to help researchers identify and access data products that best align with their research objectives, thereby advancing our understanding of the ocean's evolving carbonate chemistry. The list will be updated periodically to incorporate new data products. The most up-to-date list is available at https://oceanco2.github.io/co2-products/ (Gregor and Jiang, 2026).

1 Introduction

Since the onset of the Industrial Revolution in 1750, human activities, such as the burning of fossil fuels, cement production, and land-use change, have emitted ~ 2600 Gt carbon dioxide (CO_2) (1 Gt $= 10^{15}$ g, 1 Gt $CO_2 = 0.273$ Gt C, or Gt Carbon) into the atmosphere, causing the atmospheric CO_2 levels to increase by ~ 50 % (DeVries, 2022a; Friedlingstein et al., 2025; Tans and Keeling, 2026). The global carbon cycle, encompassing the exchange of CO_2 among the atmosphere, oceans, terrestrial ecosystems, and geosphere, plays a critical role in regulating atmospheric CO_2 levels (Archer, 2010; DeVries, 2022a; Friedlingstein et al., 2025; Lee et al., 2026). As the largest dynamic CO_2 reservoir, the ocean holds approximately 45 times the amount of carbon found in the atmosphere currently and actively exchanges it with the air above and sediments below. On timescales from decades to millennia, the ocean imposes a dominant control over atmospheric CO_2 levels (Revelle and Suess, 1957; Broecker, 1982; Archer et al., 2009; DeVries, 2022a).

The ocean currently absorbs about a quarter of human-caused CO_2 emissions (Sabine et al., 2004; Gruber et al., 2019a, 2023; Carroll et al., 2022; Crisp et al., 2022; Terhaar et al., 2022a; DeVries et al., 2023; Müller et al., 2023a; Schimel and Carroll, 2024; Terhaar, 2025). The chemistry of the ocean has been shifting as a result of anthropogenic CO_2 increase in the ocean (Feely et al., 2023; Ma et al., 2023; Müller et al., 2023a; Fassbender et al., 2023; Keppler et al., 2023a; Jiang et al., 2023; Müller and Gruber, 2024a; Terhaar et al., 2020, 2021a, 2024a). Since the beginning of the Industrial Revolution, the total amount of dissolved inorganic carbon (DIC) in the layer from 0 to 200 m has risen from 1690 to 1730 Gt of Carbon, and from 35 400 to 35 560 Gt C below 200 m (Sabine et al., 2004; Müller et al., 2023a). The seemingly small increase of 0.5 % results in a substantial drop of the oceans' buffer capacity (DeVries, 2022a). Buffer capacity refers to the ocean's ability to resist changes in pH, and thus also the partial pressure of CO_2 (pCO_2), when CO_2 or any other acid or base is added or removed.

As anthropogenic CO_2 enters seawater, it reacts with water to form carbonic acid. This is the first in a series of rapid acid-base reactions that release protons (H^+) and decrease the availability of carbonate ions, which are building materials that many marine organisms, such as mollusks, crustaceans, and corals, use to construct their shells and skeletons (Gattuso and Hansson, 2011). This process, referred to as "ocean acidification (OA)", has already decreased surface ocean pH by roughly 0.11 (~ 30 % increase in acidity) since 1750 (Orr et al., 2005; Jiang et al., 2019a, 2023; Kwiatkowski et al., 2020; IPCC, 2023). In some parts of the subsurface ocean, the trends of some acidification variables, e.g., pH, and total hydrogen ion content ($[H^+]_{total}$), can be even greater due to the increasing sensitivity of $[H^+]$ to DIC changes at depth (Chen et al., 2017; Pérez et al., 2021; Fassbender et al., 2023; Müller and Gruber, 2024a). This ongoing acidification threatens critical ocean ecosystem services, including food security, fisheries, aquaculture, and the broader Blue Economy, for billions of people globally (Cooley and Doney, 2009; Pérez et al., 2018; Doney et al., 2020).

In some parts of the ocean, OA is driven not only by the uptake of carbon but also by other processes (Delaigue et al., 2024), for example via alkalinity changes driven by freshening of the Arctic Ocean (Terhaar et al., 2021a) or changes in the carbon and alkalinity export from the Pacific Ocean and Arctic rivers (Terhaar et al., 2019; Qi et al., 2017, 2022; Bertin et al., 2023). Local anthropogenic inputs through rivers or from air pollution also contribute to OA (e.g. Sarma et al., 2015; Sridevi and Sarma, 2021). Furthermore, eutrophication and hypoxia in coastal regions may exacerbate OA in oxygen-deficient bottom waters, as biologically produced CO_2 weakens the natural buffering capacity of seawater (Cai et al., 2011). If anthropogenic CO_2 emissions continue without mitigation, as per the shared socioeconomic pathway (SSP5-8.5) scenario, surface ocean pH

could decrease by a further 0.3 to 0.4 by 2100, equivalent to a 100 %–150 % increase in acidity (Kwiatkowski et al., 2020; Jiang et al., 2023). If society, however, succeeds in reducing emissions, the future acidity level becomes highly uncertain as it sensitively depends on the transient response of the Earth system and the amount of reductions of non-CO_2 radiative agents (Terhaar et al., 2023).

In summary, monitoring ocean carbonate chemistry is essential for (a) tracking the evolving ocean carbon sink, and (b) understanding OA and its ecological impacts. Additionally, monitoring ocean carbonate chemistry is crucial when considering marine carbon dioxide removal (mCDR) strategies such as ocean alkalinity enhancement (OAE), artificial upwelling, ocean fertilization, and electrochemical ocean CO_2 removal (Kheshgi, 1995; Bach et al., 2019; Schimel and Carroll, 2024; Oschlies et al., 2025). The ocean's vast and interconnected nature necessitates that data from individual oceanographic cruises be meticulously preserved, subject to rigorous quality-control, and uniformly formatted to promote their usability (Brett et al., 2020; Schoderer et al., 2024). Following Lange et al. (2023), we curate an exhaustive catalogue of synthesis products pertaining to ocean carbonate chemistry, including cruise data compilations, gridded gap-filled data products, and other derived data products. This compilation spans both global and regional scales, providing a holistic view of the current state of ocean biogeochemistry data aggregation.

2 Methods

In this paper, data products are defined as outputs that quality-control, aggregate, and transform individual datasets from multiple sources into a unified, structured format to support research, decision-making, or operational needs for specific end users. The data products included in this study were identified through a literature review and discussions with researchers via the Ocean Acidification Information Exchange (OAIE) platform.

The products are organized into six categories based on end-user needs and listed within each class with no particular order (Fig. 1):

1. Cruise data compilations (no interpolation or gap-filling).
2. Time-series data products (no interpolation or gap-filling).
3. Derived gap-filled (e.g., interpolated) products for the surface ocean, starting with products offering a climatological snapshot of the ocean, followed by those showing temporal changes.
4. Derived gap-filled (e.g., interpolated) products for the interior ocean, also starting with products offering a climatological snapshot of the ocean, followed by those showing temporal changes.
5. Multi-product analyses of 3 and 4. These compilations also include hindcast model simulations of the ocean carbon cycle and biogeochemistry.
6. Model and hybrid data products projecting ocean carbonate system variables into the future [Note: Here the term 'model' refers to ocean biogeochemical models (Fennel et al., 2022). If a statistical model or machine learning model is used for gap-filling, the product is not categorized as a model output product in this compilation.]

Each category includes numbered descriptions of each data product in that class, as well as a summary table of the data products with corresponding IDs so the user can easily jump to the associated product description. For each data product, the description is followed by its access links. Persistent identifiers (e.g., digital object identifiers, or DOIs) and links to all data products are also summarized in the table in Sect. 4 "Data availability".

Although some data products, such as Surface Ocean CO_2 Atlas (SOCAT) and Lamont-Doherty Earth Observatory (LDEO) surface pCO_2 Database report only one ocean carbonate system variable, i.e., fugacity of carbon dioxide (fCO_2) or pCO_2, they provide a foundation from which additional variables can be derived using empirical algorithms. For instance, total alkalinity content (TA) can be estimated from salinity and temperature and other factors (Lee et al., 2006) and by neural network approaches such as those developed by Velo et al. (2013) and Broullón et al. (2019). Beyond TA, neural network algorithms have been extended to estimate DIC as demonstrated by Broullón et al. (2020a), and even the full marine carbonate system (MCS) through frameworks like CANYON-B/CONTENT (Bittig et al., 2018) and Empirical Seawater Property Estimation Routines (ESPERs) (Carter et al., 2021). While these methods primarily employ neural networks, both Velo et al. (2013) and Carter et al. (2021) provide alternative estimation approaches based on local interpolation, through their 3-dimensional moving window multilinear regression algorithm (3DwMLR) and locally interpolated regression (LIR) methods, respectively. Utilizing such derived data, the complete suite of ocean carbonate system variables can then be calculated using computer software, such as CO2SYS (Lewis and Wallace, 1998; Orr et al., 2018; Sharp et al., 2023) or its Python implementation PyCO2SYS (Humphreys et al., 2022). An in-depth explanation of the methods employed for these calculations can be found in the Supplement of Jiang et al. (2022a).

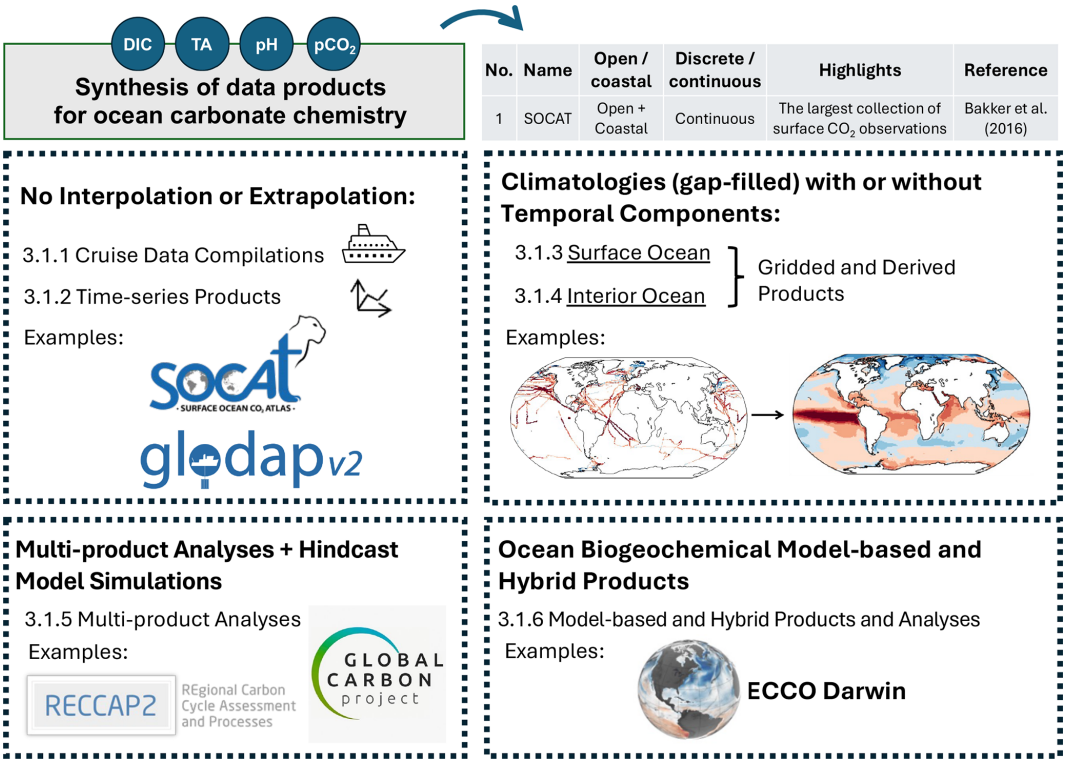

Figure 1. An overview diagram outlining the paper's structure and flow.

3 Results and discussion

3.1 Data products for ocean carbonate chemistry

3.1.1 Cruise data compilations (no interpolation or gap-filling)

The data compilations described in this section standardize datasets collected from individual research vessels, ships of opportunity, and uncrewed platforms, presenting them in a uniform format for easy access (Table 1). These datasets typically undergo both primary QC (identifying outliers and obvious errors within an individual cruise dataset) and secondary QC (when possible, to objectively compare data from one cruise against another or a previously synthesized dataset to quantify systematic differences in reported values). It is important to note that data providers are expected to carry out rigorous QC prior to data submission.

1. SOCAT: the Surface Ocean CO_2 Atlas features surface fCO_2 measurements from both the open ocean and the coastal ocean, predominantly sourced from research vessels, ships of opportunity, and autonomous platforms including fixed moorings and uncrewed surface vehicles (USVs) (Bakker et al., 2016). It represents the most extensive collection of observational ocean CO_2 data for the global surface ocean. Since 2013, SOCAT has been updated annually. Dataset flags indicate the estimated uncertainty and completeness of metadata in SOCAT synthesis products. The SOCAT gridded product (monthly $1° \times 1°$) contains fCO_2 values with an estimated uncertainty of less than 5 µatm. To access the latest version of the SOCAT data product (with 40 million data points), visit https://socat.info/ (last access: 7 January 2026) (Bakker et al., 2025).

2. LDEO Surface pCO_2 Database: Dr. Taro Takahashi at LDEO in Palisades, New York started synthesizing global surface ocean CO_2 data in 1997, compiling three decades of observations ($\sim$ 250 000 measurements) to create inaugural monthly global surface pCO_2 maps (Takahashi et al., 1997, 2002). The most recent version (V2019) expanded this dataset to approximately 14.2 million surface water pCO_2 measurements spanning 1957–2019. Distinct from the SOCAT database, the LDEO database reports pCO_2 instead of fCO_2, exclusively from equilibrator-CO_2 analyzer systems, with an average estimated uncertainty of ± 2.5 µatm. The database is also interpolated onto a global surface ocean $4° \times 5°$ grid for a reference year 2000 (Takahashi et al., 2009) and 2010 (Fay et al., 2024a). Access to the LDEO Surface pCO_2 database (Version 2019) is provided by the Ocean Carbon and Acidification Data System (OCADS, Jiang et al., 2023a) at https://www.ncei.noaa.gov/data/oceans/ncei/ocads/metadata/0160492.html (last access: 7 January 2026) (Takahashi et al., 2017).

Additionally, a dedicated webpage for the LDEO Database is available at https://www.ncei.noaa.gov/access/ocean-carbon-acidification-data-system/oceans/LDEO_Underway_Database/ (last access: 7 January 2026).

3. GLODAPv2: the Global Ocean Data Analysis Project Version 2 (GLODAPv2) aggregates biogeochemical data collected from discrete bottle samples, offering extensive global coverage from the surface to depth (Key et al., 2015; Olsen et al., 2016; Lauvset et al., 2024). While GLODAP is primarily a product for basin-scale hydrographic data, it also includes coastal datasets and observations from a few time-series. The GLODAPv2 data product provides rigorously quality-controlled measurements for 14 essential oceanographic variables: temperature, salinity, dissolved oxygen (DO), nitrate, silicate, phosphate, DIC, TA, pH, chlorofluorocarbons (CFC-11, CFC-12, CFC-113), carbon tetrachloride (CCl_4), and sulfur hexafluoride (SF_6). These variables, excluding temperature, undergo both primary and secondary quality-control procedures to detect outliers and adjust for significant measurement biases. GLODAPv2 was first published in 2016 and was updated annually through a living data process in Earth System Science Data from 2019 through "v2023" which was published in 2024. For these updates, new data (including historical data not previously included in the data product) are quality-controlled and adjusted to the 2016 version (Olsen et al., 2019, 2020; Lauvset et al., 2021, 2022, 2024). Since the global repeat hydrography programs operate with decadal repetitions, the aim is to produce a completely new version of GLODAP, where all cruise datasets will be reevaluated, every decade. Release of the GLODAPv3 data product is planned for 2026, and is expected to evolve the secondary data quality-control practices relative to those used in GLODAPv2. For more information on the secondary quality-control process, refer to Tanhua et al. (2010) and Lauvset and Tanhua (2015). GLODAPv2 offers two kinds of products: the compilation of quality-controlled data from discrete bottle samples taken at sampling location (Key et al., 2015; Olsen et al., 2016, 2019, 2020; Lauvset et al., 2021, 2022, 2024), and a gridded product, interpolated to a $1° \times 1°$ grid and the 33 standard depth levels of World Ocean Atlas (WOA) (Lauvset et al., 2016). All versions of the GLODAPv2 data product can be accessed at https://glodap.info/ (last access: 7 January 2026.

   GLODAPv2 builds upon three foundational data products: the original GLODAP (Sabine et al., 2004), CARbon dioxide IN the Atlantic Ocean (CARINA, Key et al., 2010), and PACIFic ocean Interior Carbon (PACIFICA, Suzuki et al., 2013). These data products remain available at NCEI: https://www.ncei.noaa.gov/data/oceans/ncei/ocads/metadata/0001644.html (last access: 7 January 2026) (GLODAP, Sabine et al., 2005), https://www.ncei.noaa.gov/data/oceans/ncei/ocads/metadata/0113899.html (last access: 7 January 2026) (CARINA, Tanhua et al., 2013), and https://www.ncei.noaa.gov/data/oceans/ncei/ocads/metadata/0110865.html (last access: 7 January 2026) (PACIFICA, Suzuki et al., 2013), respectively.

4. Quality Edited Hydrographic Data: the Quality Edited Hydrographic Data product offers both a user-friendly application and a library of ocean profile data curated by Jim Swift (Scripps Institution of Oceanography, La Jolla, California, United States). Similar to GLODAPv2, this data product serves as a comprehensive repository of quality-controlled discrete bottle-based measurements (and limited CTD), spanning from the surface to the depths of the global ocean. Unlike GLODAPv2, this data product does not apply offset corrections. It encompasses a range of oceanographic variables including temperature, salinity, DO, DIC, TA, silicate, phosphate, nitrate, nitrite, CFC-11, CFC-12, and SF_6. To access the application and data, visit: https://joa.ucsd.edu/ (last access: 7 January 2026). Currently, there is not a peer-reviewed paper or public-accessible report for this data product. Cite the data product itself as: Swift and Osborne (2025).

5. WOD: in addition to the GLODAPv2 (No. 3) and Quality Edited Hydrographic Data (No. 4), users can also access historical and recent original biogeochemical data collected from discrete bottle samples in a uniform format and units, along with their originator quality-control (QC) flags, through the World Ocean Database (WOD) (Mishonov et al., 2024). Like the Quality Edited Hydrographic Data, these measured data remain unaltered. The WOD allows users to filter and subset data by specific variables, platforms, institutions, projects, regions, or time periods (Garcia et al., 2024). Users can visualize sampling locations on a "distribution plot" and access a cruise list for all selected data and variables. Users also have the option of exporting data in NetCDF or Comma-Separated Value (CSV) formats. Additionally, all data in the WOD are reproducible and traceable to their original data sources archived at NOAA's National Centers for Environmental Information (NCEI). The WOD is accessible at https://www.ncei.noaa.gov/products/world-ocean-database (last access: 7 January 2026).

6. SNAPO-CO_2: Metzl et al. (2024) aggregated over 44 400 measurements of DIC and TA from a series of research cruises and ships of opportunity across various oceanic regions from 1993–2022, under several French research programs, to create a product called "Service National d'Analyse des Paramètres Océaniques

du CO_2 (SNAPO-CO_2)". The majority of the samples were analyzed by the Service National d'Analyse des Paramètres Océaniques du CO_2 (SNAPO-CO_2) at the LOCEAN laboratory in Paris, France. Sampling was performed either from CTD-rosette casts (Niskin bottles) or collected from the ship's flow-through system (intake at roughly 5 m depth). DIC and TA determinations were conducted simultaneously through potentiometric titration in a closed-cell setup, calibrated with certified reference material to achieve an accuracy of $\pm 4\,\mu mol\,kg^{-1}$ for both variables, following Edmond (1970). This methodology was also applied for real-time measurements during OISO cruises, with data from the South Indian Ocean for 1998–2018 included in this compilation. The data are split into two sets: one for the global ocean and coastal zones, and another for the Mediterranean Sea, both accessible in the same format at https://doi.org/10.17882/95414 (Metzl et al., 2023). Additionally, this data product is available at OCADS: https://www.ncei.noaa.gov/data/oceans/ncei/ocads/metadata/0285681.html (last access: 7 January 2026) (Metzl et al., 2023).

7. CODAP-NA: Jiang et al. (2021) synthesized two decades of discrete measurements of carbonate system variables, DO, and nutrient data from the North American continental shelves to generate the first version of Coastal Ocean Data Analysis Data Product in North America (CODAP-NA). The 2021 release encompasses 3391 oceanographic profiles from 61 research cruises spanning the North American continental shelves from Alaska to Mexico in the west and from Canada to the Caribbean in the east. It includes 14 key variables, including temperature, salinity, DO, DIC, TA, pH, carbonate ion, fCO_2, silicate, phosphate, nitrate, all of which have undergone rigorous quality-control. Note that certain datasets meeting the GLODAPv2 QC standards are also included in the GLODAPv2 since its 2022 release (No. 3 above). CODAP-NA is available at https://www.ncei.noaa.gov/data/oceans/ncei/ocads/metadata/0219960.html (last access: 7 January 2026) (Jiang et al., 2020).

8. AZMP Carbon: Gibb et al. (2023) compiled ocean carbonate system variables data from the Canadian Atlantic Zone Monitoring Program (AZMP Carbon) since 2014. More than 100 seagoing missions are represented in this dataset. The sampling strategy generally corresponds to full-depth water samples mostly collected along standardized hydrographic sections. The majority of these data were collected as part of the Atlantic Zone Monitoring Program (AZMP) of Fisheries and Oceans Canada (DFO). Implemented in 1998, the AZMP aims to characterize and understand the causes of oceanic variability at the seasonal, interannual and decadal scales in support of, among other things, fisheries management in the Atlantic Zone (including the Gulf of St. Lawrence, the Scotian shelf and the Newfoundland and Labrador shelf). Since 2014, a minimum of two of the three following carbonate system variables, DIC, TA, and pH, are also acquired by the program at standardized hydrographic stations across the zone (sampled up to three times a year). Each measurement is completed with corresponding temperature, salinity and, when available, nutrients and DO concentration data. This dataset also includes samples collected as part of ships of opportunity, fishing and other scientific trips. The entire dataset comprises 19 531 discrete samples [last updated 21 August 2024]. Among this number, 18 085 have at least two of the three carbonate system variables (e.g., TA, DIC and pH), allowing the derivation of other variables such as the saturation state relative to aragonite and calcite (Ω_{arag} and Ω_{calc}) and pCO_2 (in µatm). The full dataset of measured and derived variables is available from the Federated Research Data Repository: https://doi.org/10.20383/102.0673 (Cyr et al., 2022) and is updated annually.

9. MOCHA: Kennedy et al. (2023) curated a comprehensive coastal ocean data product called "Multistressor Observations of Coastal Hypoxia and Acidification (MOCHA)", encompassing temperature, salinity, DO, ocean carbonate system variables (DIC, TA, pH, pCO_2, fCO_2), nutrients, and chlorophyll measurements from the full water column along the US west coast. The synthesis integrates observations from 71 different sources, including high-resolution autonomous sensors, synoptic oceanographic cruises, and shoreline samples. The MOCHA synthesis spans from the shoreline to well beyond the continental shelf and incorporates observations from CODAP-NA (see No. 7 above), California Cooperative Oceanic Fisheries Investigations (CalCOFI), and other large-scale oceanographic cruises to facilitate linking nearshore, high-resolution observations to broader oceanographic conditions. As of 2025, MOCHA includes 15.9 million temperature readings, 5.0 million salinity measurements, 3.9 million DO records, and 2.3 million pH measurements, along with 8368 DIC, 10 144 TA, and 505 000 pCO_2/fCO_2 measurements, with limited additional chlorophyll and nutrient observations. To reduce the computational load from high-resolution sensors, the synthesis is also available as a "daily aggregated" dataset, with all data sources averaged by day, location, and depth. All data in the MOCHA synthesis product has been quality-controlled to a "plausible and reasonable" standard, but researchers requiring high-precision coastal data may need to apply additional QC tests. The data product is available at https://www.ncei.noaa.gov/data/oceans/ncei/ocads/metadata/0277984.html (last access: 7 Jan-

uary 2026) (Kennedy et al., 2023), while the methods and the product are described in Kennedy et al. (2024).

10. ARIOS: the Acidification in the Rias and the Iberian Continental Shelf (ARIOS) project involved compiling and analyzing the historical record of ocean carbonate system measurements and associated variables conducted by the Instituto de Investigacións Mariñas (IIM-CSIC) in Vigo, Spain. This dataset comprises 3343 oceanographic stations and 17 653 discrete samples, combining measurements of pH, TA, and other physical (pressure, temperature, and salinity) and biogeochemical variables (DO, nitrate, phosphate, and silicate) off the northwestern Iberian Peninsula from June 1976 to September 2018 (Padin et al., 2020). The oceanography cruises funded by 24 projects were primarily carried out in the Ría de Vigo coastal inlet, but also in an area ranging from the Bay of Biscay to the Portuguese coast. Robust seasonal cycles and long-term trends were calculated along a longitudinal section, gathering data from the coastal and oceanic zones of the Iberian upwelling system. The data product is available at https://doi.org/10.20350/digitalCSIC/12498 (Pérez et al., 2020).

11. Marine Inorganic Carbonate Chemistry in the Northern Gulf of Alaska: Monacci et al. (2023) compiled a data product of discrete seawater samples collected each May and September over a 10-year period from 2008 to 2017 along the long-term hydrographic line in the Gulf of Alaska (GAK Line). Samples were collected from a sampling rosette on a profiling CTD. Data variables include profiled seawater temperature, salinity, and DO. Discrete sample variables include DO (i.e., Winkler titrations), macronutrients (nitrate, nitrite, phosphate, silicic acid), DIC, and TA. This data product is available at https://www.ncei.noaa.gov/data/oceans/ncei/ocads/metadata/0277034.html (last access: 7 January 2026) (Monacci et al., 2023), and the synthesis paper can be accessed at https://doi.org/10.5194/essd-16-647-2024 (Monacci et al., 2024).

12. Coral Reef Carbonate Chemistry Off the Florida Keys: Palacio-Castro et al. (2023) compiled discrete seawater samples from 38 permanent stations located along 10 inshore-offshore transects at the Florida Coral Reef. These samples were collected as part of NOAA's National Coral Reef Monitoring Program (NCRMP) and the South Florida Ecosystem Restoration Research (SFER) cruises. Sampling efforts commenced in 2010, with every two months collections initiated in 2015, resulting in a total of 47 sampling cruises and 1538 discrete seawater samples. For all samples, a minimum of two of the carbonate system variables (TA, DIC) were measured, in addition to salinity and temperature. The Ω_{arag}, pCO_2, and pH were derived from the measured variables using the R package seacarb (Gattuso et al., 2021a). The time-series analysis provides insight into the dynamic carbonate conditions spanning the inshore to offshore gradients, encompassing four distinct regions of the Florida Coral Reef: Biscayne Bay, the Upper Keys, Middle Keys, and Lower Keys. Data is available at https://www.ncei.noaa.gov/access/metadata/landing-page/bin/iso?id=gov.noaa.nodc:NCRMP-CO3-Atlantic (last access: 7 January 2026) (Manzello et al., 2018).

13. Salish Cruise Data Package and Multi-stressor Data Product: Alin et al. (2025a) compiled data from 61 individual cruise data sets that sampled marine waters of the southern Salish Sea and northern Washington coast (United States) from 2008 to 2024. Since 2014, ongoing seasonal sampling has occurred during April, July, and September for Puget Sound cruises and most frequently during May and October for Sound-to-Sea cruises, which sample from Puget Sound through the Strait of Juan de Fuca to the northern Washington coast. The Salish cruise data package contains observations from water column profiles, with CTD sensor measurements of temperature, salinity, and DO; as well as discrete measurements of DO, nutrients (nitrate, phosphate, silicate, ammonium, nitrite), DIC, and TA. A follow-on data product is also available, containing only samples with complete records for temperature, salinity, and DO from sensors, and DO, nutrients, DIC, and TA from discrete measurements, along with the most commonly used calculated carbonate system variables: pH (total scale), fCO_2, pCO_2, Ω_{arag}, and Ω_{calc} (Alin et al., 2025b). The data package is available at https://www.ncei.noaa.gov/access/ocean-carbon-acidification-data-system/oceans/SalishCruise_DataPackage.html (last access: 7 January 2026). The multi-stressor data product is available at https://www.ncei.noaa.gov/access/ocean-carbon-acidification-data-system/oceans/SalishCruises_DataProduct.html (last access: 7 January 2026). Two synthesis papers describing the Salish cruises, as well as seasonality and extreme ocean acidification conditions observed during the 2008–2018 part of the time-series, can be found at https://essd.copernicus.org/articles/16/837/2024/ (last access: 7 January 2026) (Alin et al., 2024a) and https://bg.copernicus.org/articles/21/1639/2024/ (last access: 7 January 2026) (Alin et al., 2024b). A preliminary description of the 2019–2024 Salish cruises can be found at https://www.psp.wa.gov/psmarinewatersoverview.php (last access: 7 January 2026) (Alin et al., 2025c).

14. Line P Marine Carbonate Chemistry Compilation: this dataset contains marine carbonate system measurements collected during 55 Line P cruises from 1990

to 2019 in the subarctic Northeast Pacific. The dataset contains discrete profiles of DIC, TA, seawater temperature, salinity, DO and nutrients. From a total of 27 hydrographic time-series stations, only the five major stations where DIC and TA are routinely sampled were included in this compilation. Among them is the outermost station P26, also known as Ocean Station Papa (Freeland, 2007). Cruises were conducted approximately three times per year, typically in February, May/June and August/September. Each vertical profile was individually inspected and contrasted with the whole pool of data (including historical data) relative to salinity, density, and oxygen to detect and flag poor quality data following the World Ocean Circulation Experiment (WOCE) quality-control convention (Jiang et al., 2022a). Additionally, the recommended cruise-specific adjustments from PACIFICA were applied (Suzuki et al., 2013). The Line P marine carbonate chemistry compilation is described and analyzed in (Franco et al., 2021a) and is publicly available as a single synthesis product at https://www.ncei.noaa.gov/data/oceans/ncei/ocads/metadata/0234342.html (last access: 7 January 2026) (Franco et al., 2021b). The Line P carbonate chemistry timeseries is maintained by Fisheries and Oceans Canada and continues to the present day. Data are available and continuously updated in the Line P repository, which can be publicly accessed after generating an account at https://waterproperties.ca (last access: 7 January 2026).

15. Anthropogenic Carbon in the Arctic Ocean: this dataset includes anthropogenic carbon estimates in the Arctic Ocean based on measurements of transient tracers, such as CFC-12 and SF_6 (Terhaar et al., 2020; Tanhua et al., 2009). Using the transient time distribution (TTD) method, anthropogenic carbon estimates were estimated at measurement locations across all basins of the Arctic Ocean between 1983 and 2005. In addition to these estimates, adjusted estimates of anthropogenic carbon at these locations are provided to account for differences in the saturation of transient tracers and anthropogenic carbon in Arctic Ocean surface waters that caused anthropogenic carbon estimates to be biased low (Terhaar et al., 2020). It is recommended to use the adjusted estimates. This dataset can be accessed at https://doi.org/10.17882/103920 (Terhaar et al., 2024a).

3.1.2 Time-series products (no interpolation or gap-filling)

The time-series products described in this section include observations collected at regular time intervals, over a sustained period, and at fixed locations (Table 2). The data often represent changes in a particular oceanographic variable over time, such as temperature, salinity, TA and DIC. The list below includes both climate-quality time-series data products compiled at selected stations, and data products compiling time-series measurements at multiple locations. Additionally, some hydrographic sections are measured frequently enough to constitute a time-series, e.g., Line P in the northeast Pacific (Franco et al., 2021b; Freeland, 2007), sections in the northwest Pacific (Ishii et al., 2011a), the Observatoire de la Variabilité Interannuelle à DÉcennale (OVIDE) lines (Mercier et al., 2024). Measurements from these sections are typically included in cruise data compilations (Sect. 3.1.1) and are not listed separately here.

16. BATS: the Bermuda Atlantic Time-series Study (BATS) observations and data products extend over forty years of observations of DIC and TA and OA indicators, and constitute the longest continuous record of warming, salinification, ocean deoxygenation, and OA in the open ocean (Bates and Johnson, 2023). The sustained observations at the BATS site began in October 1988, approximately 80 km to the southeast of Bermuda (https://bios.asu.edu/bats, last access: 7 January 2026). The program comprises monthly cruises with CTD, water-column biogeochemical sampling and rate measurements (e.g., primary and export production) plus additional cruises in the spring period and annual transects between the Gulf Stream and Puerto Rico. CO_2-carbonate chemistry sampling includes full-depth bottle DIC and TA data (including additional surface measurements going back to 1983 collected at the Hydrostation S site). Hydrostation S is located $\sim$ 25 km southeast of Bermuda (https://bios.asu.edu/research/projects/hydrostation-s, last access: 7 January 2026) and began in 1954 with biweekly cruises each year. Underway fCO_2/pCO_2 data collected from the R/V *Atlantic Explorer* that supports the BATS and Hydrostation S sites constitutes part of the annual data submission to SOCAT. The BATS project page at the Biological and Chemical Oceanography Data Management Office (BCO-DMO) includes metadata and data streams (https://demo.bco-dmo.org/project/2124, last access: 7 January 2026). Hydrostation S data and DOIs are also available at BCO-DMO (https://www.bco-dmo.org/project/859583, last access: 7 January 2026).

17. HOT: the Hawaii Ocean Time-series (HOT) CO_2 measurement program documents more than 35 years of inorganic carbon dynamics in the open waters of the central North Pacific. Since October 1988, full ocean depth profiles of DIC and TA have been analyzed, and direct measurements of pH have been made over most of this longest-running Pacific Ocean time-series study. The program is based on shipboard observations and experiments conducted on $\sim$ 10 expeditions per year to Station ALOHA (22.75° N, 158° W). HOT program background information and details of sampling

Table 1. Ocean carbonate chemistry data products out of cruise data compilations (no gridding or gap-filling).

No.	Name	Open ocean or coastal ocean	Surface or water column	Discrete bottle or continuous	Highlights	Reference
1	SOCAT	Open ocean + Coastal ocean	Surface	Continuous	The largest collection of in situ surface ocean fCO_2 measurements	Bakker et al. (2016)
2	LDEO Surface pCO_2 Database	Open ocean + Coastal ocean	Surface	Continuous	The LDEO database reports pCO_2 exclusively from equilibrator-CO_2 analyzer systems	Takahashi et al. (2017)
3	GLODAPv2	Open ocean	Water column	Discrete bottle	Adjustments are applied by comparing data in the deep ocean ($>$ 2000 m) using a crossover and inversion method as described by Johnson et al. (2001)	Lauvset et al. (2024)
4	Quality Edited Hydrographic Data	Open ocean	Water column	Discrete bottle	Similar to GLODAPv2, with no adjustments	Swift and Osborne (2025)
5	WOD	Open ocean	Water column	Discrete bottle	Similar to GLODAPv2, with no adjustments	Mishonov et al. (2024)
6	SNAPO-CO_2	Open ocean + Coastal ocean	Water column	Discrete bottle and semi-continuous	A compilation of cruises from multiple French initiatives	Metzl et al. (2024)
7	CODAP-NA	Coastal ocean	Water column	Discrete bottle	Like GLODAPv2, but for the coastal ocean	Jiang et al. (2021)
8	AZMP Carbon	Continental shelf and Slope	Water column	Discrete bottle	A compilation of cruises from the Atlantic Zone Monitoring Program (AZMP) since 2014	Gibb et al. (2023)
9	MOCHA	Coastal ocean	Water column	Discrete bottle + Continuous	US West Coast	Kennedy et al. (2024)
10	ARIOS	Coastal ocean	Water column	Discrete bottle	An OA Database for the Galician Upwelling Ecosystem off the NW Iberian Peninsula from 1976 to 2018	Padin et al. (2020)
11	Marine Inorganic Carbonate Chemistry in the Northern Gulf of Alaska	Coastal ocean	Water column	Discrete bottle	A synthesis of twenty cruises from 2008 to 2017 on the Gulf of Alaska (GAK) Line	Monacci et al. (2023)
12	Coral Reef Carbonate Chemistry Off the Florida Keys	Coastal/Regional	Water column	Discrete bottle	Temporal trends of DIC, TA, pCO_2, pH, Ω_{arag}, in different areas of the Florida Keys	Palacio-Castro et al. (2023)

Table 1. Continued.

No.	Name	Open ocean or coastal ocean	Surface or water column	Discrete bottle or continuous	Highlights	Reference
13	Salish Cruise Data Package and Multi-stressor Data Product	Coastal/Estuarine	Water column	Discrete bottle	A data compilation and multi-stressor (OA, hypoxia, temperature) data product based on cruises from 2008 to 2024 in the southern Salish Sea and Washington coast	Alin et al. (2025a, b)
14	Line P Marine Carbonate Chemistry Compilation	Open ocean	Water column	Discrete bottle	A compilation of fifty-five Line P cruises containing discrete DIC and TA profiles at five stations in the Northeast Pacific Ocean. Sampled approximately three times per year from 1990 to 2019	Franco et al. (2021a, b)
15	Anthropogenic carbon in the Arctic Ocean	Open ocean	Water column	Discrete bottle (adjusted to 2005)	Observation-based estimates of anthropogenic carbon in the Arctic Ocean	Tanhua et al. (2009), Terhaar et al. (2020)

strategy may be found in Karl and Lukas (1996) and Karl et al. (2001). Results from the HOT CO_2 measurement program can be found in Winn et al. (1994, 1998), Dore et al. (2003, 2009, 2014), and Knor et al. (2023, 2025). The HOT project page, metadata, data streams and data identifiers are listed at https://www.bco-dmo.org/project/2101 (last access: 7 January 2026). A MAPCO_2 system on the Woods Hole Oceanographic Institution Hawaii Ocean Time-series Site mooring (WHOTS; https://www.soest.hawaii.edu/whots/, last access: 7 January 2026) has provided a near-continuous record of surface pCO_2 since 2004, and is anchored by the longer high-accuracy HOT ship-based program (see Sutton et al., 2019 and Knor et al., 2023). A surface ocean data product that includes CO2SYS-calculated values of pCO_2, carbonate mineral saturation states and other derived quantities may be found at https://hahana.soest.hawaii.edu/hot/hotco2/hotco2.html (last access: 7 January 2026) and https://doi.org/10.5281/zenodo.15060931 (Dore et al., 2025).

18. ESTOC: the European Station for Time-series in the Ocean (ESTOC) began carbon dioxide monitoring in October 1995, providing a 30-year record on DIC, TA, and pH. This dataset represents the longest continuous monthly record of warming, rising carbon dioxide levels, and acidification in the eastern North Atlantic (González-Dávila and Santana-Casiano, 2023a). ESTOC is located 100 km north of the Canary Islands archipelago (https://plocan.eu/en/installations/ocean-observatory, last access: 7 January 2026). The program includes a ship-based observation system, measuring physical, chemical, and biological variables throughout the 3670 m water column. It also features a moored platform for surface meteorological and oceanic observations as well as subsurface measurements, maintained by the Canary Island Oceanic Platform (PLOCAN, https://plocan.eu/en, last access: 7 January 2026) and the University of Las Palmas de Gran Canaria (https://iocag.ulpgc.es/research/research-units/quima, last access: 7 January 2026). Carbonate system measurements include full-depth bottle sampling for photometric pH, TA, and DIC, conducted monthly from 1995 to 2008, every two months until 2018, and semiannually in recent years due to limited ship time, timed to coincide with moored structure maintenance. ESTOC is also visited every two weeks by a volunteer observing ship, ES-SOOP-CanOA (https://meta.icos-cp.eu/resources/stations/OS_687B, last access: 7 January 2026), part of the European Research Infrastructure ICOS (https://www.icos-cp.eu/observations/ocean/stations, last access: 7 January 2026), which provides

real-time surface data on carbon dioxide fluxes and OA. The program also includes the CO_2-ESTOC oceanographic buoy (https://meta.icos-cp.eu/labeling/, last access: 7 January 2026). The full dataset with DOIs is accessible on Pangaea (González-Dávila and Santana-Casiano, 2023a).

19. Point B Time-series: the Point B Time-series documents the carbonate chemistry at a coastal site in the Bay of Villefranche (43.686200°N 7.314800° E) in Villefranche-sur-mer, France, northwestern Mediterranean Sea. Since January 2007, seawater is sampled weekly at 1 and 50 m, and analyzed for DIC and TA (Kapsenberg et al., 2017). Salinity and temperature are extracted from CTD profiles. Variables of the carbonate system such as pH (total scale) are calculated using the R package seacarb (Gattuso et al., 2021a). Data are available at Pangaea: https://doi.org/10.1594/PANGAEA.727120 (Gattuso et al., 2021b).

20. Ny-Ålesund Time-series: the Ny-Ålesund Time-series documents the carbonate chemistry at a coastal site of Kongsfjorden, Spitsbergen (78.930660° N 11.920030° E) during the period 2015–2021. It is the first high-frequency (1 h), multi-year (6 years) dataset of salinity, temperature, pCO_2, pH, as well as calculated DIC and TA in the High-Arctic Ocean (Gattuso et al., 2023a). Data are available at Pangaea: https://doi.org/10.1594/PANGAEA.957028 (Gattuso et al., 2023b).

21. SPOTS: the Synthesis Product for Ocean Time-Series (SPOTS) is a ship-based biogeochemical pilot, aiming at regularly providing high quality data from fixed time-series stations with consistent format and semantics (Lange et al., 2024a). The pilot includes data from 12 fixed ship-based time-series programs with a focus on the Global Ocean Observing System's biogeochemical essential ocean variables. These stations represent unique marine environments across a variety of spatiotemporal resolutions and ranges, with data from 1983 to 2021. While implementing the FAIR principles (Wilkinson et al., 2016) and promoting open data, the metadata of the time-series stations were enhanced to interoperate with the IOC-UNESCO Ocean Data and Information System (ODIS). Additionally, an extensive quality assessment resulted in enhanced intra- and inter-station comparability. Data are available at https://www.bco-dmo.org/dataset/896862 (last access: 7 January 2026) (Lange et al., 2024b).

22. pCO_2 and pH Time-series from 40 Surface Buoys: Sutton et al. (2019) established a living dataset comprising 40 individual autonomous moored surface ocean pCO_2 time-series established between 2004 and 2013, 17 of which also include autonomous pH measurements. These time-series characterize a wide range of surface ocean carbonate system conditions, across a variety of environments, including 17 oceanic and 13 coastal locations, as well as 10 coral reefs. Data are available at https://www.ncei.noaa.gov/data/oceans/ncei/ocads/metadata/0173932.html (last access: 7 January 2026) (Sutton et al., 2018). Additionally, a dedicated webpage for this project is available at https://www.ncei.noaa.gov/access/ocean-carbon-acidification-data-system/oceans/Moorings/ndp097.html (last access: 7 January 2026).

3.1.3 Gridded and derived products – surface ocean

Although cruise data compilations are valuable for making data available in a uniform format, they often are constrained by their sampling strategies and can have significant gaps in space and time. Gridded and derived data products address this limitation by making some variables available at all grid points on a standardized spatial grid and at standardized depth levels through processes such as interpolation and gap-filling. This section describes gridded data products that have been derived from observations through interpolation and other gap-filling procedures, depicting the surface ocean. Note that this compilation focuses primarily on data products with global coverage, acknowledging that many regional gap-filled products became available in recent years and shall be include in future updates.

23. Takahashi Delta fCO_2 and Flux Climatology: following on previous climatologies published by the late Taro Takahashi in 1997 and 2009, Fay et al. (2024a) created a legacy climatology using his methodology and the updated SOCAT database of observations. This product provides 12 months of delta fCO_2 values and corresponding fluxes for a reference year of 2010 at $4° \times 5°$ resolution, and subsequently regridded to $1° \times 1°$ resolution and near-global coverage. This climatology represents the mean of ocean conditions over the last four decades and is distinctive relative to many other mechanistic machine learning approaches in that it interpolates in time and space using only the available fCO_2 data and a surface water advection scheme rather than using proxy variables for gap-filling. It uses the median of observations to determine a reference year of 2010 and fluxes are provided using air–sea partial pressure differences and inputs from the SeaFlux product (Fay et al., 2021). The climatology product is available at https://www.ncei.noaa.gov/data/oceans/ncei/ocads/metadata/0282251.html (last access: 7 January 2026). The related manuscript is available at ESSD: https://doi.org/10.5194/essd-16-2123-2024 (Fay et al., 2024a).

Table 2. Time-series based ocean carbonate chemistry data synthesis products.

No.	Name	Open ocean or coastal ocean	Surface or water column	Discrete bottle or continuous	Highlights	Reference
16	BATS	Open ocean	Top 4600 m	CTD profiles, discrete bottle data from hydrocast, rate measurements (primary, export and bacterial production), biomass and other biological measurements, underway measurements	One of the longest continuous records of warming, salinification, ocean deoxygenation, and OA in the open ocean	Bates and Johnson (2020, 2023)
17	HOT	Open ocean	Top 4500 m	Discrete bottle for shipboard measurements; sensor measurements on WHOTS mooring	35+ years of inorganic carbon dynamics in the open waters of the central North Pacific	Dore et al. (2009)
18	ESTOC	Open ocean	Top 3570 m	Discrete bottle for shipboard measurements; sensor measurements on ESTOC mooring	The longest continuous monthly record of warming, rising carbon dioxide levels, and OA in the eastern North Atlantic	González-Dávila and Santana-Casiano (2023a)
19	Point B Time-series	Coastal ocean	5 and 50 m	CTD profiles, discrete bottle data	Carbonate chemistry at a coastal site of the Bay of Villefranche, France	Kapsenberg et al. (2017)
20	Ny-Ålesund Time-series	Coastal ocean	12 m	CTD, discrete bottle data, sensor measurements at the COSYNA/MOSES-AWIPEV underwater observatory	Carbonate chemistry at a coastal site of Kongsfjorden, Spitsbergen	Gattuso et al. (2023a, b)
21	SPOTS	Open ocean + Coastal ocean	Water column	Discrete	The pilot includes biogeochemical data from 12 fixed ship-based time-series programs	Lange et al. (2024a, b)
22	pCO_2 and pH Time-series from 40 Surface Buoys	Open ocean + Coastal ocean	Surface	Continuous	Based on 40 moored surface pCO_2 time-series, with 17 of them containing pH	Sutton et al. (2019)

24. MPI-ULB-SOM-FFN: Landschützer et al. (2020a) created a uniform pCO_2 climatology combining open and coastal oceans. It is a monthly gridded global surface ocean pCO_2 data product without adjusting for a specific reference year. Developed on a higher-resolution $0.25° \times 0.25°$ global surface-ocean grid, this product is the result of combining two neural network-based pCO_2 products: the open ocean product described below (i.e., Landschützer et al., 2016) and the coastal product created by Laruelle et al. (2017). Consequently, it represents coastal zones better. Data collected between 1998 and 2015 from the SOCAT database (Version 5) were used to create this data product. The merged climatology product is available at https://www.ncei.noaa.gov/data/oceans/ncei/ocads/metadata/0209633.html (last access: 7 Jan-

uary 2026). Additionally, a dedicated web page for this project is available at https://www.ncei.noaa.gov/access/ocean-carbon-acidification-data-system/oceans/MPI-ULB-SOM_FFN_clim.html (last access: 7 January 2026).

25. VLIZ-SOM-FFN: Landschützer et al. (2016) employed the Self-Organizing-Map Feed-Forward Network (SOM-FFN) neural network method (Landschützer et al., 2013) to map sea surface pCO_2 from SOCAT (see No. 1 above) (Bakker et al., 2014) to generate monthly pCO_2 fields on a $1° \times 1°$ global surface ocean grid, covering the period from 1982 to near present. It is based on the gridded pCO_2 measurements from SOCAT and is updated regularly. The creation of the pCO_2 fields involves a two-step neural network approach, which has been extensively detailed and validated in previous works by Landschützer et al. (2013, 2014, 2016). In the initial step, the global ocean is clustered into biogeochemical provinces, and subsequently, the non-linear relationship between CO_2 driver variables and gridded data from SOCAT (Bakker et al., 2016) is reconstructed. Air–sea CO_2 fluxes are also computed based on the air–sea pCO_2 difference, utilizing a bulk gas transfer formulation as described by Landschützer et al. (2013, 2014, 2016). The product is available at https://www.ncei.noaa.gov/data/oceans/ncei/ocads/metadata/0160558.html (last access: 7 January 2026). Additionally, a dedicated page for this project is available at https://www.ncei.noaa.gov/access/ocean-carbon-acidification-data-system/oceans/SPCO2_1982_present_ETH_SOM_FFN.html (last access: 7 January 2026).

26. JMA-MLR: Iida et al. (2021) developed a monthly data product for inorganic carbonate variables on a $1° \times 1°$ global surface ocean grid for the period 1993–2018. Variables include DIC, TA, pCO_2, air–sea CO_2 flux, pH, and Ω_{arag}. They leveraged data products such as SOCAT.v2019 (Bakker et al., 2016) and GLODAPv2.2019 (Olsen et al., 2019), as well as satellite-based variables, including sea-surface dynamic height (SSDH), mixed layer depth (MLD), and chlorophyll a. The product is updated annually using the latest SOCAT and GLODAPv2 data. The data product can be accessed at https://www.data.jma.go.jp/kaiyou/english/co2_flux/co2_flux_data_en.html (last access: 7 January 2026).

27. OceanSODA-ETHZ:

    a. OceanSODA-ETHZv1 is a monthly gridded global surface ocean data product for multiple ocean carbonate system variables, including DIC, TA, pCO_2, pH (total scale), Ω_{arag}, and Ω_{calc} (Gregor and Gruber, 2020, 2021, 2023; Ma et al., 2023). This dataset is structured on a $1° \times 1°$ global surface ocean grid with monthly resolution from 1982–2022, facilitating research on OA over seasonal to decadal scales. The OceanSODA-ETHZ data product was created by extrapolating in time and space the surface ocean observations of fCO_2 from SOCATv2022 (Bakker et al., 2016) and TA from GLODAPv2.2022 using the newly developed Geospatial Random Cluster Ensemble Regression (GRaCER) method (Gregor, 2021). TA and pCO_2 were then used to calculate the remaining variables of the marine carbonate system with the PyCO2SYS software (Humphreys et al., 2022). Phosphate and silicate from WOA 2018 product was used (Boyer et al., 2018; Garcia et al., 2018a). The OceanSODA-ETHZ data product is available at https://www.ncei.noaa.gov/data/oceans/ncei/ocads/metadata/0220059.html (last access: 7 January 2026).

    b. OceanSODA-ETHZv2 is a surface fCO_2 product with a $0.25° \times 0.25°$ spatial resolution and an 8 d temporal resolution, providing estimates starting from 1982 (Gregor et al., 2024a, b). The high-resolution outputs are suitable for investigating the shorter- and finer-scale dynamics of surface fCO_2. Despite sharing a name with its predecessor, OceanSODA-ETHZv2 does not provide TA estimates and employs a different methodology, as described in the following steps: (1) the atmospheric trend of CO_2 is removed by subtracting marine boundary layer CO_2 concentrations from SOCAT fCO_2 producing a new target Δ^*CO_2 to reduce the biases at the start and end of the time-series. (2) An 8 d seasonal climatology of Δ^*CO_2 is estimated using Gradient Boosted Decision Trees (GBDT), which is later used as a predictor. (3) The non-seasonal thermal component is removed from Δ^*CO_2, resulting in a new target, $\Delta^*CO_2^{nonT}$. (4) The new target is estimated using a feed-forward neural network, with the GBDT as one of the forcing variables. (5) Steps 4 through to 1 are inverted to arrive at fCO_2. (6) Air–sea CO_2 fluxes are computed using ERA5 winds. Data are available at https://doi.org/10.5281/zenodo.11206366 (Gregor et al., 2024b) and are updated annually.

28. LDEO-HPD fCO_2: the LDEO Hybrid Physics Data (LDEO-HPD) estimates the temporal evolution of surface ocean fCO_2 and air–sea CO_2 exchange, utilizing the strengths of observations and global ocean biogeochemical models (GOBMs) (Gloege et al., 2022). GOBMs are internally consistent, mechanistic representations of the ocean circulation and carbon cycle, and have long been the standard for making

spatiotemporally resolved estimates of air–sea CO_2 fluxes. However, there is often a bias between the modelled fCO_2 and available surface ocean measurements (Fay and McKinley, 2021). The LDEO-HPD approach trains an eXtreme Gradient Boosting (XGB) algorithm to learn a non-linear relationship between model-data fCO_2 mismatch and observed predictor variables: sea surface temperature (SST), sea surface salinity (SSS), chlorophyll concentration, mixed layer depth). The GOBM fCO_2 is then corrected with the predicted model-data misfit to estimate real-world fCO_2 for the observation period (Gloege et al., 2022). This results in reconstructed monthly surface ocean fCO_2 and air–sea CO_2 fluxes on a $1° \times 1°$ grid in the open ocean beginning in 1982. Additional information can be found at oceancarbon.ldeo.columbia.edu. The data product is available at https://doi.org/10.5281/zenodo.4760205 (Gloege et al., 2021).

29. LDEO-HPD with Extended Temporal Coverage: building on the work of Gloege et al. (2022), the LDEO-HPD product as mentioned above (No. 28) can be extended back in time to predict fCO_2 for all available model years. Bennington et al. (2022a) find that the largest component of the GOBM corrections is climatological. The smaller corrections at other timescales suggest either that these are well captured by the GOBMs or the data are insufficient. The dominance of climatological corrections supports the extension of the LDEO-HPD fCO_2 product backwards in time. A climatology of model-observation misfits for the best-observed period (2000–present) is applied to the GOBMs for 1959–1981, while an interannually varying correction is used for 1982 onward. (Bennington et al., 2022a). This results in reconstructed monthly surface ocean fCO_2 and air–sea CO_2 fluxes on a $1° \times 1°$ grid covering the open ocean, beginning in 1959. Since 2022, the LDEO-HPD Back in Time product has been included in the annual release of the Global Carbon Budget (GCB). Additional information can be found at https://oceancarbon.ldeo.columbia.edu/ (last access: 7 January 2026). The data product can be accessed via Zenodo at https://doi.org/10.5281/zenodo.13891722 (Fay et al., 2024b).

30. LDEO fCO_2 – Residual Method: a frequently used approach for estimating full-coverage fCO_2 is to train a machine learning algorithm on sparse in situ fCO_2 data and associated physical and biogeochemical observations. While these associated variables have well-known relationships to fCO_2, it is often unclear how they mechanistically drive fCO_2 around the world. The LDEO fCO_2-Residual method takes the basic approach and enhances connections between physical understanding and reconstructed fCO_2. The novel approach used here includes applying pre-processing to the fCO_2 data to remove the direct effect of temperature – a relationship well-documented in literature and lab experiments (Takahashi et al., 2002). This enhances the biogeochemical/physical component of fCO_2 in the target variable (now fCO_2-Residual) and reduces the complexity that the machine learning must disentangle. The resulting algorithm has physically understandable connections between input data and the output biogeochemical/physical component of fCO_2 (Bennington et al., 2022b). This results in reconstructed monthly surface ocean fCO_2 and air–sea CO_2 fluxes on a $1° \times 1°$ grid covering the open ocean, beginning in 1982 and extended to the most recent year of available data. Additional information can be found at oceancarbon.ldeo.columbia.edu. The data product can be accessed via Zenodo at https://doi.org/10.5281/zenodo.13941548 (Bennington et al., 2024).

31. CMEMS-LSCE Surface Ocean Carbonate Data Products:

    a. CMEMS-LSCEv1: monthly surface ocean pCO_2 and air–sea CO_2 fluxes on a $1° \times 1°$ grid in both the open ocean and coastal seas from 1985–2019 were reconstructed by Chau et al. (2022a). CMEMS-LSCE is short for Copernicus Marine Environment Monitoring Service – Laboratoire des Sciences du Climat et de l'Environnement. This product is generated from an ensemble-based reconstruction of pCO_2 maps trained with gridded data from SOCATv2020 (Bakker et al., 2016). Sea-surface pCO_2 values (converted from the original fCO_2 values in SOCATv2020) were regressed against a set of predictors with non-linear functions, i.e., feed-forward neural network (FFNN) models. The predictors include: sea-surface height (SSH), SST, SSS, MLD, chlorophyll *a* (Chl *a*), atmospheric CO_2 mole fraction (xCO_2), and geographical coordinates (longitudes and latitudes). This data product is accessible at https://data.ipsl.fr/catalog/srv/eng/catalog.search#/metadata/a2f0891b-763a-49e9-af1b-78ed78b16982 (last access: 7 January 2026).

    b. CMEMS-LSCEv2: CMEMS-LSCEv2 corresponds to the latest version of the CMEMS-LSCE FFNN. It uses the same ensemble-based reconstruction method for pCO_2 maps as CMEMS-LSCEv1. Improvements include downscaling the spatial resolution to $0.25° \times 0.25°$ and reproducing additional surface ocean carbonate system variables on a global grid from 1985 onwards (Chau et al., 2024a). The additional surface ocean carbonate system variables are: pCO_2, DIC, TA, pH, Ω_{arag}, and Ω_{calc}. Surface ocean pCO_2 is reconstructed based on an en-

semble of neural network models mapping gridded observation-based data provided by SOCATv2022 (Bakker et al., 2016). Surface ocean TA is estimated with a multiple linear regression approach (Carter et al., 2016, 2017). The remaining carbonate variables are calculated from pCO_2 and TA using a MATLAB version of CO2SYS (Lewis and Wallace, 1998; Sharp et al., 2023). The CMEMS-LSCE product is updated yearly for surface ocean pCO_2, air–sea fluxes, and the carbonate system variables. Updates are phased with release of the SOCAT database. For surface ocean pCO_2 and air–sea fluxes the temporal coverage is extended to the present date with a latency of 1 month (Chau et al., 2024b). Both the multi-year reconstruction and the near-real time prediction can be accessed through the CMEMS portal: https://doi.org/10.48670/moi-00047 (Chau et al., 2024c).

32. CarboScope (Jena-MLS): the Jena Mixed-Layer Scheme (within the CarboScope family of data-based estimates of carbon-cycle variability) is based on observed sea surface pCO_2 from SOCAT (see above No. 1) (Bakker et al., 2014). It provides daily global fields of pCO_2 and air–sea CO_2 fluxes from 1957 to the year before present, on a resolution of $2.5° \times 2°$ degrees. In the original method (Rödenbeck et al., 2013), a diagnostic model of the carbon balance in the ocean mixed layer is being fitted to the pCO_2 data, by adjusting the ocean-interior sources and sinks of carbon of the mixed layer. The multi-decadal trend is derived from the data-based Ocean Circulation Inverse Model (OCIM) estimate provided by DeVries (2022b). Since a later extension described in Rödenbeck et al. (2022), the variability in the ocean-interior sources and sinks is first regressed against variability in SST and wind speed. The regression step is followed by a correction step with explicit temporal variability, to also represent data variability not yet represented by the predictors of the regression. The CarboScope product is updated yearly. The results from current and previous releases can be downloaded from https://www.bgc-jena.mpg.de/CarboScope/ (last access: 7 January 2026).

33. UOEx-Watson: this product is an estimate of the atmosphere-ocean flux of CO_2 that takes into account near-surface temperature deviations (Watson et al., 2020). Most estimates use data on surface ocean pCO_2 without considering corrections due to temperature gradients within the uppermost few millimeters of the sea surface ("Skin temperature effects") or small effects due to changes in temperature that occur during sampling and measurement, especially when the measurement is from a commercial vessel rather than a research ship. This product takes these effects into account by recalculating pCO_2 from the SOCAT data base (v2019) using co-located satellite observations of skin temperature. The result is a substantial increase in the calculated net global uptake of CO_2. In other respects, the methodology for this data product follows the two-step neural network approach described by Landschützer et al. (2013, 2014). The gridded data set of sea surface fCO_2 adjusted to satellite-derived subskin surface temperature, is available at https://doi.org/10.1594/PANGAEA.905316 (Holding et al., 2019). Ocean-atmosphere fluxes interpolated to monthly and $1° \times 1°$ spatial resolution is available at https://www.ncei.noaa.gov/data/oceans/ncei/ocads/metadata/0301544.html (last access: 7 January 2026).

34. NIES-ML3: the ensemble product of three machine learning methods (ML3) from the National Institute for Environmental Studies (NIES), Japan, includes monthly global surface ocean fCO_2 in 1982–2024 on $1° \times 1°$ grids. Using a leave-one-year-out (LOYO) validation method and three machine learning models, Zeng et al. (2022) found that the time variant trends of ocean CO_2 could be estimated approximately by a harmonic function fitting of the annual atmospheric CO_2. They removed the estimated trends from the ocean CO_2 and applied the LOYO to the trend-removed data to obtain the trend that could not be approximated by the fitting for trend correction. The trend-removed data by the corrected trends were used to train the models. The gap-filled CO_2 maps were constructed by adding the trends to model predictions. The product is available at NIES: https://doi.org/10.17595/20220311.001 (Zeng, 2022).

35. CSIR-ML6: provides monthly $1° \times 1°$ estimates of surface pCO_2 (Gregor et al., 2019a). The approach uses the conceptual two-step approach of clustering and performing regressions for each cluster as Landschützer et al. (2016). CSIR-ML6 investigates the efficacy of various machine learning (ML) methods in estimating surface pCO_2, namely, feed-forward neural networks (FFNN), extremely randomized trees (ERT), gradient boosting machines (GBM), and support vector regression (SVR). It is found that the ensemble of all but the ERT method resulted in the best estimate, highlighting the fact that various ML methods do not produce the same outcome, particularly when data is sparse. Further, the variance between ensemble members can inform us about regions where uncertainty may be large due to methodological differences. Despite this, all methods achieve roughly the same uncertainty – a barrier, or wall beyond which the community has yet to overcome. The data are available at https://www.ncei.noaa.gov/data/oceans/ncei/ocads/metadata/0206205.html (last access: 7 January 2026) (Gregor et al., 2019b). The product is one of the six ensemble members of the SeaFlux dataset.

36. Stepwise-FFNN: Zhong et al. (2022) constructed a monthly global $1° \times 1°$ surface ocean pCO_2 product from January 1992 to December 2024, by combining the stepwise regression algorithm and a feed-forward neural network (FFNN) to select predictors of pCO_2 based on the mean absolute error in each of the 11 biogeochemical provinces defined by the self-organizing map (SOM) method. The methodology for this data product used regionally optimal predictors to account for differences in pCO_2 drivers, lowering local biases relative to a single global predictor set. The developed data product is available at https://doi.org/10.12157/IOCAS.20250814.001 (Zhong, 2025).

37. AOML-ET: Wanninkhof et al. (2024, 2025) developed a monthly global ocean data product of seawater pCO_2 and air–sea CO_2 fluxes, referred to as AOML-ET, using an extremely randomized trees (ET) machine learning technique. These maps are created on $1° \times 1°$ spatial grids, providing global surface ocean coverages from 1998 to 2023. AOML-ET incorporates several predictor variables, including time, location, SST, SSS, MLD, and chlorophyll a. The model was trained using the v2020 and v2023 releases of the SOCAT data product (No. 1). Air–sea CO_2 fluxes were calculated using the air–sea CO_2 partial pressure difference (ΔpCO_2) and a bulk gas transfer formulation incorporating windspeed. The dataset contains monthly $1° \times 1°$ NetCDF files of the AOML-ET outputs, along with the predictor variables. The data product is available at https://www.ncei.noaa.gov/data/oceans/ncei/ocads/metadata/0298989.html (last access: 7 January 2026) (Wanninkhof et al., 2024).

38. ULB-SOM-FFN-Coastalv2.1: Roobaert et al. (2024) present high-resolution ($0.25° \times 0.25°$ grid) monthly maps showing the distribution of sea surface pCO_2 across the global coastal ocean, spanning from 1982 to 2020. This product (ULB-SOM-FFN-coastalv2.1) builds upon the work by Laruelle et al. (2017), incorporating a two-step methodology that utilizes Self Organizing Maps (SOM) and Feed Forward Networks (FFN). This updated product now captures temporal variability, enabling the assessment of interannual variability and long-term trends in coastal air–sea CO_2 exchange, unlike the product by Laruelle et al. (2017), which only offers a climatology for a short period (1998–2015). The enhancements include additional environmental predictors and an expanded dataset for training and validation, featuring approximately 18 million direct coastal observations from the SOCAT database, specifically the SOCATv2022 release (Bakker et al., 2016). The product is available at https://www.ncei.noaa.gov/data/oceans/ncei/ocads/metadata/0279118.html (last access: 7 January 2026) (Roobaert et al., 2023).

39. RFR-LME: Sharp et al. (2024a) developed a data product delineating the temporal trends of OA indicators mapped on a $0.25° \times 0.25°$ spatial grid, across eleven US Large Marine Ecosystems (LMEs), with monthly coverage from 1998–2023. These indicators, which include the pCO_2, pH, Ω_{arag}, DIC, TA, Revelle Factors, among others, were derived from SOCATv2023, along with other oceanographic properties, e.g., SST, SSS, SSH, and MLD. The methodology combined Gaussian Mixture Models to categorize the data into environmentally similar subregions, Random Forest Regressions for the spatial and temporal extrapolation of observational fCO_2 data, and regressions to estimate TA (Carter et al., 2021) to provide a second carbonate system constraint. The resulting maps are available at https://www.ncei.noaa.gov/data/oceans/ncei/ocads/metadata/0287551.html (last access: 7 January 2026) (Sharp et al., 2024b), while an online portal at https://ecowatch.noaa.gov/thematic/ocean-acidification (last access: 7 January 2026) presents regionally averaged time-series for three key indicators: pCO_2, Ω_{arag}, and pH.

40. ReCAD-NAACOM-pCO_2: Wu et al. (2025) developed a reconstructed pCO_2 product for the North American Atlantic Coastal Ocean Margins (NAACOM), spanning from the Gulf of Mexico/Gulf of America to the Grand Banks, called the Reconstructed Coastal Acidification Database-pCO_2 (ReCAD-NAACOM-pCO_2). This product employed a two-step approach combining random forest regression and linear regression to generate monthly pCO_2 data at 0.25° spatial resolution from 1993–2021. The model was trained using SOCAT v2023 observations as ground-truth values, incorporating various satellite-derived and reanalysis environmental variables known to influence sea surface pCO_2. The ReCAD-NAACOM-pCO_2 dataset is publicly accessible (https://doi.org/10.5281/zenodo.11500974, Wu et al., 2024) and will be updated regularly.

41. Gridded Surface OA Indicators in the Northern Caribbean Sea: this dataset contains a high-quality dataset of derived products from over a million observations of surface water partial pressure/fugacity of carbon dioxide (pCO_2w/fCO_2w), for the Caribbean Sea, Gulf of Mexico/Gulf of America and North–West Atlantic Ocean covering the timespan from 1 January 2002 to 30 December 2019. The derived quantities include TA, acidity (pH), Ω_{arag} and air–sea CO_2 flux (Wanninkhof et al., 2020). This data product is available at https://www.ncei.noaa.gov/data/oceans/

ncei/ocads/metadata/0207749.html (last access: 7 January 2026) (Wanninkhof et al., 2019).

42. OA Data in the Gulf of Mexico/Gulf of America and Wider Caribbean: the Acidification, Climate, and Coral Reef Ecosystems Team (ACCRETE) Lab within AOML's Ocean Chemistry and Ecosystems Division (OCED) developed a data product for tracking OA in the Caribbean and Gulf of Mexico/Gulf of America from 2014 to 2020 (van Hooidonk, 2022). Utilizing satellite imagery and a data-assimilative hybrid model, the tool maps key indicators of the water's carbonate system, including pCO_2, TA, pH, Ω_{arag}, and Ω_{calc}. This innovation builds upon an update to the experimental OA Product Suite (OAPS) developed by NOAA's Coral Reef Watch. The data product is available at https://www.ncei.noaa.gov/data/oceans/ncei/ocads/metadata/0245950.html (last access: 7 January 2026) (van Hooidonk, 2022).

43. pCO_2 Climatology of the Baltic Sea: Bittig et al. (2024) used biogeochemical model output to inform the mapping of sea surface pCO_2 observations in the Baltic Sea and to build a mean monthly climatology for the period 2003 to 2021, with spatial resolutions of $0.10° \times 0.05°$ (approximately 3 nautical miles in both directions). In a first step, spatial patterns of variability were extracted from 20 years of model surface pCO_2 data by an EOF analysis. These spatial patterns were then used to map surface pCO_2 observations from SOCAT (see above No. 1) (Bakker et al., 2014) onto the Baltic Sea domain. By using an ensemble approach with varying number of EOF patterns, the spatial scales of the mapping were locally adjusted based on the observation's data density. Mapped monthly fields of pCO_2 from 2003–2021 were combined for the product into a mean monthly climatology and a spatially-resolved linear trend. The climatology product is available at PANGAEA: https://doi.org/10.1594/PANGAEA.961119 (Bittig et al., 2023).

44. INCOIS-ReML: the Indian National Centre for Ocean Information Services-Regional Machine Learning model (INCOIS-ReML) pCO_2 data product offers machine learning based monthly climatological sea surface pCO_2 and the corresponding air–sea CO_2 flux for the Bay of Bengal (Joshi et al., 2024). This data product integrates publicly available open-ocean observations with data from the Indian Exclusive Economic Zone. This high-resolution ($0.083° \times 0.083°$) monthly climatological pCO_2 data product is available from the INCOIS Portal: https://las.incois.gov.in (last access: 7 January 2026), and from OCADS: https://www.ncei.noaa.gov/data/oceans/ncei/ocads/metadata/0307627.html (last access: 7 January 2026) (Joshi et al., 2025a).

45. INCOIS_TA: the Indian National Centre for Ocean Information Services-Total Alkalinity (INCOIS_TA) data product offers a machine learning based monthly interannual surface TA from 1993–2020 for the North Indian Ocean (Joshi et al., 2025b). This data product integrates publicly available open-ocean observations with data collected during Indian scientific expeditions and from the Indian Exclusive Economic Zone. This high-resolution ($0.083° \times 0.083°$) long-term monthly TA data product is available from the INCOIS Portal: https://las.incois.gov.in (last access: 7 January 2026, and from OCADS: https://www.ncei.noaa.gov/data/oceans/ncei/ocads/metadata/0307789.html (last access: 7 January 2026) (Joshi et al., 2025c).

3.1.4 Gridded and derived products – interior ocean

This section describes gridded data products derived from observations through interpolation and other gap-filling procedures, depicting the interior ocean (Table 4).

46. GLODAPv2 Climatology (referenced to 2002): Lauvset et al. (2016) generated a comprehensive set of global interior ocean climatologies, mapping key biogeochemical variables on a $1° \times 1°$ grid for 33 depth levels from the surface to 5500 m. These climatologies cover temperature, salinity, DO, nitrate, phosphate, silicate, DIC, TA, pH, Ω_{arag}, and Ω_{calc}. This data product was created based on the quality-controlled and internally consistent GLODAPv2.2016 (Olsen et al., 2016) using the data-interpolating variational analysis (DIVA) method (Barth et al., 2014). The conceivably confounding temporal trends in DIC, pH, Ω_{arag} and Ω_{calc} due to anthropogenic influence were removed prior to mapping by normalizing their values to a reference year of 2002 using first-order calculations of anthropogenic carbon accumulation rates. For all variables, all data from the full 1972–2013 period were used, including data that did not receive full secondary quality-control. This data product is not updated each year along with the main GLODAPv2 data product. The mapped data product is available at https://www.ncei.noaa.gov/data/oceans/ncei/ocads/metadata/0286118.html (last access: 7 January 2026) (Lauvset et al., 2023a). It can also be accessed from the GLODAP website: https://glodap.info/ (last access: 7 January 2026) For reference, the original GLODAP Climatology (Version 1.1) is accessible at https://www.ncei.noaa.gov/data/oceans/ncei/ocads/metadata/0001644.html (last access: 7 January 2026) (Sabine et al., 2005).

47. Aragonite Saturation State Climatology: Jiang et al. (2015) developed a global interior-ocean Ω_{arag} cli-

Table 3. Gridded and derived ocean carbonate chemistry data synthesis products in the surface ocean.

No.	Name	Open ocean or coastal ocean	Spatial resolution	Temporal resolution	Methodology	Highlights	Reference
23	Takahashi Delta fCO_2 and Flux Climatology	Open ocean	1° × 1°	12-month climatology referenced to 2010	Advection Scheme	Does not use proxy variables for extrapolation. Only produced as monthly climatology	Fay et al. (2024a)
24	MPI-ULB-SOM-FFN	Open ocean + Coastal ocean	0.25° × 0.25°	12-Month climatology without a reference year	2-step machine learning: Merged product of the SOM-FFN approach applied to the open ocean (Landschützer et al., 2016) and the coastal ocean (Laruelle et al., 2017)	Monthly gridded pCO_2 without adjusting for a specific reference year, high-resolution coastal ocean coverage	Landschützer et al. (2020a)
25	VLIZ SOM-FFN	Open ocean	1° × 1°	Monthly from January 1982 onwards	2-step machine learning: Self organizing map clustering followed by a feed forward network (SOM-FFN)	Monthly gridded pCO_2 from 1982 through near present	Landschützer et al. (2016)
26	JMA-MLR	Open ocean	1° × 1°	Monthly from January 1990 onwards	Multiple linear regressions	Temporal trends of DIC, TA, pCO_2, air–sea CO_2 flux, pH, and Ω_{arag}	Iida et al. (2021)
27(a)	OceanSODA-ETHZv1	Open ocean	1° × 1°	Monthly from 1982 to 2023	Ensemble of 2-step members: K-means clustering with gradient boosting and SVR regression	Temporal trends of DIC, TA, pCO_2, pH, Ω_{arag}, and Ω_{calc}	Gregor and Gruber (2021)
27(b)	OceanSODA-ETHZv2	Open ocean + Coastal ocean	0.25° × 0.25°	8 d from 1982 to 2022	FFNN	Highlighting fine-scale and short-term variability of the ocean carbon sink	Gregor et al. (2024a, b)

Table 3. Continued.

No.	Name	Open ocean or coastal ocean	Spatial resolution	Temporal resolution	Methodology	Highlights	Reference
28	LDEO-HPD fCO_2	Open ocean	1° × 1°	Monthly from 1982	XGBoost algorithm	Temporal evolution of surface ocean fCO_2 and air–sea CO_2 exchange	Gloege et al. (2022)
29	LDEO-HPD with Extended Temporal Coverage	Open ocean	1° × 1°	Monthly from 1959	XGBoost algorithm	Uses model-data misfit climatology to extend estimate back in time to 1959	Fay et al. (2024b)
30	LDEO fCO_2 – Residual Method	Open ocean	1° × 1°	Monthly from 1982	XGBoost algorithm	Removes the temperature component before ML	Bennington et al. (2022b)
31(a)	CMEMS-LSCEv1	Open ocean + Coastal ocean	1° × 1°	Monthly from 1985 to 2019	FFNN	Seamless reconstruction from coastal to open ocean	Chau et al. (2022a)
31(b)	CMEMS-LSCEv2	Open ocean + Coastal ocean	0.25° × 0.25°	Monthly from 1985 to 2025	FFNN	Yearly extension of time-series and monthly reconstruction at low latency	Chau et al. (2024a, b)
32	CarboScope (Jena-MLS)	Open ocean	2.5° × 2°	Daily from 1957	Multi-linear regression against long-term predictors, plus auto-regressive correction	Variability of pCO_2 and air–sea CO_2 fluxes since 1957, sensitivities to SST and wind speed variations	Rödenbeck et al. (2022)
33	UOEx-Watson	Open ocean	1° × 1°	Monthly from January 1992	Two-step neural network approach described by Landschützer et al. (2013, 2014, 2016)	Air–sea fluxes of CO_2 with adjusted skin temperature effect	Watson et al. (2020)

Table 3. Continued.

No.	Name	Open ocean or coastal ocean	Spatial resolution	Temporal resolution	Methodology	Highlights	Reference
34	NIES-ML3	Open ocean	1° × 1°	Monthly from 1982 to 2023	FNN, GBM, RF	The prediction of a ML method was obtained from ten trainings with different seeds. The mean of the three methods was taken as the final prediction	Zeng (2022), Zeng et al. (2022)
35	CSIR-ML6	Open ocean	1° × 1°	Monthly from 1982 to 2016	Ensemble: FFNN, SVR, ERT, Gradient Boosted Trees	Various ML methods produce different results when data is sparse, but all still achieving roughly the same uncertainty	Gregor et al. (2019a)
36	Stepwise-FFNN	Open ocean	1° × 1°	Monthly from 1992 to 2024	SOM, FFNN, Stepwise regression	ML-based selection of predictors considering regional differences of pCO_2 drivers	Zhong et al. (2022)
37	AOML-ET	Open ocean	1° × 1°	Monthly from 1998 to 2023	Extremely randomized trees (ET) machine learning technique	Monthly global air–sea CO_2 flux maps in modern era	Wanninkhof et al. (2025)
38	ULB-SOM-FFN-Coastalv2.1	Coastal ocean	0.25° × 0.25°	Monthly from 1982 to 2020	2-step machine learning: Self organizing map clustering followed by a feed forward network (SOM-FFN)	Global temporal trends of coastal pCO_2 and air–sea CO_2 fluxes based on SOCATv2022 with data collected from 1982–2020	Roobaert et al. (2024)

Table 3. Continued.

No.	Name	Open ocean or coastal ocean	Spatial resolution	Temporal resolution	Methodology	Highlights	Reference
39	RFR-LME	Coastal ocean	0.25° × 0.25°	Monthly from 1998 to 2023	Gaussian mixture models and random forest regressions	Temporal trends of OA indicators and estimated uncertainties across 11 US Large Marine Ecosystems (LMEs), with monthly coverage from 1998–2023	Sharp et al. (2024a)
40	ReCAD-NAACOM-pCO_2	Coastal ocean	0.25° × 0.25°	Monthly from 1993 to 2021	2-step machine learning: random forest regression followed by linear regression	Sea surface pCO_2 in the North American Atlantic Coastal Ocean Margins (NAACOM)	Wu et al. (2025)
41	Gridded Surface OA Indicators in the Northern Caribbean Sea	Coastal ocean	1° × 1°	Monthly from 2002 to 2019	Gridding of the observations of fCO_2, SST and SSS was performed by binning and averaging the data in (1° × 1° by month) cells	A 17-year record of fCO_2, TA, pH, Ω_{arag}, and air–sea CO_2 flux in the Caribbean Sea	Wanninkhof et al. (2020)
42	OA data in the Gulf of Mexico/Gulf of America and Wider Caribbean	Regional	0.088° × 0.88°	Monthly from 2014 to 2020	Utilizing satellite imagery and a data-assimilative hybrid model, the tool maps key indicators of the water's carbonate system, including pCO_2, TA, pH, Ω_{arag}, and Ω_{calc}.	A new tool to monitor OA over the wider Caribbean and Gulf of Mexico/Gulf of America	van Hooidonk (2022)
43	pCO_2 Climatology of the Baltic Sea	Regional	0.10° × 0.05°	12-month climatology referenced to 2013; linear trend 2003–2021	Extrapolation using model-based patterns of variability	Does not use proxy variables for extrapolation. Spatial scales adjust locally to data density	Bittig et al. (2024)

Table 3. Continued.

No.	Name	Open ocean or coastal ocean	Spatial resolution	Temporal resolution	Methodology	Highlights	Reference
44	INCOIS-ReML	Regional	$0.083° \times 0.083°$	Monthly climatology referenced to 2015.	Xtreme Gradient Boosting (XGB) based Machine Learning Model	This data product integrates publicly available open-ocean observations with data from the Indian EEZ region in the Bay of Bengal to provide surface pCO_2 and air–sea CO_2 flux estimates	Joshi et al. (2024)
45	INCOIS_TA	Regional	$0.083° \times 0.083°$	Monthly from 1993 to 2020	Xtreme Gradient Boosting (XGB) based Machine Learning Model	Integrates publicly available open-ocean observations with data collected during Indian scientific expeditions and from the Indian Exclusive Economic Zone to provide surface TA estimates for the North Indian Ocean	Joshi et al. (2025b)

matology (referenced to 2000), on a $1° \times 1°$ grid at 9 standardized depth levels from the surface down to 4000 m. This was accomplished by integrating data from the first version of GLODAP (Key et al., 2004), CARINA (Key et al., 2010), and PACIFICA (Suzuki et al., 2013), along with additional recent cruise datasets up to 2012. Temporal adjustments were made to a reference year of 2000, accounting for an annual fCO_2 increase of 1.6 µatm in the surface mixed layer (SML), with a rate that decreases linearly to 0 µatm yr^{-1} from the bottom of the SML to a depth of 1000 m (Sabine et al., 2008). The data product is available at https://www.ncei.noaa.gov/data/oceans/ncei/ocads/metadata/0139360.html (last access: 7 January 2026) (Jiang and Feely, 2015).

48. Mapped Observation-Based Oceanic Dissolved Inorganic Carbon (MOBO-DIC):

    a. MOBO-DIC (Version 2020): Keppler et al. (2020a) produced a global interior ocean DIC monthly climatology (average climatological values for January through December) on a $1° \times 1°$ grid at 33 standardized depth levels from the surface to 2000 m. The MOBO-DIC mapping method adapts and extends the SOM-FFN technique originally introduced by Landschützer et al. (2013). It starts by categorizing the ocean into clusters with compa-

rable physical and biogeochemical characteristics using self-organizing maps (SOM). Subsequently, within each SOM-defined cluster, a feed-forward network (FFN) is employed to estimate and enforce the statistical correlation between the targeted DIC data and the predictor data available in globally mapped fields. The product uses data from January 2004 to December 2017, and is thus centered around the years 2010/2011. The data product is available at https://www.ncei.noaa.gov/access/ocean-carbon-acidification-data-system/oceans/ndp_104/ndp104.html (last access: 7 January 2026).

b. MOBO-DIC (Version 2023): Keppler et al. (2023a) extended the temporal resolution of MOBO-DIC to resolve monthly fields from January 2004 to December 2019, as opposed to the average climatological values in Keppler et al. (2020a). This data product is on a $1° \times 1°$ grid at 28 depth levels from the surface to 1500 m. The data product is available at https://www.ncei.noaa.gov/data/oceans/ncei/ocads/metadata/0277099.html (last access: 7 January 2026) (Keppler et al., 2023b).

49. Monthly Interior Ocean TA Climatology: Broullón et al. (2019) developed a monthly global interior ocean TA climatology using a feed-forward neural network approach. This dataset offers a spatial resolution of $1° \times 1°$ in the horizontal, spans 102 depth levels (ranging from 0–5500 m) in the vertical dimension, and features a temporal resolution that varies from monthly (0–1500 m) to annual (1550–5500 m). The development of this climatology was based on the analysis of TA in relation to several key predictor variables, including temperature, salinity, nutrients (phosphate, nitrate, and silicate), DO, and sampling position (coordinates and depth), as outlined in Velo et al. (2013). Both TA and these predictor variables were sourced from GLODAPv2 (version 2016) (Olsen et al., 2016). The global interior ocean TA climatology was constructed by leveraging the established relationships between TA and the predictor variables, as well as the monthly climatologies of temperature, salinity, and DO from the WOA 2013 (Locarnini et al., 2013; Zweng et al., 2013; Garcia et al., 2014), and nutrients data that were obtained through the CANYON-B neural network process, applied to the previously mentioned fields. The data product is available at https://www.ncei.noaa.gov/data/oceans/ncei/ocads/metadata/0222470.html (last access: 7 January 2026) (Broullón et al., 2020b).

50. Monthly Interior Ocean DIC Climatology: Broullón et al. (2020a) employed a feed-forward neural network approach to create a monthly global interior ocean DIC climatology, centered around the year 1995. This dataset offers a $1° \times 1°$ spatial resolution in the horizontal domain, encompassing 102 depth levels ranging from 0–5500 m vertically. The temporal resolution varies, ranging from monthly (0–1500 m) to annual (1550–5500 m). In contrast to their previous work on TA (Broullón et al., 2019), this analysis includes the variable "year" to account for anthropogenic DIC pool changes. It also incorporates data from the LDEO pCO_2 database (Takahashi et al., 2017) alongside GLODAPv2.2019 (Olsen et al., 2019) to establish relationships between DIC and its input variables: temperature, salinity, DO, as well as location, pressure, and time. The DIC climatology was derived using these relationships, along with monthly climatological data for temperature, salinity, and DO from WOA 2013 (Locarnini et al., 2013; Zweng et al., 2013; Garcia et al., 2014), as well as phosphate, nitrate, and silicate values computed from the CANYON-B neural network fed with the aforementioned fields. The data product is available at https://www.ncei.noaa.gov/data/oceans/ncei/ocads/metadata/0222469.html (last access: 7 January 2026) (Broullón et al., 2020c).

51. Acidification Metrics in the Ocean Interior: Fassbender et al. (2023) generated estimates of global interior ocean changes to pH, $[H^+]$, Ω_{arag}, pCO_2, and the Revelle sensitivity factor driven by the accumulation of anthropogenic carbon (C_{ant}) from the preindustrial period to 2002, and quantified the component of these changes caused by carbonate system nonlinearities. For each OA metric, the dataset includes year 2002 values and quasi-preindustrial values, which were estimated by subtracting C_{ant} from the year 2002 carbonate chemistry information and recomputing each OA metric without considering any warming, circulation, or biological changes that may have occurred since the preindustrial era. Data from the upper 2000 m of the GLODAPv2 Climatology (No. 46, Lauvset et al., 2016) and from the preformed properties product of Carter et al. (2021) were used to make these estimates on the $1° \times 1°$ GLODAPv2 Climatology grid for 26 depth levels from the surface to 2000 m. The provided uncertainties were estimated using a 1000-iteration Monte Carlo simulation. Calculation details are described in Fassbender et al. (2023). Year 2002 Ω_{arag} and pH values, and their uncertainties, are reproduced from the GLODAPv2 Climatology and are provided in this dataset for user convenience with the permission of the original data producer. This data product is available at https://www.ncei.noaa.gov/data/oceans/ncei/ocads/metadata/0290073.html (last access: 7 January 2026) (Fassbender, 2024).

52. Ocean Interior Acidification Over the Industrial Era: building on the total anthropogenic carbon estimates for 1994 from Sabine et al. (2005) and the decadal

changes between 1994 and 2014 reconstructed by Müller et al. (2023a), Müller and Gruber (2024a) quantified ocean interior acidification over the industrial era. To convert the increasing anthropogenic carbon concentrations into acidification estimates, their approach relied on time-invariant climatologies of ocean interior DIC, TA, temperature, salinity, and other relevant variables to determine the background state of the marine carbonate system. Hence, their estimates resolve exclusively the acidification driven by the anthropogenic carbon accumulation. In contrast to direct observations of acidification variables, such as those collected at time-series stations, this approach does not account for changes in the natural carbon cycle or the displacement of water masses. The approach by Müller and Gruber (2024a) is conceptually similar to that of Fassbender et al. (2023), but provides temporally resolved estimates, enabling the tracking of both the spatial distribution and temporal evolution of ocean interior acidification. The data product is available at https://www.ncei.noaa.gov/data/oceans/ncei/ocads/metadata/0298993.html (last access: 7 January 2026) (Müller and Gruber, 2024b).

53. Decadal changes of anthropogenic CO_2:

    a. Anthropogenic CO_2 from 1994 to 2007: Gruber et al. (2019a) estimated the decadal time-scale changes in the oceanic content of anthropogenic CO_2 (ΔC_{ant}) between 1994 to 2007. The results were derived from the GLODAPv2.2016 product (Olsen et al., 2016), utilizing the eMLR(C^*) methodology pioneered by Clement and Gruber (2018). The product is combined with the estimated amount of C_{ant} for 1994 derived by Sabine et al. (2004) from GLODAPv1 to infer C_{ant} for 2007. All estimates are geospatially distributed on a horizontal grid with a resolution of $1° \times 1°$. Two primary files are available: one providing the complete three-dimensional distribution of ΔC_{ant}, and the other containing vertically integrated values, i.e., the column inventories. This data product is available at https://www.ncei.noaa.gov/data/oceans/ncei/ocads/metadata/0186034.html (last access: 7 January 2026) (Gruber et al., 2019b).

    b. Decadal Trends in Anthropogenic CO_2 from 1994 to 2014: Müller et al. (2023a) extended the analysis by Gruber et al. (2019a) to reconstruct decadal trends in the oceanic storage of ΔC_{ant} in the global ocean interior from mid-year 1994 to mid-year 2004, and further to mid-year 2014. They applied the extended multiple linear regression (eMLR) method (Clement and Gruber, 2018) to ship-borne observations of DIC and other biogeochemical variables from GLODAPv2.2021 (Lauvset et al., 2021). All estimates are provided on a $1° \times 1°$ horizontal grid. Two principal data files are provided: one featuring the comprehensive three-dimensional distribution of ΔC_{ant} for the two time periods, and the other presenting the vertically integrated quantities, i.e., the column inventories. The data product is available at https://www.ncei.noaa.gov/data/oceans/ncei/ocads/metadata/0279447.html (last access: 7 January 2026) (Müller et al., 2023b).

54. Tracer-based rapid anthropogenic carbon estimation from 1750 to 2500: Carter et al. (2025) developed a method for estimating C_{ant} based on a machine learning translation of ocean circulation information inferred from transient tracer distributions. They applied it to the gridded GLODAPv2 climatology to obtain estimates of the past and projected C_{ant} distribution between 1750 and 2500. Projections are made using a range of simple assumptions and shared socioeconomic pathway projections. Estimates are provided on $1° \times 1°$ spatial grids at 33 standard depth levels in micromoles C_{ant} per kg of seawater. This data product is available at https://doi.org/10.5281/zenodo.15003059 (Carter, 2025).

55. Preformed TA and other biogeochemical properties: Carter et al. (2020) estimated preformed seawater TA, nitrate, silicate, phosphate, and oxygen using empirical seawater property estimation routines (Carter et al., 2017) with ocean circulation pathway information from ocean circulation transport matrices (John et al., 2020). Preformed properties are estimated property contents that seawater had when it last left contact with the atmosphere, and are used as an aid in interpretation of measured ocean property distributions. This data product is available at https://doi.org/10.5281/zenodo.3745002 (BRCScienceProducts, 2020).

56. Monthly Interior Ocean pH Climatology: Zhong et al. (2025) developed a monthly $1° \times 1°$ gridded global seawater pH (total scale) climatology from 1992 to 2020 at in situ temperature, derived using a machine learning algorithm trained on pH observations from GLODAPv2 (Lauvset et al., 2024). The product spans from 1992 to 2020 and covers depths from the surface to 2000 m across 41 vertical levels. Its development involved a three-step machine-learning approach: (1) regional division using a self-organizing map neural network, (2) predictor selection via stepwise regression, which iteratively adds or removes variables based on their impact on reconstruction error, and (3) nonlinear regression using feedforward neural networks (FFNNs). The developed data product is available at https://doi.org/10.12157/IOCAS.20230720.001 (Zhong et al., 2023).

57. CODAP-NA Climatology: Jiang et al. (2024) developed a coastal OA indicators climatology on a $1° \times 1°$ grid, covering North American ocean margins from the surface to 500 m at 14 standardized depth levels. This product includes 10 key oceanographic variables: fCO_2, pH, $[H^+]_{total}$, free hydrogen ion content ($[H^+]_{free}$), carbonate ion content ($[CO_3^{2-}]$), Ω_{arag}, Ω_{calc}, DIC, TA, and Revelle Factor (RF), as well as temperature and salinity. The climatology was produced with the WOA gridding technologies of the NOAA National Centers for Environmental Information (NCEI), based on the recently released Coastal Ocean Data Analysis Product in North America (CODAP-NA) (Jiang et al., 2021), along with GLODAPv2.2022 (Lauvset et al., 2022). The relevant variables were adjusted to the year of 2010 before the gridding. The first-guess fields for this analysis were calculated using ESPERs (Carter et al., 2021), based on the WOA (Version 2018) climatologies for salinity (Zweng et al., 2019), temperature (Locarnini et al., 2019) and DO (Garcia et al., 2018b). The data product is available in NetCDF at https://www.ncei.noaa.gov/data/oceans/ncei/ocads/metadata/0270962.html (last access: 7 January 2026) (Jiang et al., 2022b). Additionally, maps of these indicators are available in jpeg at https://www.ncei.noaa.gov/access/ocean-carbon-acidification-data-system/synthesis/nacoastal.html (last access: 7 January 2026) (Jiang et al., 2022b).

3.1.5 Multi-product analyses

This section includes data products that have been generated by community synthesis efforts designed to inform the GCB (Table 5).

58. SeaFlux: harmonization of air–sea CO_2 fluxes from surface pCO_2 data products using a standardized approach (Gregor and Fay, 2021). This resource provides an ensemble of six pCO_2 products with air–sea CO_2 fluxes computed consistently. The six included products are: CMEMS-LSCEv1, CSIR-ML6, JENA-MLS, JMA-MLR, MPI-SOMFFN, and NIES-FNN. First, missing areas of pCO_2 estimates (mostly high-latitude and marginal seas) are filled using a linear-regression approach, thus addressing differences in spatial coverage between the mapping products. Further, it also accounts for methodological inconsistencies in flux calculations. Fluxes are calculated using three wind products (CCMPv2, ERA5, and JRA55) along with the application of a scaled gas exchange coefficient for each of the wind products. Through these steps, SeaFlux presents an ensemble product of interpolated global surface ocean pCO_2 and air–sea carbon flux estimates for the years 1990–2019. For more details, refer to Fay et al. (2021).

59. RECCAP2: in the context of the second iteration of the project REgional Carbon Cycle Assessment and Processes (RECCAP2), the ocean carbon community compiled, quality-controlled, and harmonized (in the sense of providing output on the same regular grid at the same spatial and temporal resolution) 12 GOBMs simulations, 11 pCO_2 products, one ocean interior DIC product, and three data assimilation models to constrain the ocean carbon sink between 1985 and 2018. The RECCAP2 synthesis effort stands as a distinct but complementary resource to the GCB project (Friedlingstein et al., 2025), which primarily focuses on anthropogenically perturbed surface CO_2 fluxes from a global budgeting perspective. The individual chapters of RECCAP2 were published in this special issue of *Global Biogeochemical Cycles*: https://agupubs.onlinelibrary.wiley.com/doi/toc/10.1002/(ISSN)2169-8961.RECCAP2 (last access: 7 January 2026). The data products of this assessment are available on a $1° \times 1°$ horizontal grid, with monthly resolution for surface ocean variables such as air–sea CO_2 fluxes, and annual resolution for interior ocean variables, such as DIC content. The data compilation, which is described in detail in DeVries et al. (2023) and evaluated in Terhaar et al. (2024b), is available at https://doi.org/10.5281/zenodo.7990823 (Müller, 2023).

60. Global Carbon Budget: the GCB collects annually updated estimates of the ocean carbon sink from currently nine fCO_2-products and ten GOBMs for the period 1959 to the past calendar year (https://globalcarbonbudget.org/gcb-2025, last access: 7 January 2026, Friedlingstein et al., 2025). In contrast to Earth System Models (ESMs), the GOBMs are here forced with atmospheric reanalysis that ingested atmosphere and ocean observations and are thus thought to be closer to the observed climate. Gridded fields are provided on a $1° \times 1°$ horizontal grid and monthly resolution. In addition, globally and regionally integrated air–sea CO_2 fluxes from the native model grids are provided. Globally integrated time-series are adjusted for full ocean coverage and model bias and drift and are available for each individual fCO_2-product and GOBM (https://globalcarbonbudget.org/download/1442/?tmstv=1731323337, last access: 7 January 2026). The model data goes well beyond surface fluxes and includes data to analyze drivers of carbon fluxes, including several 3D variables. The model data request has been updated since RECCAP2 and also provides, for example, monthly interior ocean data of DIC, TA, nutrients and DO. The GOBM data request was also updated to have all variables available that are needed to serve as a testbed for fCO_2-products (e.g., sea surface height). Gridded

Table 4. Gridded and derived ocean carbonate chemistry data synthesis products in the subsurface ocean.

No.	Name	Open ocean or coastal ocean	Resolution	Temporal resolution	Methodology	Highlights	Reference
46	GLODAPv2 Climatology	Open ocean	1° × 1°	Referenced to 2002	Data Interpolating Variational Analysis (DIVA)	Ocean interior climatology for multiple variables from the surface to the bottom of the ocean (referenced to 2002)	Lauvset et al. (2016)
47	Aragonite Saturation State Climatology	Open ocean	1° × 1°	Referenced to 2000	Data Interpolating Variational Analysis (DIVA)	Ocean interior climatology for Ω_{arag} from the surface to 4000 m (referenced to 2000)	Jiang et al. (2015)
48(a)	MOBO-DIC (Version 2020)	Open ocean	1° × 1°	Monthly climatology referenced to January 2011	Machine learning	Seasonal variability of DIC in the interior ocean from the surface to 2000 m	Keppler et al. (2020a)
48(b)	MOBO-DIC (Version 2023)	Open ocean	1° × 1°	Monthly from January 2004 to December 2019	Machine learning	Temporal trends and interannual variability of DIC in the interior ocean from the surface to 1500 m	Keppler et al. (2023a, b)
49	Monthly Interior Ocean TA Climatology	Open ocean	1° × 1°	Monthly climatology	Machine learning	Ocean interior climatology for TA from the surface to the bottom	Broullón et al. (2019, 2020b)
50	Monthly Interior Ocean DIC Climatology	Open ocean	1° × 1°	Monthly from 1957 to 2018	Machine learning	Ocean interior climatology for DIC from the surface to the bottom (referenced to 1995)	Broullón et al. (2020a, c)

Table 4. Continued.

No.	Name	Open ocean or coastal ocean	Resolution	Temporal resolution	Methodology	Highlights	Reference
51	Acidification Metrics in the Ocean Interior	Open ocean	1° × 1°	2002 and preindustrial	Reproduced from GLODAPv2 Climatology (Lauvset et al., 2016) and the preformed properties of Carter et al. (2021)	Metrics of acidification in the ocean interior (to 2000 m) and the component of those changes caused by carbonate system nonlinearities	Fassbender et al. (2023)
52	Ocean Interior Acidification over the Industrial Era	Open ocean	1° × 1°	1800,1994, 2004, 2014	Conversion of anthropogenic carbon accumulation into acidification rates	Temporal trends in the progression of acidification in the interior ocean are resolved	Müller and Gruber (2024a)
53(a)	Anthropogenic CO_2 from 1994 to 2007	Open ocean	1° × 1°	From 1994 to 2007	eMLR(C^*) extended Multiple Linear Regression applied to the tracer C^*	The oceanic sink for anthropogenic CO_2 over the period 1994 to 2007	Gruber et al. (2019a)
53(b)	Decadal Trends in Anthropogenic CO_2 from 1994 to 2014	Open ocean	1° × 1°	Decadal from 1994 to 2014	eMLR(C^*) extended Multiple Linear Regression applied to the tracer C^*	Temporal trends in the accumulation of anthropogenic CO_2 in the interior ocean are resolved	Müller et al. (2023a)
54	Anthropogenic carbon from 1750 to 2500 (TRACE)	Open ocean	1° × 1°	Referenced to 20 years ranging from ∼ 1750 to 2500	Estimated from atmospheric transients and ocean tracer distributions	Estimates over time based on assumptions of steady state ocean circulation and CO_2 exchange	Carter et al. (2025)
55	Preformed TA and other bio-geochemical properties	Open ocean	1° × 1°	Not referenced in time	Empirical algorithms with inversions to find source outcrops	Estimates of the properties of seawater at the time of last contact with the atmosphere	Carter et al. (2021)

Table 4. Continued.

No.	Name	Open ocean or coastal ocean	Resolution	Temporal resolution	Methodology	Highlights	Reference
56	Monthly Interior Ocean pH Climatology	Open ocean	1° × 1°	Monthly from January 1992 to December 2020	Machine learning	Temporal variability of pH in the interior ocean from the surface to 2000 m over 3 decades	Zhong et al. (2025)
57	CODAP-NA Climatology	Coastal ocean	1° × 1°	Referenced to 2010	Objective analysis approach of the WOA	The first discrete bottle-based climatology in the North American ocean margins	Jiang et al. (2024)

surface data of sea surface fugacity and air–sea CO_2 flux of all fCO_2-products and GOBMs as used in the latest release of GCB (Version 2024) are published on Zenodo (https://doi.org/10.5281/zenodo.14639761, Hauck et al., 2025). All other GOBM output is available via https://globalcarbonbudgetdata.org/closed-access-requests.html (last access: 7 January 2026).

3.1.6 Model-based and hybrid products and analyses

Model-based projections of biogeochemical variables are often available from global and regional models, such as those in the Seventh Coupled Model Intercomparison Project (CMIP7) (Dunne et al., 2025; Durack et al., 2025). This section further includes hybrid data products, which adjust model estimates towards observation-based constraints (Table 6).

61. Decadal Trends in the Ocean Carbon Sink: The DeVries et al. (2019) analysis examines decadal trends in global and regional air–sea CO_2 fluxes from a variety of ocean biogeochemical models that contributed to the GCB (see No. 60). Three sets of model simulations were performed. Simulation A uses variable climate forcing (e.g., variable wind stress, heat and freshwater fluxes) and observed atmospheric CO_2 forcing, simulation B uses constant (repeated) climate forcing and observed atmospheric CO_2, and simulation C uses both constant climate forcing and constant atmospheric CO_2 concentrations. With these simulations, the authors partitioned decadal trends in ocean CO_2 uptake into those driven by climate variability and those driven by atmospheric CO_2. They found that climate variability drove a weakening trend of the ocean carbon sink during the 1990s, and a strengthening trend during the first decade of the 2000s. The magnitude of these trends agreed with those of an OCIM that was trained to replicate tracer data from the 1990s and 2000s (DeVries et al., 2017), indicating that the decadal trends may be driven by variability in ocean circulation. The data from this analysis are accessible at https://doi.org/10.6084/m9.figshare.8091161.v1 (DeVries, 2019).

62. ECCO-Darwin: Carroll et al. (2022) used the Estimating the Circulation and Climate of the Ocean-Darwin (ECCO-Darwin) global-ocean biogeochemistry state estimate to generate a data-constrained DIC budget and investigate how spatiotemporal variability in advection and mixing, air–sea CO_2 flux, and the biological pump have modulated the ocean sink for 1995–2018. ECCO-Darwin assimilates ocean circulation and physical tracers, including temperature, salinity, and sea ice, derived from the Estimating the Circulation and Climate of the Ocean (ECCO) LLC270 global-ocean and sea-ice data synthesis (Zhang et al., 2018). Additionally, it assimilates biogeochemical observations encompassing the cycling of carbon, nitrogen, phosphorus (PO_4), iron (Fe), silica (SiO_2), DO, and TA. This inclusive approach enhances the model's fidelity by aligning it with a diverse array of observations. All ECCO-Darwin model output is available on the ECCO Data Por-

Table 5. Ocean carbonate chemistry data product synthesis and harmonizations.

No.	Name	Open ocean or coastal ocean	Surface or water column	Spatial resolution	Temporal resolution	Methodology	Highlights	Reference
58	SeaFlux	Open ocean + Coastal ocean	Surface only	1° × 1°	Monthly from 1990 to 2022	Consistent flux calculations for 6 pCO_2 products to produce an ensemble estimate	Careful consideration of flux calculation provides a resource and code to the community for independent flux calculations	Gregor and Fay (2021)
59	RECCAP2	Open ocean + Coastal ocean	Surface + Water column	1° × 1° (open) 0.25° × 0.25° (coastal)	Monthly from 1985 to 2018	Harmonized compilation of surface fCO_2 products, model simulations and ocean interior products	Quality-controlled data compilation with a harmonized horizontal grid and temporal resolution	Müller (2023), DeVries et al. (2023), Resplandy et al. (2024)
60	Global Carbon Budget	Open ocean + Coastal ocean	Surface + Water column	1° × 1°	Monthly from 1959 to 2023	Harmonized compilation of surface fCO_2 products, and GOBM simulations	Annually updated and quality-controlled datasets. Availability of monthly 4D ocean model output.	Friedlingstein et al. (2025)

tal: https://data.nas.nasa.gov/ecco/ (last access: 7 January 2026). The model code and platform-independent instructions for running ECCO-Darwin simulations can be found at https://github.com/MITgcm-contrib/ecco_darwin (last access: 7 January 2026).

63. Global Surface Ocean Acidification Indicators:

    a. Surface pH and Revelle Factor: Jiang et al. (2019a) produced a high-resolution (1° × 1°) data product delineating a regionally varying view of global surface ocean pH, acidity, and Revelle Factor (RF) from 1770 to 2100 by amalgamating recent observational seawater CO_2 data from the SOCAT database (Version 6) (Bakker et al., 2016) and temporal trends at individual locations of the global surface ocean from an Earth System Model, i.e., GFDL-ESM2M (Dunne et al., 2013). The calculations were conducted under historical atmospheric CO_2 levels (pre-2005) and four Representative Concentrations Pathways (post-2005) corresponding to the Intergovernmental Panel on Climate Change (IPCC)'s 5th Assessment Report, specifically RCP2.6, RCP4.5, RCP6.0, and RCP8.5. Surface ocean TA was calculated from SSS and SST using the updated locally interpolated alkalinity regression (LIARv2) method (Carter et al., 2017). Surface ocean pH, acidity, and RF were then calculated using a MATLAB version of the CO2SYS program (Orr et al., 2015). The data product is available at https://www.ncei.noaa.gov/data/oceans/ncei/ocads/metadata/0206289.html (last access: 7 January 2026) (Jiang et al., 2019b).

    b. Surface OA Indicators: Jiang et al. (2023b) developed a comprehensive model-data fusion product that delineates the trajectory of 10 OA indicators: fCO_2, pH, $[H^+]_{total}$, $[H^+]_{free}$, $[CO_3^{2-}]$, Ω_{arag}, Ω_{calc}, DIC, TA, and RF, as well as temperature and salinity at all locations of the global surface ocean from 1750 to 2100. This product marks a significant improvement in OA forecasting by refining

temporal trends with data from 14 ESMs within CMIP6, and by applying bias and drift corrections using three updated observational ocean carbonate system data products: SOCAT (Version 2022) (Bakker et al., 2016), GLODAPv2.2022 (Lauvset et al., 2022), and CODAP-NA (Jiang et al., 2021). This dataset offers 10-year averages on a $1° \times 1°$ global surface ocean grid, capturing trends from preindustrial times (1750) through historical conditions (1850–2010), and projects future conditions to 2100 across five Shared Socioeconomic Pathways: SSP1-1.9, SSP1-2.6, SSP2-4.5, SSP3-7.0, and SSP5-8.5. The gridded data product is available in NetCDF at https://www.ncei.noaa.gov/data/oceans/ncei/ocads/metadata/0259391.html (last access: 7 January 2026) (Jiang et al., 2022c), and global maps of these indicators are available in JPEG at https://www.ncei.noaa.gov/access/ocean-carbon-acidification-data-system/synthesis/surface-oa-indicators.html (last access: 7 January 2026) (Jiang et al., 2022c).

64. Simulated and Constrained Global and Southern Ocean Carbon Sink: these two datasets include spatially-integrated and annually averaged values for the ocean carbon sink from 1850 to 2100 for different scenarios over the 21st century for the global ocean (Terhaar et al., 2022a, b) and the Southern Ocean (Terhaar et al., 2021b, c). All results are based on CMIP5 and CMIP6 models. For the global ocean carbon sink, values are available for SSP1-2.6, SSP2-4.5, and SSP5-8.5. For the Southern Ocean, values are also available for SSP1-2.6, SSP2-4.5, and SSP5-8.5 and additionally for RCP2.6, RCP4.5, and RCP8.5. In addition, to the raw simulated values, constrained estimates of the annually averaged ocean carbon sink estimates are available. These constrained estimates adjusted the simulated carbon sink estimates for biases on the ocean's circulation and surface carbonate chemistry (see Terhaar et al., 2021b, 2022a for details). It is recommended to use the constrained estimates. The datasets are available at https://doi.org/10.17882/103934 (Terhaar et al., 2022b) and https://doi.org/10.17882/103938 (Terhaar et al., 2021c).

65. Composite model-based estimate of the ocean carbon sink from 1959 to 2022: this data product, developed by Terhaar (2025), presents an estimate of the global ocean carbon sink by combining forced hindcast simulations and simulations made by coupled ESMs. Hindcast models manage to adequately simulate the short-term variability of the ocean, but struggle to simulate the long-term climate change trend (Huguenin et al., 2022; Takano et al., 2023; Hollitzer et al., 2024). ESMs cannot simulate the observed short-term variability by definition, but accurately simulate long-term trends (Takano et al., 2023; Hollitzer et al., 2024). The composite model-based estimate combines the simulated short-term variability from hindcast simulations and the long-term trend from ESMs. The output is supplied with the associated study (https://doi.org/10.5194/bg-22-1631-2025) (Terhaar, 2025).

66. pCIBR_Clim and pCIBR_Int: a machine learning (ML) model is employed to correct biases in surface pCO_2 simulations generated by the INCOIS-BIO-ROMS model (pCO_2model) over the period 1980–2019. The ML model is trained using the differences between observed (pCO_2obs) and modeled pCO_2 to estimate the spatio-temporal deviations (pCO_2obs-pCO_2model). These interannually and climatologically varying deviations are then added back to the original model output, resulting in two improved data products: pCIBR_Int and pCIBR_Clim (Ghoshal et al., 2025a). Evaluation against independent datasets, including moored observations (BOBOA), the gridded SOCAT product, and other ML-based pCO_2 products (such as CMEMS-LSCEv2 and OceanSODA), demonstrates a significant improvement of approximately $40\,\% \pm 3.31\,\%$ in RMSE compared to the original model. This high-resolution ($0.083° \times 0.083°$), long-term monthly pCO_2 data product is available from the INCOIS Portal (https://las.incois.gov.in, last access; 7 January 2026) and from OCADS: https://www.ncei.noaa.gov/data/oceans/ncei/ocads/metadata/0307788.html (last access: 7 January 2026) (Ghoshal et al., 2025b).

67. INCOIS-BIO-ROMS Simulated Surface pCO_2 and pH for the Indian Ocean: this data product presents a comprehensive assessment of OA trends across the Indian Ocean and its sub-regions from 1980 to 2019, leveraging outputs from a regional, high-resolution coupled ocean-ecosystem model (INCOIS-BIO-ROMS), an offline biogeochemical (BGC) model, and two machine learning-based products (Chakraborty et al., 2024). INCOIS-BIO-ROMS, configured at 1/12° resolution for the Indian Ocean, was developed in accordance with the "RECCAP-2: Ocean Modeling Protocol" for regional oceans. The INCOIS-BIO-ROMS simulated surface pCO_2 and pH data product is available from the INCOIS Portal (https://las.incois.gov.in, last access: 7 January 2026) and from OCADS: https://www.ncei.noaa.gov/data/oceans/ncei/ocads/metadata/0307663.html (last access: 7 January 2026) (Chakraborty et al., 2025).

68. Ocean Circulation Inverse Model (OCIM): DeVries (2022b) utilized a two-step procedure to estimate anthropogenic carbon in the ocean interior using an ocean inverse model. First, a steady-state ocean circulation inverse model (OCIM) was fit to observations of physical circulation tracers such as temperature,

salinity, radiocarbon, and CFCs (Holzer et al., 2021). Then, the circulation model was coupled to an abiotic carbon cycle model, spun up to equilibrium in 1780 and then forced by observed atmospheric CO_2 time history from 1781–2020. Simulations were run with and without historical changes in sea surface temperatures. The difference between preindustrial and transient simulations represents the anthropogenic carbon accumulation in the ocean. Results are provided on a regular grid with a nominal resolution of 2° in the horizontal with 48 depth levels. The output is available at https://doi.org/10.6084/m9.figshare.19341974.v2 (DeVries, 2022c).

3.2 Overlaps and history

Many of the data products described above exhibit significant overlap in various forms. In some cases, one or more products are used to generate new ones, while in others, the same collection-level cruise datasets underpin multiple products. There are a few foundational data products, such as GLODAPv2 and SOCAT, which are widely utilized to develop other data products, including their respective gridded products (e.g., Lauvset et al., 2016). For instance, SOCAT forms the backbone of nearly all derived products listed in Table 3, serving as a key resource for product development or validation. Some derived products, such as the JMA-MLR (No. 26) and OceanSODA-ETHZv1 (No. 27a), incorporate both SOCAT and GLODAPv2 during development. Having overlaps in data and derived products has provided opportunities for data quality-control and intercomparison of different approaches to gap-filling that would not have been available otherwise. Additional overlaps between these data products are provided below:

3.2.1 SOCAT and LDEO

The quality-control and synthesis of global surface ocean CO_2 data began in 1997 with Dr. Taro Takahashi and his colleagues at LDEO in Palisades, New York. His pioneering work led to the creation of the LDEO Surface pCO_2 Database (No. 2), which focused on high-quality data collected by his team and from various US and international expeditions. Over time, this data set expanded to include contributions from other laboratories, resulting in a highly influential collection of pCO_2 data and several seminal papers on global surface ocean CO_2 variations and air–sea CO_2 fluxes (Takahashi et al., 1997, 2002, 2009). The last update to the LDEO database was in 2019, following Dr. Takahashi's passing, and no further updates are anticipated (Takahashi et al., 2017).

The SOCAT project was developed to address questions around the current and future drivers of CO_2 fluxes raised at the 2007 Surface Ocean CO_2 Variability and Vulnerability (SOCOVV) workshop in Paris, France (Metzl et al., 2007). SOCAT was developed to synthesize all of the publicly available, discoverable, and citable surface CO_2 data. Following the GLODAP model, there was a strong emphasis on an open and transparent secondary quality-control process to ensure the highest data quality. The first data release came in 2011 (Pfeil et al., 2013; Sabine et al., 2013) and included contributions from numerous laboratories, as well as the freely available CO_2 data from the LDEO database. As of 2024, SOCAT contains ∼ 40 million data points, with new observations added annually. All data are rigorously standardized, and recalculated as fCO_2. SOCAT represents an ongoing global community effort, with participants from all continents contributing data and participating in the quality-control process. Initially new versions were released every other year, however automation allowed annual public releases since version 4.

3.2.2 GLODAPv2 and quality edited hydrographic data

Starting in the late 1980s, the WOCE, Joint Global Ocean Flux Study (JGOFS), and the NOAA Ocean-Atmosphere Exchange Study (OACES) collaborated in a multinational effort to conduct a decadal global hydrographic survey of unparalleled quality and quantity. At the conclusion of the survey at the end of the 1990s, GLODAP combined and publicly released all of the available hydrographic data with high-quality ocean carbonate system measurements as a single database (Key et al., 2004; Sabine et al., 2005). The data were subjected to extensive secondary quality-control checks where cruise tracks intersected one another, making it the most comprehensive and highest-quality ocean inorganic carbon dataset ever generated. A gridded, full-depth global ocean carbon climatology was also created and released as part of the project. These data and associated climatology have been extensively used to evaluate carbon distributions as well as the accumulation of anthropogenic CO_2 in the ocean. Other regional datasets, like the CARINA data synthesis project, an international collaborative effort of the European Union CARBOOCEAN program (Key et al., 2010; Tanhua et al., 2010), and PACIFICA, an international synthesis of Pacific Ocean data organized through the North Pacific Marine Science Organization (PICES) (Ishii et al., 2011b; Suzuki et al., 2013), were combined with GLODAP after its initial release. The GLODAP database is continuing to grow with new data collected as part of the Global Ocean Ship-Based Hydrographic Investigations Program (GO-SHIP).

For discrete bottle measurements spanning the entire oceanic water column, GLODAPv2 (No. 3) and the Quality Edited Hydrographic Data (No. 4) are the primary data products. Most cruise datasets contributing to these two data products overlap, but the key difference lies in their approach to data adjustment. The former applies crossover and inversion analysis for bias correction, while the latter presents the data without such adjustments. GLODAPv2 achieves consistency by applying adjustments based on deep-ocean offsets,

Table 6. Model based data synthesis products and analyses for ocean carbonate chemistry.

No.	Name	Open ocean or coastal ocean	Surface or water column	Spatial resolution	Temporal resolution	Highlights	Reference
61	Decadal Trends in the Ocean Carbon Sink	Open ocean	Surface	Variable	Decadal	Climate variability drove weakened ocean CO_2 uptake in the 1990s, and strengthened CO_2 uptake in the 2000s	DeVries et al. (2019)
62	ECCO-Darwin	Open ocean + Coastal ocean	Water column	1/3° × 1/3°	3-hourly, daily, and month fields available	Model-data synthesis product based on the Estimating the Circulation and Climate of the Ocean (ECCO) ocean state estimate. Fully-closed, physically-consistent 3D biogeochemical budgets	Carroll et al. (2020, 2022, 2024)
63(a)	Surface pH and Revelle Factor	Open ocean	Surface	1° × 1°	Decadal from 1770 to 2100	A model-observation fusion product for pH, acidity and Revelle Factor, leveraging GFDL-ESM2M and SOCATv6	Jiang et al. (2019a)
63(b)	Surface OA Indicators	Open ocean	Surface	1° × 1°	Decadal from 1750 to 2100	A model-observation fusion product for all major OA indicators, leveraging a consortium of 14 ESMs and 3 observational data products	Jiang et al. (2023b)

Table 6. Continued.

No.	Name	Open ocean or coastal ocean	Surface or water column	Spatial resolution	Temporal resolution	Highlights	Reference
64	Simulated and Constrained Global and Southern Ocean Carbon Sink	Open ocean	Surface	Spatially integrated	Annual from 1850 to 2100	A constrained estimate of the ocean carbon sink based on the simulated carbon sink from CMIP5 and CMIP6 models and constrained with observations of the ocean physics and carbonate chemistry	Terhaar et al. (2021b, 2022a)
65	Composite model-based estimate of the ocean carbon sink from 1959 to 2022	Open ocean	Surface	Spatially integrated	Annual from 1959 to 2022	A model-based estimate of the ocean carbon sink combining the respective strengths of hindcast simulations and simulations by coupled ESMs	Terhaar (2025)
66	pCIBR_Clim and pCIBR_Int	Open ocean + Coastal ocean	Surface	$0.083° \times 0.083°$	Monthly	This data product has been developed by employing an innovative hybrid approach, where a machine learning algorithm was used to correct high-resolution (1/12°) coupled ocean-ecosystem model outputs using observational data from SOCAT (1984–2019) and SAS (1991–2019) for the Indian Ocean	Ghoshal et al. (2025a)

Table 6. Continued.

No.	Name	Open ocean or coastal ocean	Surface or water column	Spatial resolution	Temporal resolution	Highlights	Reference
67	INCOIS-BIO-ROMS Simulated Surface pCO_2 and pH for the Indian Ocean	Open ocean + Coastal ocean	Surface	$0.083° \times 0.083°$	Monthly from 1980 to 2019	INCOIS-BIO-ROMS was developed in accordance with the "RECCAP-2: Ocean Modeling Protocol" for regional oceans. By integrating model simulations with available field observations and reconstructed data products, this study advances the current understanding of OA in the Indian Ocean	Chakraborty et al. (2024)
68	Ocean Circulation Inverse Model (OCIM)	Open ocean	Surface and Water column	$2° \times 2°$ horizontal, 48 vertical layers	Annual from 1780 to 2020	Data-constrained estimate of anthropogenic CO_2 accumulation in the ocean from inverting physical ocean circulation tracers	DeVries (2022b)

whereas Quality Edited Hydrographic Data provides the data in its original form. While there is substantial overlap between the two, data from a specific expedition might differ slightly due to GLODAPv2's secondary quality-control adjustments. Both GLODAPv2 and Quality Edited Hydrographic Data offer global coverage, but several independent regional data products are also available, such as SNAPO-CO_2 (No. 6), CODAP-NA (No. 7), AZMP Carbon (No. 8), MOCHA (No. 9), and ARIOS (No. 10). Data from these regional products often partially or fully overlap with GLODAPv2 and Quality Edited Hydrographic Data.

(a) GLODAPv2 and CODAP-NA

All cruise datasets contributing to CODAP-NA were forwarded to the GLODAPv2 quality-control team in 2022. Data from select cruises with deep-water sampling (> 1500 m), enabling crossover analysis, were subsequently incorporated into the GLODAPv2.2022 data product update (Lauvset et al., 2022).

(b) GLODAPv2 and SPOTS

Some time-series data are included in both GLODAPv2 and the Synthesis Product for Ocean Time-Series (SPOTS). Usu-

ally, data present in both products were not measured on dedicated time-series cruises but rather were collected as part of a larger cruise passing by a time-series location. As the quality-control of SPOTS is restricted to assigning method flags, adjustments that are applied as a result of the QC of GLODAP are not present in SPOTS. Additional crossover analyses between SPOTS and GLODAP have revealed good consistency (Lange et al., 2024a).

3.2.3 RECCAP2 and GCB

RECCAP2 and GCB are not data products themselves, but analyses and syntheses of data-based and model-based products. Users should be aware that there is a large degree of overlap between the fCO_2 products and GOBMs that contributed to both RECCAP2 and GCB, and of the resulting datasets. However, the RECCAP2 and GCB analyses serve different purposes. GCB is updated annually to the latest complete calendar year and its main purpose is to present and estimate the magnitude (and uncertainty) of the ocean CO_2 sink and the role of CO_2 and climate drivers since 1959 with a focus on the last year, while RECCAP2 presents a deeper analysis of the magnitude, trends, and variability of the global and regional ocean CO_2 sink over the period 1985–2018.

3.2.4 Jiang et al. (2019a, 2023)

Both products contain the projection of surface ocean pH, $[H^+]_{total}$, and buffer capacity from 1750 to 2100. However, the former is based on one GFDL model ESM2M, while the latter is based on a consortium of 14 ESMs, and additional observational data. The latter also contains the projection of seven other OA variables, including carbonate ions, Ω_{arag}, Ω_{calc}, fCO_2, DIC, TA, and $[H^+]_{free}$.

4 Data availability

Access links for all data products mentioned in this paper are provided in their respective paragraphs. Additionally, access links for all products are available in Table 7.

5 Summary

The synthesis and gridded data products presented here reflect significant community-based efforts that have been made to advance understanding of the ocean's role in global carbon cycling. This synthesis provides an overview of key data compilations and gridded data products essential for coastal and global ocean carbonate chemistry research. It highlights the key features of each product, serving as a resource for researchers seeking the necessary data for their work. The list will be updated periodically to incorporate new data products. The most up-to-date list is available at https://oceanco2.github.io/co2-products/ (Gregor and Jiang, 2026). A submission interface is also available on the data product page. After submitting a new data product, please send a notification to noaa.ocads@noaa.gov to ensure the submission is reviewed and added to the webpage.

Author contributions. LQJ prepared the initial draft. LG designed and implemented the GitHub webpage and supporting scripts to present the most current list of products. AR prepared Fig. 1. All authors contributed to the writing of the manuscript. The first 23 authors are listed based on their contributions, while the remaining authors are listed alphabetically by their last names.

Competing interests. At least one of the (co-)authors is a member of the editorial board of *Earth System Science Data*. The peer-review process was guided by an independent editor, and the authors also have no other competing interests to declare.

Disclaimer. Publisher's note: Copernicus Publications remains neutral with regard to jurisdictional claims made in the text, published maps, institutional affiliations, or any other geographical representation in this paper. The authors bear the ultimate responsibility for providing appropriate place names. Views expressed in the text are those of the authors and do not necessarily reflect the views of the publisher.

Acknowledgements. We extend our gratitude to all scientists who collected and measured the original data and those who compiled and quality-controlled these data products. We thank Pierre Friedlingstein (University of Exeter, Exeter, UK), Bronte Tilbrook (CSIRO Oceans and Atmosphere and Australian Antarctic Program Partnership, University of Tasmania, Australia), and Dwight Gledhill (NOAA/OAR Ocean Acidification Program, United States) for their valuable insights and discussions, which helped shape the vision of this paper. Additionally, we thank Xinping Hu (University of Texas at Austin, United States), Tessa Hill (University of California, Davis, United States), and Patrick Duke (University of Victoria, Canada) for recommending numerous data products incorporated into this compilation. This is PMEL contribution 5728. This is INCOIS contribution no. 596.

Financial support. Funding for Li-Qing Jiang was from NOAA Ocean Acidification Program (https://ror.org/02bfn4816, last access: 7 January 2026) and NOAA grant NA24NESX432C0001 (Cooperative Institute for Satellite Earth System Studies – CISESS) at the Earth System Science Interdisciplinary Center, University of Maryland. Jens Daniel Müller acknowledges funding by Carbon to Sea through the Windward Fund and support from Google for OAEMIP. Maciej Telszewski acknowledge funding from the United States National Science Foundation (grant no. OCE-2513154) to the Scientific Committee on Oceanic Research (SCOR, United States) for the International Ocean Carbon Coordination Project (IOCCP) and from the United Nations Educational, Scientific and Cultural Organization (UNESCO) to the Institute of

Table 7. Access links for the compiled ocean carbonate chemistry data products. n/a is short for not applicable. Last access date for all URLs mentioned in this table: 7 January 2026.

No.	Name	Data access link	DOI	Reference
1	SOCAT	https://socat.info/	https://doi.org/10.25921/648f-fv35	Bakker et al. (2016, 2025)
2	LDEO Surface pCO_2 Database	https://www.ncei.noaa.gov/data/oceans/ncei/ocads/metadata/0160492.html	https://doi.org/10.3334/cdiac/otg.ndp088(v2015)	Takahashi et al. (2017)
3	GLODAPv2	https://glodap.info/	https://doi.org/10.25921/zyrq-ht66	Lauvset et al. (2023b, 2024)
4	Quality Edited Hydrographic Data	https://joa.ucsd.edu/	n/a	Swift and Osborne (2025)
5	WOD	https://www.ncei.noaa.gov/products/world-ocean-database	https://doi.org/10.25923/z885-h264	Mishonov et al. (2024)
6	SNAPO-CO_2	https://www.ncei.noaa.gov/data/oceans/ncei/ocads/metadata/0285681.html	https://doi.org/10.17882/95414	Metzl et al. (2023, 2024)
7	CODAP-NA	https://www.ncei.noaa.gov/data/oceans/ncei/ocads/metadata/0219960.html	https://doi.org/10.25921/531n-c230	Jiang et al. (2020, 2021)
8	AZMP Carbon	n/a	https://doi.org/10.20383/102.0673	Cyr et al. (2022)
9	MOCHA	https://www.ncei.noaa.gov/data/oceans/ncei/ocads/metadata/0277984.html	https://doi.org/10.25921/2vve-fh39	Kennedy et al. (2023)
10	ARIOS	https://digital.csic.es/handle/10261/205135	https://doi.org/10.20350/digitalCSIC/12498	Pérez et al. (2020)
11	Marine Inorganic Carbonate Chemistry in the Northern Gulf of Alaska	https://www.ncei.noaa.gov/data/oceans/ncei/ocads/metadata/0277034.html	https://doi.org/10.25921/x9sg-9b08	Monacci et al. (2023, 2024)
12	Coral Reef Carbonate Chemistry Off the Florida Keys	https://www.ncei.noaa.gov/access/metadata/landing-page/bin/iso?id=gov.noaa.nodc:NCRMP-CO3-Atlantic	https://doi.org/10.25921/vfz0-dg77	Manzello et al. (2018)
13	Salish Cruise Data Package and Multi-stressor Data Product	https://www.ncei.noaa.gov/access/ocean-carbon-acidification-data-system/oceans/SalishCruise_DataPackage.html, https://www.ncei.noaa.gov/access/ocean-carbon-acidification-data-system/oceans/SalishCruises_DataProduct.html	https://doi.org/10.25921/jgrz-v584, https://doi.org/10.25921/4y18-rw26	Alin et al. (2024a, b, 2025a, b, c)
14	Line P Marine Carbonate Chemistry Compilation	https://www.ncei.noaa.gov/data/oceans/ncei/ocads/metadata/0234342.html	https://doi.org/10.25921/zrw8-kn24	Franco et al. (2021a, b)

Table 7. Continued.

No.	Name	Data access link	DOI	Reference
15	Anthropogenic Carbon in the Arctic Ocean	https://www.seanoe.org/data/00927/103920/	https://doi.org/10.17882/103920	Terhaar et al. (2024a)
16	BATS	https://demo.bco-dmo.org/project/2124	https://doi.org/10.26008/1912/bco-dmo.894099.6, https://doi.org/10.26008/1912/bco-dmo.893182.6, https://doi.org/10.26008/1912/bco-dmo.926534.4, https://doi.org/10.26008/1912/bco-dmo.893521.6, https://doi.org/10.26008/1912/bco-dmo.917255.5, https://doi.org/10.26008/1912/bco-dmo.939210.9, https://doi.org/10.26008/1912/bco-dmo.3782.8, https://doi.org/10.26008/1912/bco-dmo.3918.10, https://doi.org/10.26008/1912/bco-dmo.881861.6	Bates et al. (2024a, b, c, d, e, 2025), Johnson et al. (2025a, b), Steinberg and Cope (2025)
17	HOT	https://www.bco-dmo.org/project/2101, https://doi.org/10.5281/zenodo.15060931	https://doi.org/10.26008/1912/bco-dmo.3773.3, https://doi.org/10.5281/zenodo.15060931	Winn et al. (1994, 1998), Dore et al. (2003, 2009, 2014, 2025), Knor et al. (2023, 2025, White et al. (2025)
18	ESTOC	n/a	https://doi.org/10.1594/PANGAEA.959856, https://doi.org/10.1594/PANGAEA.856590, https://doi.org/10.1594/PANGAEA.856615 , https://doi.org/10.1594/PANGAEA.856608, https://doi.org/10.1594/PANGAEA.856616, https://doi.org/10.1594/PANGAEA.856593, https://doi.org/10.1594/PANGAEA.856612, https://doi.org/10.1594/PANGAEA.856614, https://doi.org/10.1594/PANGAEA.856607, https://doi.org/10.1594/PANGAEA.956272	González-Dávila and Santana-Casiano (2023b), González-Dávila and Melchor (2016a, b, c, d, e, f, g, h), González-Dávila et al. (2023)
19	Point B Time-series	n/a	https://doi.org/10.1594/PANGAEA.727120	Gattuso et al. (2021b)
20	Ny-Ålesund Time-series	n/a	https://doi.org/10.1594/PANGAEA.957028	Gattuso et al. (2023b)

Table 7. Continued.

No.	Name	Data access link	DOI	Reference
21	SPOTS	https://www.bco-dmo.org/dataset/896862	https://doi.org/10.26008/1912/bco-dmo.896862.2	Lange et al. (2024a, b)
22	pCO_2 and pH Time-series from 40 Surface Buoys	https://www.ncei.noaa.gov/data/oceans/ncei/ocads/metadata/0173932.html	https://doi.org/10.7289/v5db8043	Sutton et al. (2018)
23	Takahashi delta fCO_2 and flux climatology	https://www.ncei.noaa.gov/data/oceans/ncei/ocads/metadata/0282251.html	https://doi.org/10.25921/295g-sn13	Fay et al. (2023)
24	MPI-ULB-SOM-FFN	https://www.ncei.noaa.gov/data/oceans/ncei/ocads/metadata/0209633.html	https://doi.org/10.25921/qb25-f418	Landschützer et al. (2020a, b)
25	VLIZ SOM-FFN	https://www.ncei.noaa.gov/data/oceans/ncei/ocads/metadata/0160558.html	https://doi.org/10.7289/v5z899n6	Landschützer et al. (2016), Jersild et al. (2017)
26	JMA-MLR	https://www.data.jma.go.jp/kaiyou/english/co2_flux/co2_flux_data_en.html	n/a	Iida et al. (2021)
27(a)	OceanSODA-ETHZv1	https://www.ncei.noaa.gov/data/oceans/ncei/ocads/metadata/0220059.html	https://doi.org/10.25921/m5wx-ja34	Gregor and Gruber (2020)
27(b)	OceanSODA-ETHZv2	https://doi.org/10.5281/zenodo.11206366	https://doi.org/10.5281/zenodo.11206366	Gregor et al. (2024b)
28	LDEO-HPD fCO_2	https://doi.org/10.5281/zenodo.4760205	https://doi.org/10.5281/zenodo.4760205	Gloege et al. (2021)
29	LDEO-HPD with Extended Temporal Coverage	https://doi.org/10.5281/zenodo.13891722	https://doi.org/10.5281/zenodo.13891722	Fay et al. (2024b)
30	LDEO fCO_2 – Residual Method	https://doi.org/10.5281/zenodo.13941548	https://doi.org/10.5281/zenodo.13941548	Bennington et al. (2024)
31(a)	CMEMS-LSCEv1	https://data.ipsl.fr/catalog/srv/eng/catalog.search#/metadata/a2f0891b-763a-49e9-af1b-78ed78b16982	https://doi.org/10.14768/a2f0891b-763a-49e9-af1b-78ed78b16982	Chau et al. (2022b)
31(b)	CMEMS-LSCEv2	https://data.marine.copernicus.eu/product/MULTIOBS_GLO_BIO_CARBON_SURFACE_MYNRT_015_008/services	https://doi.org/10.48670/moi-00047	Chau et al. (2024a, b, c)
32	CarboScope (Jena-MLS)	https://www.bgc-jena.mpg.de/CarboScope/?ID=oc	https://doi.org/10.17871/CarboScope-oc_v2024E (or analogously for previous and upcoming releases)	Rödenbeck (2024), Rödenbeck et al. (2022)
33	UOEx-Watson	https://www.ncei.noaa.gov/data/oceans/ncei/ocads/metadata/0301544.html	https://doi.org/10.25921/2dp5-xm29	Watson et al. (2025)

Table 7. Continued.

No.	Name	Data access link	DOI	Reference
34	NIES-ML3	https://db.cger.nies.go.jp/DL/10.17595/20220311.001.html.en	https://doi.org/10.17595/20220311.001	Zeng (2022), Zeng et al. (2022)
35	CSIR-ML6	https://www.ncei.noaa.gov/data/oceans/ncei/ocads/metadata/0206205.html	https://doi.org/10.25921/z682-mn47	Gregor et al. (2019b)
36	Stepwise-FFNN	https://msdc.qdio.ac.cn/data/metadata-special-detail?id=1955061943609876482	https://doi.org/10.12157/IOCAS.20250814.001	Zhong (2025), Zhong et al. (2022)
37	AOML-ET	https://www.ncei.noaa.gov/data/oceans/ncei/ocads/metadata/0298989.html	https://doi.org/10.25921/0s8y-q287	Wanninkhof et al. (2024, 2025)
38	ULB-SOM-FFN-coastalv2.1	https://www.ncei.noaa.gov/data/oceans/ncei/ocads/metadata/0279118.html	https://doi.org/10.25921/4sde-p068	Roobaert et al. (2023, 2024)
39	RFR-LME	https://www.ncei.noaa.gov/data/oceans/ncei/ocads/metadata/0287551.html	https://doi.org/10.25921/h8vw-e872	Sharp et al. (2024a, b)
40	ReCAD-NAACOM-pCO2	https://doi.org/10.5281/zenodo.11500974	https://doi.org/10.5281/zenodo.11500974	Wu et al. (2024, 2025)
41	Gridded Surface OA Indicators and Air–sea CO_2 Fluxes in the Northern Caribbean Sea	https://www.ncei.noaa.gov/data/oceans/ncei/ocads/metadata/0207749.html	https://doi.org/10.25921/2swk-9w56	Wanninkhof et al. (2019)
42	OA data in the Gulf of Mexico/Gulf of America and Wider Caribbean	https://www.ncei.noaa.gov/data/oceans/ncei/ocads/metadata/0245950.html	https://doi.org/10.25921/tt1c-dx53	van Hooidonk (2022)
43	pCO_2 Climatology of the Baltic Sea	n/a	https://doi.org/10.1594/PANGAEA.961119	Bittig et al. (2023)
44	INCOIS-ReML	https://www.ncei.noaa.gov/data/oceans/ncei/ocads/metadata/0307627.html	https://doi.org/10.25921/2sjr-pg16	Joshi et al. (2024, 2025a)
45	INCOIS_TA	https://www.ncei.noaa.gov/data/oceans/ncei/ocads/metadata/0307789.html	https://doi.org/10.25921/7as7-et15	Joshi et al. (2025b, c)
46	GLODAPv2 Climatology	https://www.ncei.noaa.gov/data/oceans/ncei/ocads/metadata/0286118.html	https://doi.org/10.3334/cdiac/otg.ndp093_glodapv2	Lauvset et al. (2016, 2023a)
47	Aragonite Saturation State Climatology	https://www.ncei.noaa.gov/data/oceans/ncei/ocads/metadata/0139360.html	https://doi.org/10.7289/v5q81b4p	Jiang and Feely (2015), Jiang et al. (2015)

Table 7. Continued.

No.	Name	Data access link	DOI	Reference
48(a)	MOBO-DIC (Version 2020)	https://www.ncei.noaa.gov/access/ocean-carbon-acidification-data-system/oceans/ndp_104/ndp104.html	https://doi.org/10.25921/yvzj-zx46	Keppler et al. (2020b)
48(b)	MOBO-DIC (Version 2023)	https://www.ncei.noaa.gov/data/oceans/ncei/ocads/metadata/0277099.html	https://doi.org/10.25921/z31n-3m26	Keppler et al. (2023a, b)
49	Monthly Interior Ocean TA Climatology	https://www.ncei.noaa.gov/data/oceans/ncei/ocads/metadata/0222470.html	https://doi.org/10.25921/5p69-y471	Broullon et al. (2019, 2020b)
50	Monthly Interior Ocean DIC Climatology	https://www.ncei.noaa.gov/data/oceans/ncei/ocads/metadata/0222469.html	https://doi.org/10.25921/ndgj-jp24	Broullón et al. (2020a, c)
51	Acidification Metrics in the Ocean Interior	https://www.ncei.noaa.gov/data/oceans/ncei/ocads/metadata/0290073.html	https://doi.org/10.25921/rdtr-9t74	Fassbender et al. (2023), Fassbender (2024)
52	Ocean Interior Acidification over the Industrial Era	https://www.ncei.noaa.gov/data/oceans/ncei/ocads/metadata/0298993.html	https://doi.org/10.25921/tefm-x802	Müller and Gruber (2024a, b)
53(a)	Anthropogenic CO_2 from 1994 to 2007	https://www.ncei.noaa.gov/data/oceans/ncei/ocads/metadata/0186034.html	https://doi.org/10.25921/wdn2-pt10	Gruber et al. (2019a, b)
53(b)	Decadal Trends in Anthropogenic CO_2 From 1994 to 2014	https://www.ncei.noaa.gov/data/oceans/ncei/ocads/metadata/0279447.html	https://doi.org/10.25921/ppcf-w020	Müller et al. (2023a, b)
54	Anthropogenic carbon from 1750 to 2500 (TRACE)	https://github.com/BRCScienceProducts/TRACEv1	https://doi.org/10.5281/zenodo.15003059	Carter (2025), Carter et al. (2025)
55	Preformed TA and other bio-geochemical properties	https://github.com/BRCScienceProducts/PreformedPropertyEstimates	https://doi.org/10.5281/zenodo.3745002	BRCScienceProducts (2020), Carter et al. (2020)
56	Monthly Interior Ocean pH Climatology	https://doi.org/10.12157/IOCAS.20230720.001	https://doi.org/10.12157/IOCAS.20230720.001	Zhong et al. (2023, 2025)
57	CODAP-NA Climatology	https://www.ncei.noaa.gov/data/oceans/ncei/ocads/metadata/0270962.html	https://doi.org/10.25921/g8pb-zy76	Jiang et al. (2022b, 2024)
58	SeaFlux	https://doi.org/10.5281/zenodo.5482547	https://doi.org/10.5281/zenodo.5482547	Gregor and Fay (2021)
59	RECCAP2	https://doi.org/10.5281/zenodo.7990823	https://doi.org/10.5281/zenodo.7990823	Müller (2023)

Table 7. Continued.

No.	Name	Data access link	DOI	Reference
60	Global Carbon Budget	https://doi.org/10.5281/zenodo.14639761, https://globalcarbonbudget.org/download/1442/?tmstv=1731323337, https://globalcarbonbudgetdata.org/closed-access-requests.html	https://doi.org/10.5281/zenodo.14639761	Hauck et al. (2025)
61	Decadal Trends in the Ocean Carbon Sink	n/a	https://doi.org/10.6084/m9.figshare.8091161.v1	DeVries (2019), DeVries et al. (2019)
62	ECCO-Darwin	https://data.nas.nasa.gov/ecco/	n/a	Carroll et al. (2020)
63(a)	Surface pH and Revelle Factor	https://www.ncei.noaa.gov/data/oceans/ncei/ocads/metadata/0206289.html	https://doi.org/10.25921/kgqr-9h49	Jiang et al. (2019a, b)
63(b)	Surface OA Indicators	https://www.ncei.noaa.gov/data/oceans/ncei/ocads/metadata/0259391.html	https://doi.org/10.25921/9ker-bc48	Jiang et al. (2022c, 2023)
64	Simulated and Constrained Global and Southern Ocean Carbon Sink	https://www.seanoe.org/data/00927/103934/, https://www.seanoe.org/data/00927/103938/	https://doi.org/10.17882/103934, https://doi.org/10.17882/103938	Terhaar et al. (2021c, 2022b)
65	Composite model-based estimate of the ocean carbon sink from 1959 to 2022	https://bg.copernicus.org/articles/22/1631/2025/ (the data is in the annex)	https://doi.org/10.5194/bg-22-1631-2025	Terhaar (2025)
66	pCIBR_Clim and pCIBR_Int	https://www.ncei.noaa.gov/data/oceans/ncei/ocads/metadata/0307788.html	https://doi.org/10.25921/r2q9-d197	Ghoshal et al. (2025a, b)
67	INCOIS-BIO-ROMS Simulated Surface pCO_2 and pH for the Indian Ocean	https://www.ncei.noaa.gov/data/oceans/ncei/ocads/metadata/0307663.html	https://doi.org/10.25921/z2x4-vt48	Chakraborty et al. (2024, 2025)
68	Ocean Circulation Inverse Model (OCIM)	https://figshare.com/articles/dataset/OCIM2-48L_abiotic_ocean_carbon_cycle_model_output/19341974	https://doi.org/10.6084/m9.figshare.19341974.v2	DeVries (2022b, c)

Oceanology of Polish Academy of Sciences for the GOOS Biogeochemistry Panel (4500540682). Siv K. Lauvset and Nico Lange acknowledge funding from OceanICU. OceanICU was funded by the European Union under grant agreement no. 101083922. Views and opinions expressed are however those of the author(s) only and do not necessarily reflect those of the European Union or European Research Executive Agency. Neither the European Union nor the granting authority can be held responsible for them. Funding for GLODAPv2 was provided by the EU FP7 project CarboChange (grant agreement 264879) and the Research Council of Norway project DECApH (grant agreement 214513), and the 2019–2023 updates were funded by the EU Horizon 2020 innovation action EuroSea (grant agreement 862626). Andrea J. Fassbender, Simone R. Alin, and Richard A. Feely were supported by the NOAA Pacific Marine Environmental Laboratory. Galen A. McKinley was funded by NOAA NA24OARX431G0151-T1-01. Jean-Pierre Gattuso was supported by the Service d'Observation Rade de Villefranche (SO-Rade), the Service d'Observation en Milieu Littoral (SOMLIT/CNRS-INSU), the Coastal Observing System for Northern and Arctic Seas (COSYNA), the two Helmholtz large-scale infrastructure projects: ACROSS and MOSES, the French Polar Institute (IPEV), and the European Commission, Horizon 2020 Framework Programme (grant nos. 871153, 951799, 727890 and 869154). Discrete samples reported by were analyzed for CT and AT by the Service National d'Analyse des Paramètres Océaniques du CO_2. Anton Velo and Fiz F. Pérez were supported by BOCATS2 (PID2019-104279GB-C21) project funded by MICIU/AEI/10.13039/501100011033, by FICARAM+ (PID2023-148924OB-100) and by EuroGO-SHIP project (Horizon Europe #101094690). Nicolas Metzl and Claire Lo Monaco acknowledge Institut National des Sciences de l'Univers du Centre National de la Recherche Scientifique (INSU/CNRS) and Observatoire des Science de l'Univers (OSU ECCE-Terra) for supporting the SNAPO-CO_2 facility housed by the LOCEAN laboratory in Paris/France. The AZMP Carbon dataset is a contribution to Fisheries and Oceans Canada Atlantic Zone Monitoring Program. Funding for the HOT program and WHOTS mooring maintenance were provided by the National Science Foundation (grant no. OCE-2241005). CMEMS-LSCE is supported by the European Copernicus Marine Environment Monitoring Service (CMEMS, grant no. 83-CMEMSTAC-MOB). The work of Luke Gregor was supported by the ESA OceanHealth-OA project (contract number 4000137603/22/I-DT), the European Space Agency (OceanSODA project, grant no. 4000112091/14/I-LG), the European Commission (COMFORT project, grant no. 820989), and the Horizon 2020 (4C project, grant no. 821003). Peter Landschützer received funding through the Horizon Europe research and innovation program under grant agreement No. 101137682 (AI4PEX), the Horizon2020 program (4C project, grant no. 821003) and through Schmidt Sciences (OBVI InMOS). Judith Hauck received funding from the Initiative and Networking Fund of the Helmholtz Association (Helmholtz Young Investigator Group Marine Carbon and Ecosystem Feedbacks in the Earth System [MarESys], Grant VH-NG-1301), and from the ERC-2022-STG OceanPeak (Grant 101077209). Alex Kozyr was funded by the NOAA Global Ocean Monitoring and Observing program (https://ror.org/037bamf06, last access: 7 January 2026). Jens Terhaar was funded by the Swiss National Science Foundation under grant # PZ00P2_209044 (ArcticECO). Henry C. Bittig acknowledges funding by the German Federal Ministry of Education and Research under grants no. 03F0877D (C-SCOPE project) and 03F0773A (BONUS INTEGRAL project). Tim DeVries acknowledges support from the US National Science Foundation through Grant # 1948955. Rik Wanninkhof, Leticia Barbero, Adrienne J. Sutton, Simone R. Alin, and Richard A. Feely acknowledge support from the Office of Oceanic and Atmospheric Research of NOAA, US Department of Commerce, including resources from the Global Ocean Monitoring and Observing Program and the Ocean Acidification Program (Open Funder Registry numbers 100018302 and 100018228, respectively). Simone R. Alin and Richard A. Feely acknowledge support from the Washington Ocean Acidification Center. Natalie M. Monacci acknowledges support from the Alaska Ocean Observing System (AOOS), the Exxon Valdez Oil Spill Trustee Council (EVOS), Gulf Watch Alaska, and the North Pacific Research Board (NPRB). Kunal Chakraborty acknowledges the support of the Development of Climate Change Advisory Services project, undertaken by the Indian National Centre for Ocean Information Services (INCOIS) under the Deep Ocean Mission programme of the Ministry of Earth Sciences (MoES), Government of India. Liang Xue was supported by the National Key R&D Program of China (2023YFE0113101 and 2023YFC3108102), the National Natural Science Foundation of China (42176051and 42376048), and the Taishan Scholar Project of Shandong Province (tsqn202306294). Kumiko Azetsu-Scott and Debby Ianson acknowledge funding from Fisheries and Oceans Canada, including, but not limited to, Aquatic Climate Change Adaptation Service Program. Debby Ianson and Ana Franco acknowledge funding from Canada's Marine Environmental Observation Prediction and Response Network-OxyNet. Funding for the MOCHA synthesis was provided by California Ocean Protection Council (grant no. R/OPCOAH-04), the NOAA Ocean Acidification Program (grant no. 2906368), the National Park Service (grant no. P17AC01416), and the National Science Foundation (grant no. 1734999). Ian Enochs, Nicole Besemer and Ana M. Palacio-Castro acknowledge support from the NOAA Ocean Acidification Program (grant no. 25027), and the Coral Reef Conservation program (grant no. 743).

Review statement. This paper was edited by Sebastiaan van de Velde and reviewed by Meg Yoder and one anonymous referee.

References

Alin, S. R., Newton, J. A., Feely, R. A., Greeley, D., Curry, B., Herndon, J., and Warner, M.: A decade-long cruise time series (2008–2018) of physical and biogeochemical conditions in the southern Salish Sea, North America, Earth Syst. Sci. Data, 16, 837–865, https://doi.org/10.5194/essd-16-837-2024, 2024a.

Alin, S. R., Newton, J. A., Feely, R. A., Siedlecki, S., and Greeley, D.: Seasonality and response of ocean acidification and hypoxia to major environmental anomalies in the southern Salish Sea, North America (2014–2018), Biogeosciences, 21, 1639–1673, https://doi.org/10.5194/bg-21-1639-2024, 2024b.

Alin, S. R., Newton, J., Ikeda, C., Boyar, A., Greeley, D., Herndon, J., Curry, B., Kozyr, A., and Feely, R. A.: SalishCruise-

DataPackage_v2025: An updated compiled data package of sensor profile and discrete physical and biogeochemical measurements from 61 individual cruise data sets collected from a variety of ships in the southern Salish Sea and northern California Current System (Washington state marine waters) from 2008-02-04 to 2024-10-22 (NCEI Accession 0307188), NOAA National Centers for Environmental Information [data set], https://doi.org/10.25921/jgrz-v584, 2025a.

Alin, S. R., Newton, J., Feely, R. A., Ikeda, C., Boyar, A., Greeley, D., Herndon, J., and Kozyr, A.: SalishCruiseMultistressor_v2025: An updated multi-stressor data product for marine heatwave, hypoxia, and ocean acidification research, including calculated inorganic carbon parameters from the southern Salish Sea and northern California Current System from 2008-02-04 to 2024-10-22 (NCEI Accession 0307626), NOAA National Centers for Environmental Information [data set], https://doi.org/10.25921/4y18-rw26, 2025b.

Alin, S. R., Newton, J., Feely, R. A., Boyar, A., and Ikeda, C.: The second half decade of Washington Ocean Acidification Center cruises, in: PSEMP Marine Waters Workgroup 2025, Puget Sound marine waters: 2024 overview, edited by: Apple, J., Wold, R., Stark, K., and Newton, J., 24–25, https://pspwa.app.box.com/s/7ye4t366v5uzil8zybrqtyx11qd32779 (last access: 7 January 2026), 2025c.

Archer, D.: The Global Carbon Cycle, Princeton University Press, JSTOR, https://doi.org/10.2307/j.ctvcm4hx8, 2010.

Archer, D., Eby, M., Brovkin, V., Ridgwell, A., Cao, L., Mikolajewicz, U., Caldeira, K., Matsumoto, K., Munhoven, G., Montenegro, A., and Tokos, K.: Atmospheric lifetime of fossil fuel carbon dioxide, Annu. Rev. Earth Planet. Sci., 37, 117–134, https://doi.org/10.1146/annurev.earth.031208.100206, 2009.

Bach, L. T., Gill, S. J., Rickaby, R. E., Gore, S., and Renforth, P.: CO_2 removal with enhanced weathering and ocean alkalinity enhancement: Potential risks and co-benefits for marine pelagic ecosystems, Front. Clim., 1, https://doi.org/10.3389/fclim.2019.00007, 2019.

Bakker, D. C. E., Pfeil, B., Smith, K., Hankin, S., Olsen, A., Alin, S. R., Cosca, C., Harasawa, S., Kozyr, A., Nojiri, Y., O'Brien, K. M., Schuster, U., Telszewski, M., Tilbrook, B., Wada, C., Akl, J., Barbero, L., Bates, N. R., Boutin, J., Bozec, Y., Cai, W.-J., Castle, R. D., Chavez, F. P., Chen, L., Chierici, M., Currie, K., de Baar, H. J. W., Evans, W., Feely, R. A., Fransson, A., Gao, Z., Hales, B., Hardman-Mountford, N. J., Hoppema, M., Huang, W.-J., Hunt, C. W., Huss, B., Ichikawa, T., Johannessen, T., Jones, E. M., Jones, S. D., Jutterström, S., Kitidis, V., Körtzinger, A., Landschützer, P., Lauvset, S. K., Lefèvre, N., Manke, A. B., Mathis, J. T., Merlivat, L., Metzl, N., Murata, A., Newberger, T., Omar, A. M., Ono, T., Park, G.-H., Paterson, K., Pierrot, D., Ríos, A. F., Sabine, C. L., Saito, S., Salisbury, J., Sarma, V. V. S. S., Schlitzer, R., Sieger, R., Skjelvan, I., Steinhoff, T., Sullivan, K. F., Sun, H., Sutton, A. J., Suzuki, T., Sweeney, C., Takahashi, T., Tjiputra, J., Tsurushima, N., van Heuven, S. M. A. C., Vandemark, D., Vlahos, P., Wallace, D. W. R., Wanninkhof, R., and Watson, A. J.: An update to the Surface Ocean CO_2 Atlas (SOCAT version 2), Earth Syst. Sci. Data, 6, 69–90, https://doi.org/10.5194/essd-6-69-2014, 2014.

Bakker, D. C. E., Pfeil, B., Landa, C. S., Metzl, N., O'Brien, K. M., Olsen, A., Smith, K., Cosca, C., Harasawa, S., Jones, S. D., Nakaoka, S., Nojiri, Y., Schuster, U., Steinhoff, T., Sweeney, C., Takahashi, T., Tilbrook, B., Wada, C., Wanninkhof, R., Alin, S. R., Balestrini, C. F., Barbero, L., Bates, N. R., Bianchi, A. A., Bonou, F., Boutin, J., Bozec, Y., Burger, E. F., Cai, W.-J., Castle, R. D., Chen, L., Chierici, M., Currie, K., Evans, W., Featherstone, C., Feely, R. A., Fransson, A., Goyet, C., Greenwood, N., Gregor, L., Hankin, S., Hardman-Mountford, N. J., Harlay, J., Hauck, J., Hoppema, M., Humphreys, M. P., Hunt, C. W., Huss, B., Ibánhez, J. S. P., Johannessen, T., Keeling, R., Kitidis, V., Körtzinger, A., Kozyr, A., Krasakopoulou, E., Kuwata, A., Landschützer, P., Lauvset, S. K., Lefèvre, N., Lo Monaco, C., Manke, A., Mathis, J. T., Merlivat, L., Millero, F. J., Monteiro, P. M. S., Munro, D. R., Murata, A., Newberger, T., Omar, A. M., Ono, T., Paterson, K., Pearce, D., Pierrot, D., Robbins, L. L., Saito, S., Salisbury, J., Schlitzer, R., Schneider, B., Schweitzer, R., Sieger, R., Skjelvan, I., Sullivan, K. F., Sutherland, S. C., Sutton, A. J., Tadokoro, K., Telszewski, M., Tuma, M., van Heuven, S. M. A. C., Vandemark, D., Ward, B., Watson, A. J., and Xu, S.: A multi-decade record of high-quality fCO_2 data in version 3 of the Surface Ocean CO_2 Atlas (SOCAT), Earth Syst. Sci. Data, 8, 383–413, https://doi.org/10.5194/essd-8-383-2016, 2016.

Bakker, D. C. E., Alin, S. R., Aramaki, T., Barbero, L., Bates, N. R., Gkritzalis, T., Jones, S. D., Kozyr, A., Lauvset, S. K., Macovei, V., Metzl, N.; Munro, D. R., Nakaoka, S.-I., O'Brien, K. M., Olsen, A., Pierrot, D., Steinhoff, T., Sullivan, K. F., Sutton, A. J., Sweeney, C., Wada, C., Wanninkhof, R., Akl, J., Arbilla, L. A., Azetsu-Scott, K., Battisti, R., Beatty, C. M., Becker, M., Benoit-Cattin, A., Berghoff, C. F., Bittig, H. C., Bonin, J. A., Bott, R., Bozzano, R., Burger, E. F., Brunetti, F., Cantoni, C., Castelli, G., Chambers, D. P., Chierici, M., Corbo, A., Cronin, M., Cross, J. N., Currie, K. I., Dentico, C., Emerson, S. R., Enochs, I., Enright, M. P.; Enyo, K.; Ericson, Y.; Evans, W.; Fay, A. R.; Feely, R. A.; Fragiacomo, E., Fransson, A., Gehrung, M., Giani, M., Glockzin, M., Hamnca, S., Holodkov, N., Hoppema, M., Ibánhez, J. S. P., Kadono, K., Kamb, L., Kralj, M., Kristensin, T. O., Laudicella, V. A., Lefèvre, N., Leseurre, C., Lo Monaco, C., Maenner Jones, S. M., Maenza, R. A., McAuliffe, A. M., Mdokwana, B. W., Monacci, N. M., Musielewicz, S., Neill, C., Newberger, T., Nojiri, Y., Ohman, M. D., Ólafsdóttir, S. R., Olivier, L., Omar, A.; Osborne, J., Pensieri, S., Petersen, W., Plueddemann, A. J., Rehder, G., Roden, N. P., Rutgersson, A., Sallée, J.-B., Sanders, R., Sarpe, D., Schirnik, C., Schlitzer, R., Send, U., Skjelvan, I., Sutherland, S. C., T'Jampens, M., Tamsitt, V., Telszewski, M., Theetaert, H., Tilbrook, B., Trull, T., Tsanwani, M., Van de Velde, S., Van Heuven, S. M. A. C., Veccia, M. H., Voynova, Y. G., Weller, R. A., and Williams, N. L.: Surface Ocean CO_2 Atlas Database Version 2025 (SOCATv2025) (NCEI Accession 0304549), NOAA National Centers for Environmental Information [data set], https://doi.org/10.25921/648f-fv35, 2025.

Barth, A., Beckers, J.-M., Troupin, C., Alvera-Azcárate, A., and Vandenbulcke, L.: DIVAnd-1.0: n-dimensional variational data analysis for ocean observations, Geosci. Model Dev., 7, 225–241, https://doi.org/10.5194/gmd-7-225-2014, 2014.

Bates, N., Johnson, R. J., Lomas, M. W., Steinberg, D. K., Lopez, P., Hayden, M., May, R., Derbyshire, L., Lethaby, P. J., Smith, D., and Lomas, D.: Determination of carbon, nitrogen, and phosphorus content in sinking particles at the Bermuda Atlantic Time-series Study (BATS) site from December 1988 to December 2023 using a Particle Interceptor Trap System (PITS), BCO-DMO – Biological and Chemical Oceanogra-

phy Data Management Office (Version 4) Version Date 2024-11-14, https://doi.org/10.26008/1912/bco-dmo.894099.4, 2024a.

Bates, N., Johnson, R. J., Lethaby, P. J., Smith, D., and Medley, C.: Primary productivity estimates from the incubation of seawater collected at the Bermuda Atlantic Time-series Study (BATS) site from December 1988 through December 2023, BCO-DMO – Biological and Chemical Oceanography Data Management Office (Version 4) Version Date 2024-11-14, https://doi.org/10.26008/1912/bco-dmo.893182.4, 2024b.

Bates, N., Johnson, R. J., Lethaby, P. J., Smith, D., and Medley, C.: HPLC and fluorometric derived phytoplankton pigment concentrations from seawater collected on BATS Validation cruises from June 1996 to June 2023, BCO-DMO – Biological and Chemical Oceanography Data Management Office (Version 4) Version Date 2024-09-18, https://doi.org/10.26008/1912/bco-dmo.926534.4, 2024c.

Bates, N., Johnson, R. J., Lethaby, P. J., Medley, C., and Smith, D.: HPLC and fluorometric derived phytoplankton pigment concentrations from seawater collected at the Bermuda Atlantic Time-series Study (BATS) site from October 1988 through December 2023, BCO-DMO – Biological and Chemical Oceanography Data Management Office (Version 6) Version Date 2023-09-13, https://doi.org/10.26008/1912/bco-dmo.893521.6, 2024d.

Bates, N., Johnson, R. J., Smith, D., Lethaby, P .J., Lomas, M. W., and Lomas, D.: Discrete bottle samples collected during BATS Validation (BVAL) cruises from April 1991 through June 2023, BCO-DMO – Biological and Chemical Oceanography Data Management Office (Version 5) Version Date 2024-10-01, https://doi.org/10.26008/1912/bco-dmo.917255.5, 2024e.

Bates, N., Johnson, R. J., Lomas, M. W., Smith, D., Lethaby, P. J., Bakker, R., Davey, E., Derbyshire, L., Enright, M., Garley, R., Hayden, M. G., Lomas, D., May, R., Medley, C., Stuart, E., and Chambers, E.: Discrete bottle samples collected at the Bermuda Atlantic Time-series Study (BATS) site in the Sargasso Sea from October 1988 through December 2024, (Version 8) Version Date 2025-06-27, Biological and Chemical Oceanography Data Management Office (BCO-DMO) [data set], https://doi.org/10.26008/1912/bco-dmo.3782.8, 2025.

Bates, N. R. and Johnson, R. J.: Acceleration of ocean warming, salinification, deoxygenation, and acidification in the surface subtropical North Atlantic Ocean, Nat. Commun. Earth Environ., 1, 1–12, 2020.

Bates, N. R. and Johnson, R. J.: Forty years of ocean acidification observations (1983–2023) in the Sargasso Sea at the Bermuda Atlantic Time-series Study (BATS) site, Front. Mar. Sci., 10, https://doi.org/10.3389/fmars.2023.1289931, 2023.

Bennington, V., Gloege, L., and McKinley, G. A.: Variability in the global ocean carbon sink from 1959 to 2020 by correcting models with observations, Geophys. Res. Lett., 49, https://doi.org/10.1029/2022gl098632, 2022a.

Bennington, V., Galjanic, T., and McKinley, G. A.: Explicit physical knowledge in machine learning for Ocean Carbon Flux Reconstruction: The pCO_2-residual method, J. Adv. Model. Earth Syst., 14, https://doi.org/10.1029/2021ms002960, 2022b.

Bennington, V., Fay, A., and McKinley, G.: LDEO pCO_2-Residual Method (Version 2024), Zenodo [data set], https://doi.org/10.5281/zenodo.13941548, 2024.

Bertin, C., Carroll, D., Menemenlis, D., Dutkiewicz, S., Zhang, H., Matsuoka, A., Tank, S., Manizza, M., Miller, C. E., Babin, M., Mangin, A., and Le Fouest, V.: Biogeochemical river runoff drives intense coastal Arctic Ocean CO_2 outgassing, Geophys. Res. Lett., 50, https://doi.org/10.1029/2022gl102377, 2023.

Bittig, H. C., Steinhoff, T., Claustre, H., Fiedler, B., Williams, N. L., Sauzède, R., Körtzinger, A., and Gattuso, J.-P.: An alternative to static climatologies: Robust estimation of open ocean CO_2 variables and nutrient concentrations from T, S, and O_2 data using Bayesian Neural Networks, Front. Mar. Sci., 5, https://doi.org/10.3389/fmars.2018.00328, 2018.

Bittig, H. C., Jacobs, E., Neumann, T., and Rehder, G.: A regional pCO_2 climatology of the Baltic Sea, PANGAEA [data set], https://doi.org/10.1594/PANGAEA.961119, 2023.

Bittig, H. C., Jacobs, E., Neumann, T., and Rehder, G.: A regional pCO_2 climatology of the Baltic Sea from in situ pCO_2 observations and a model-based extrapolation approach, Earth Syst. Sci. Data, 16, 753–773, https://doi.org/10.5194/essd-16-753-2024, 2024.

Boyer, T. P., Garcia, H. E., Locarnini, R. A., Zweng, M. M., Mishonov, A. V., Reagan, J. R., Weathers, K. A., Baranova, O. K., Seidov, D., and Smolyar, I. V.: World Ocean Atlas 2018, NOAA National Centers for Environmental Information, https://www.ncei.noaa.gov/archive/accession/NCEI-WOA18 (last access: 7 January 2026), 2018.

BRCScienceProducts: BRCScienceProducts/PreformedPropertyEstimates: Submitted for Peer Review (Version V0), Zenodo [data set], https://doi.org/10.5281/zenodo.3745002, 2020.

Brett, A., Leape, J., Abbott, M., Sakaguchi, H., Cao, L., Chand, K., Golbuu, Y., Martin, T. J., Mayorga, J., and Myksvoll, M. S.: Ocean Data Need a sea change to help navigate the Warming World, Nature, 582, 181–183, https://doi.org/10.1038/d41586-020-01668-z, 2020.

Broecker, W. S.: Glacial to interglacial changes in ocean chemistry, Prog. Oceanogr., 11, 151–197, https://doi.org/10.1016/0079-6611(82)90007-6, 1982.

Broullón, D., Pérez, F. F., Velo, A., Hoppema, M., Olsen, A., Takahashi, T., Key, R. M., Tanhua, T., González-Dávila, M., Jeansson, E., Kozyr, A., and van Heuven, S. M. A. C.: A global monthly climatology of total alkalinity: a neural network approach, Earth Syst. Sci. Data, 11, 1109–1127, https://doi.org/10.5194/essd-11-1109-2019, 2019.

Broullón, D., Pérez, F. F., Velo, A., Hoppema, M., Olsen, A., Takahashi, T., Key, R. M., Tanhua, T., Santana-Casiano, J. M., and Kozyr, A.: A global monthly climatology of oceanic total dissolved inorganic carbon: A Neural Network approach, Earth Syst. Sci. Data, 12, 1725–1743, https://doi.org/10.5194/essd-12-1725-2020, 2020a.

Broullón, D., Pérez, F. F., Velo, A., Hoppema, M., Olsen, A., Takahashi, T., Key, R. M., Tanhua, T., González-Dávila, M., Jeansson, E., Kozyr, A., and van Heuven, S. M. A. C.: A global monthly climatology of total alkalinity (AT): a neural network approach (NCEI Accession 0222470), NOAA National Centers for Environmental Information [data set], https://doi.org/10.25921/5p69-y471, 2020b.

Broullón, D., Pérez, F. F., Velo, A., Hoppema, M., Olsen, A., Takahashi, T., Key, R. M., Tanhua, T;, Santana-Casiano, J. M., and Kozyr, A.: A global monthly climatology of oceanic total dissolved inorganic carbon (DIC): a neural network approach (NCEI Accession 0222469), NOAA National Centers for Envi-

ronmental Information [data set], https://doi.org/10.25921/ndgj-jp24, 2020c.

Cai, W.-J., Hu, X., Huang, W.-J., Murrell, M. C., Lehrter, J. C., Lohrenz, S. E., Chou, W.-C., Zhai, W., Hollibaugh, J. T., Wang, Y., Zhao, P., Guo, X., Gundersen, K., Dai, M., and Gong, G.-C.: Acidification of subsurface coastal waters enhanced by eutrophication, Nat. Geosci., 4, 766–770, https://doi.org/10.1038/ngeo1297, 2011.

Carroll, D., Menemenlis, D., Adkins, J. F., Bowman, K. W., Brix, H., Dutkiewicz, S., Fenty, I., Gierach, M. M., Hill, C., Jahn, O., Landschützer, P., Lauderdale, J. M., Liu, J., Manizza, M., Naviaux, J. D., Rödenbeck, C., Schimel, D. S., Van der Stocken, T., and Zhang, H.: The ECCO-Darwin data-assimilative global ocean biogeochemistry model: Estimates of seasonal to multidecadal surface ocean pCO_2 and air-sea CO_2 flux, J. Adv. Model. Earth Syst., 12, https://doi.org/10.1029/2019ms001888, 2020.

Carroll, D., Menemenlis, D., Dutkiewicz, S., Lauderdale, J. M., Adkins, J. F., Bowman, K. W., Brix, H., Fenty, I., Gierach, M. M., Hill, C., Jahn, O., Landschützer, P., Manizza, M., Mazloff, M. R., Miller, C. E., Schimel, D. S., Verdy, A., Whitt, D. B., and Zhang, H.: Attribution of space-time variability in global-ocean dissolved Inorganic Carbon, Global Biogeochem. Cy., 36, https://doi.org/10.1029/2021gb007162, 2022.

Carroll, D., Menemenlis, D., Zhang, H., Mazloff, M., McKinley, G., Fay, A., Dutkiewicz, S., Lauderdale, J., and Fenty, I.: Evaluation of the ECCO-Darwin Ocean Biogeochemistry State Estimate vs. In-situ Observations (ver 1.0), Zenodo [data set], https://doi.org/10.5281/zenodo.10627664, 2024.

Carter, B.: Anthropogenic carbon distributions from preindustrial to 2500 c.e. estimated using Tracer-based Rapid Anthropogenic Carbon Estimation (version 1), Zenodo [data set], https://doi.org/10.5281/zenodo.15003059, 2025.

Carter, B. R., Williams, N. L., Gray, A. R., and Feely, R. A.: Locally interpolated alkalinity regression for global alkalinity estimation, Limnol. Oceanogr.: Meth., 14, 268–277, https://doi.org/10.1002/lom3.10087, 2016.

Carter, B. R., Feely, R. A., Williams, N. L., Dickson, A. G., Fong, M. B., and Takeshita, Y.: Updated methods for global locally interpolated estimation of alkalinity, ph, and nitrate, Limnol. Oceanogr.: Meth., 16, 119–131, https://doi.org/10.1002/lom3.10232, 2017.

Carter, B. R., Feely, R. A., Lauvset, S. K., Olsen, A., DeVries, T., and Sonnerup, R.: Preformed properties for marine organic matter and carbonate mineral cycling quantification, Global Biogeochem. Cy., 35, https://doi.org/10.1029/2020gb006623, 2020.

Carter, B. R., Bittig, H. C., Fassbender, A. J., Sharp, J. D., Takeshita, Y., Xu, Y.-Y., Álvarez, M., Wanninkhof, R., Feely, R. A., and Barbero, L.: New and updated global empirical seawater property estimation routines, Limnol. Oceanogr.: Meth., 19, 785–809, https://doi.org/10.1002/lom3.10461, 2021.

Carter, B. R., Schwinger, J., Sonnerup, R., Fassbender, A. J., Sharp, J. D., Dias, L. M., and Sandborn, D. E.: Tracer-based Rapid Anthropogenic Carbon Estimation (TRACE), Earth Syst. Sci. Data, 17, 3073–3088, https://doi.org/10.5194/essd-17-3073-2025, 2025.

Chakraborty, K., Joshi, A. P., Ghoshal, P. K., Baduru, B., Valsala, V., Sarma, V. V. S. S., Metzl, N., Gehlen, M., Chevallier, F., and Lo Monaco, C.: Indian Ocean acidification and its driving mechanisms over the last four decades (1980–2019), Global Biogeochem. Cy., 38, https://doi.org/10.1029/2024gb008139, 2024.

Chakraborty, K., Joshi, A. P., Ghoshal, P. K., Baduru, B., Valsala, V., Sarma, V. V. S. S., Metzl, N., Gehlen, M., Chevallier, F., and Lo Monaco, C.: Indian ocean acidification and its driving mechanisms over the last four decades from 1980-01-01 to 2019-12-31 (NCEI Accession 0307663), NOAA National Centers for Environmental Information [data set], https://doi.org/10.25921/z2x4-vt48, 2025.

Chau, T.-T.-T., Gehlen, M., and Chevallier, F.: A seamless ensemble-based reconstruction of surface ocean pCO_2 and air–sea CO_2 fluxes over the global coastal and open oceans, Biogeosciences, 19, 1087–1109, https://doi.org/10.5194/bg-19-1087-2022, 2022a.

Chau, T. T. T., Gehlen, M., and Chevallier, F.: Global ocean surface carbon product Le Laboratoire des Sciences du Climat et de l'Environnement (LSCE), IPSL/CEA Saclay [data set], https://doi.org/10.14768/a2f0891b-763a-49e9-af1b-78ed78b16982, 2022b.

Chau, T.-T.-T., Gehlen, M., Metzl, N., and Chevallier, F.: CMEMS-LSCE: a global, 0.25°, monthly reconstruction of the surface ocean carbonate system, Earth Syst. Sci. Data, 16, 121–160, https://doi.org/10.5194/essd-16-121-2024, 2024a.

Chau, T.-T.-T., Chevallier, F. and Gehlen, M.: Global analysis of surface ocean CO_2 fugacity and air–sea fluxes with low latency, Geophys. Res. Lett., 51, e2023GL106670, https://doi.org/10.1029/2023GL106670, 2024b.

Chau, T. T. T., Gehlen, M., and Chevallier, F.: CMEMS-LSCE: Surface ocean carbon fields, EU Copernicus Marine Service Information (CMEMS). Marine Data Store (MDS) [data set], https://doi.org/10.48670/moi-00047, 2024c.

Chen, C.-T. A., Lui, H.-K., Hsieh, C.-H., Yanagi, T., Kosugi, N., Ishii, M., and Gong, G.-C.: Deep oceans may acidify faster than anticipated due to global warming, Nat. Clim. Change, 7, 890–894, https://doi.org/10.1038/s41558-017-0003-y, 2017.

Clement, D. and Gruber, N.: The EMLR(C^*) method to determine decadal changes in the global ocean storage of Anthropogenic CO_2, Global Biogeochem. Cy., 32, 654–679, https://doi.org/10.1002/2017gb005819, 2018.

Cooley, S. R. and Doney, S. C.: Anticipating ocean acidification's economic consequences for commercial fisheries, Environ. Res. Lett., 4, 024007, https://doi.org/10.1088/1748-9326/4/2/024007, 2009.

Crisp, D., Dolman, H., Tanhua, T., McKinley, G. A., Hauck, J., Bastos, A., Sitch, S., Eggleston, S., and Aich, V.: How well do we understand the land-ocean-atmosphere carbon cycle?, Rev. Geophys., 60, https://doi.org/10.1029/2021RG000736, 2022.

Cyr, F., Gibb, O., Azetsu-Scott, K., Chassé, J., Galbraith, P., Maillet, G., Pepin, P., Punshon, S., and Starr, M.: Ocean carbonate parameters on the Canadian Atlantic Continental Shelf, Federated Research Data Repository [data set], https://doi.org/10.20383/102.0673, 2022.

Delaigue, L., Sulpis, O., Reichart, G.-J., and Humphreys, M. P.: The changing biological carbon pump of the South Atlantic Ocean, Global Biogeochem. Cy., 38, https://doi.org/10.1029/2024gb008202, 2024.

DeVries, T.: Global Ocean Biogeochemical Model Air-Sea CO_2 Fluxes, figshare [data set], https://doi.org/10.6084/m9.figshare.8091161.v1, 2019.

DeVries, T.: The Ocean Carbon Cycle, Annu. Rev. Environ. Resour., 47, 317–341, https://doi.org/10.1146/annurev-environ-120920-111307, 2022a.

DeVries, T.: Atmospheric CO_2 and sea surface temperature variability cannot explain recent decadal variability of the Ocean CO_2 Sink, Geophys. Res. Lett., 49, https://doi.org/10.1029/2021gl096018, 2022b.

DeVries, T.: OCIM2-48L abiotic ocean carbon cycle model output, figshare [data set], https://doi.org/10.6084/m9.figshare.19341974.v2, 2022c.

DeVries, T., Holzer, M., and Primeau, F.: Recent increase in oceanic carbon uptake driven by weaker upper-ocean overturning, Nature, 542, 215–218, https://doi.org/10.1038/nature21068, 2017.

DeVries, T., Le Quéré, C., Andrews, O., Berthet, S., Hauck, J., Ilyina, T., Landschützer, P., Lenton, A., Lima, I. D., Nowicki, M., Schwinger, J., and Séférian, R.: Decadal trends in the ocean carbon sink, P. Natl. Acad. Sci. USA, 116, 11646–11651, https://doi.org/10.1073/pnas.1900371116, 2019.

DeVries, T., Yamamoto, K., Wanninkhof, R., Gruber, N., Hauck, J., Müller, J. D., Bopp, L., Carroll, D., Carter, B., Chau, T., Doney, S. C., Gehlen, M., Gloege, L., Gregor, L., Henson, S., Kim, J. H., Iida, Y., Ilyina, T., Landschützer, P., Le Quéré, C., Munro, D., Nissen, C., Patara, L., Pérez, F. F., Resplandy, L., Rodgers, K. B., Schwinger, J., Séférian, R., Sicardi, V., Terhaar, J., Triñanes, J., Tsujino, H., Watson, A., Yasunaka, S., and Zeng, J.: Magnitude, trends, and variability of the Global Ocean Carbon Sink from 1985 to 2018, Global Biogeochem. Cy., 37, https://doi.org/10.1029/2023gb007780, 2023.

Doney, S. C., Busch, D. S., Cooley, S. R., and Kroeker, K. J.: The impacts of ocean acidification on marine ecosystems and reliant human communities, Annu. Rev. Environ. Resour., 45, 83–112, https://doi.org/10.1146/annurev-environ-012320-083019, 2020.

Dore, J. E., Lukas, R., Sadler, D. W., and Karl, D. M.: Climate-driven changes to the atmospheric CO_2 sink in the subtropical North Pacific Ocean, Nature, 424, 754–757, https://doi.org/10.1038/nature01885, 2003.

Dore, J. E., Lukas, R., Sadler, D. W., Church, M. J., and Karl, D. M.: Physical and biogeochemical modulation of ocean acidification in the central North Pacific, P. Natl. Acad. Sci. USA, 106, 12235–12240, https://doi.org/10.1073/pnas.0906044106, 2009.

Dore, J. E., Church, M. J., Karl, D. M., Sadler, D. W., and Letelier, R. M.: Paired windward and leeward biogeochemical time series reveal consistent surface ocean CO_2 trends across the Hawaiian Ridge, Geophys. Res. Lett., 41, 6459–6467, https://doi.org/10.1002/2014GL060725, 2014.

Dore, J. E., White, A. E., and Karl, D. M.: Hawaii Ocean Time-series (HOT) Carbon Dioxide (Version 1), Zenodo [data set], https://doi.org/10.5281/zenodo.15060931, 2025.

Dunne, J. P., John, J. G., Shevliakova, E., Stouffer, R. J., Krasting, J. P., Malyshev, S. L., Milly, P. C., Sentman, L. T., Adcroft, A. J., Cooke, W., Dunne, K. A., Griffies, S. M., Hallberg, R. W., Harrison, M. J., Levy, H., Wittenberg, A. T., Phillips, P. J., and Zadeh, N.: GFDL's ESM2 global coupled climate–carbon earth system models. part II: Carbon system formulation and baseline simulation characteristics, J. Climate, 26, 2247–2267, https://doi.org/10.1175/jcli-d-12-00150.1, 2013.

Dunne, J. P., Hewitt, H. T., Arblaster, J. M., Bonou, F., Boucher, O., Cavazos, T., Dingley, B., Durack, P. J., Hassler, B., Juckes, M., Miyakawa, T., Mizielinski, M., Naik, V., Nicholls, Z., O'Rourke, E., Pincus, R., Sanderson, B. M., Simpson, I. R., and Taylor, K. E.: An evolving Coupled Model Intercomparison Project phase 7 (CMIP7) and Fast Track in support of future climate assessment, Geosci. Model Dev., 18, 6671–6700, https://doi.org/10.5194/gmd-18-6671-2025, 2025.

Durack, P. J., Taylor, K. E., Gleckler, P. J., Meehl, G. A., Lawrence, B. N., Covey, C., Stouffer, R. J., Levavasseur, G., Ben-Nasser, A., Denvil, S., Stockhause, M., Gregory, J. M., Juckes, M., Ames, S. K., Antonio, F., Bader, D. C., Dunne, J. P., Ellis, D., Eyring, V., Fiore, S. L., Joussaume, S., Kershaw, P., Lamarque, J.-F., Lautenschlager, M., Lee, J., Mauzey, C. F., Mizielinski, M., Nassisi, P., Nuzzo, A., O'Rourke, E., Painter, J., Potter, G. L., Rodriguez, S., and Williams, D. N.: The Coupled Model Intercomparison Project (CMIP): Reviewing project history, evolution, infrastructure and implementation, EGUsphere [preprint], https://doi.org/10.5194/egusphere-2024-3729, 2025.

Edmond, J. M.: High precision determination of titration alkalinity and total carbon dioxide content of sea water by potentiometric titration, Deep-Sea Res. Oceanogr. Abstr., 17, 737–750, https://doi.org/10.1016/0011-7471(70)90038-0, 1970.

Fassbender, A. J.: Near-global, upper 2000 m estimates of preindustrial and year 2002 ocean pH, aragonite saturation state, carbon dioxide partial pressure, hydrogen ion concentration, and Revelle factor values, and their total changes caused by anthropogenic carbon accumulation in addition to the component of the changes induced by carbonate system nonlinearities (NCEI Accession 0290073), NOAA National Centers for Environmental Information [data set], https://doi.org/10.25921/rdtr-9t74, 2024.

Fassbender, A. J., Carter, B. R., Sharp, J. D., Huang, Y., Arroyo, M. C., and Frenzel, H.: Amplified subsurface signals of ocean acidification, Global Biogeochem. Cy., 37, e2023GB007843, https://doi.org/10.1029/2023GB007843, 2023.

Fay, A. R. and McKinley, G. A.: Observed regional fluxes to constrain modelled estimates of the Ocean Carbon Sink, Geophys. Res. Lett., 48, https://doi.org/10.1029/2021gl095325, 2021.

Fay, A. R., Gregor, L., Landschützer, P., McKinley, G. A., Gruber, N., Gehlen, M., Iida, Y., Laruelle, G. G., Rödenbeck, C., Roobaert, A., and Zeng, J.: SeaFlux: harmonization of air–sea CO_2 fluxes from surface pCO_2 data products using a standardized approach, Earth Syst. Sci. Data, 13, 4693–4710, https://doi.org/10.5194/essd-13-4693-2021, 2021.

Fay, A. R., Munro, D. R., McKinley, G. A., Pierrot, D., Sutherland, S. C., Sweeney, C., and Wanninkhof, R.: Climatological distributions of sea-air Delta fCO_2 and CO_2 flux densities in the Global Surface Ocean (NCEI Accession 0282251), NOAA National Centers for Environmental Information [data set], https://doi.org/10.25921/295g-sn13, 2023.

Fay, A. R., Munro, D. R., McKinley, G. A., Pierrot, D., Sutherland, S. C., Sweeney, C., and Wanninkhof, R.: Updated climatological mean ΔfCO_2 and net sea–air CO_2 flux over the global open ocean regions, Earth Syst. Sci. Data, 16, 2123–2139, https://doi.org/10.5194/essd-16-2123-2024, 2024a.

Fay, A., McKinley, G., Bennington, V., Gloege, L., and Samant, D.: LDEO-pCO_2 HPD Back in Time, Zenodo [data set], https://doi.org/10.5281/zenodo.13891722, 2024b.

Feely, R. A., Jiang, L.-Q., Wanninkhof, R., Carter, B. R., Alin, S. A., Bednaršek, N., and Cosca, C. E.: Acidification of the global surface ocean: What we have learned from observations, Oceanog-

raphy, 36, 120–129, https://doi.org/10.5670/oceanog.2023.222, 2023.

Fennel, K., Mattern, J. P., Doney, S. C., Bopp, L., Moore, A. M., Wang, B., and Yu, L.: Ocean biogeochemical modelling, Nat. Rev. Meth. Primers, 2, 76, https://doi.org/10.1038/s43586-022-00154-2, 2022.

Franco, A. C., Ianson, D., Ross, T., Hamme, R. C., Monahan, A. H., Christian, J. R., Davelaar, M., Johnson, W. K., Miller, L. A., Robert, M., and Tortell, P. D.: Anthropogenic and climatic contributions to observed carbon system trends in the northeast Pacific, Global Biogeochem. Cy., 35, https://doi.org/10.1029/2020GB006829, 2021a.

Franco, A. C., Ianson, D., Ross, T., Hamme, R. C., Monahan, A. H., Christian, J. R., Davelaar, M., Johnson, W. K., Miller, L. A., Robert, M., and Tortell, P. D.: A compilation of inorganic carbon system and other hydrographic and chemical discrete profile measurements obtained during the fifty five Line P cruises in the Northeast Pacific Ocean over the period from 1990 to 2019 (NCEI Accession 0234342), NOAA National Centers for Environmental Information [data set], https://doi.org/10.25921/zrw8-kn24, 2021b.

Freeland, H.: A short history of Ocean Station Papa and Line P, Prog. Oceanogr., 75, 120–125, https://doi.org/10.1016/j.pocean.2007.08.005, 2007.

Friedlingstein, P., O'Sullivan, M., Jones, M. W., Andrew, R. M., Bakker, D. C. E., Hauck, J., Landschützer, P., Le Quéré, C., Li, H., Luijkx, I. T., Peters, G. P., Peters, W., Pongratz, J., Schwingshackl, C., Sitch, S., Canadell, J. G., Ciais, P., Aas, K., Alin, S. R., Anthoni, P., Barbero, L., Bates, N. R., Bellouin, N., Benoit-Cattin, A., Berghoff, C. F., Bernardello, R., Bopp, L., Brasika, I. B. M., Chamberlain, M. A., Chandra, N., Chevallier, F., Chini, L. P., Collier, N. O., Colligan, T. H., Cronin, M., Djeutchouang, L., Dou, X., Enright, M. P., Enyo, K., Erb, M., Evans, W., Feely, R. A., Feng, L., Ford, D. J., Foster, A., Fransner, F., Gasser, T., Gehlen, M., Gkritzalis, T., Goncalves De Souza, J., Grassi, G., Gregor, L., Gruber, N., Guenet, B., Gürses, Ö., Harrington, K., Harris, I., Heinke, J., Hurtt, G. C., Iida, Y., Ilyina, T., Ito, A., Jacobson, A. R., Jain, A. K., Jarníková, T., Jersild, A., Jiang, F., Jones, S. D., Kato, E., Keeling, R. F., Klein Goldewijk, K., Knauer, J., Kong, Y., Korsbakken, J. I., Koven, C., Kunimitsu, T., Lan, X., Liu, J., Liu, Z., Liu, Z., Lo Monaco, C., Ma, L., Marland, G., McGuire, P. C., McKinley, G. A., Melton, J., Monacci, N., Monier, E., Morgan, E. J., Munro, D. R., Müller, J. D., Nakaoka, S.-I., Nayagam, L. R., Niwa, Y., Nutzel, T., Olsen, A., Omar, A. M., Pan, N., Pandey, S., Pierrot, D., Qin, Z., Regnier, P. A. G., Rehder, G., Resplandy, L., Roobaert, A., Rosan, T. M., Rödenbeck, C., Schwinger, J., Skjelvan, I., Smallman, T. L., Spada, V., Sreeush, M. G., Sun, Q., Sutton, A. J., Sweeney, C., Swingedouw, D., Séférian, R., Takao, S., Tatebe, H., Tian, H., Tian, X., Tilbrook, B., Tsujino, H., Tubiello, F., van Ooijen, E., van der Werf, G., van de Velde, S. J., Walker, A., Wanninkhof, R., Yang, X., Yuan, W., Yue, X., and Zeng, J.: Global Carbon Budget 2025, Earth Syst. Sci. Data Discuss. [preprint], https://doi.org/10.5194/essd-2025-659, in review, 2025.

Garcia, H. E., Locarnini, R. A., Boyer, T. P., Antonov, J. I.,Baranova, O. K., Zweng, M. M., Reagan, J. R., and Johnson, D. R.: World Ocean Atlas 2013, in: Volume 3: Dissolved Oxygen, Apparent Oxygen Utilization, and Oxygen Saturation, NOAA Atlas NESDIS 75, edited by: Levitus, S. and Mishonov, A., NOAA, 27 pp., https://doi.org/10.7289/V5XG9P2W, 2014.

Garcia, H. E., Weathers, K., Paver, C. R., Smolyar, I., Boyer, T. P., Locarnini, R. A., Zweng, M. M., Mishonov, A. V., Baranova, O. K., Seidov, D., and Reagan, J. R.: World Ocean Atlas 2018, in: Volume 4: Dissolved Inorganic Nutrients (phosphate, nitrate and nitrate + nitrite, silicate), NOAA Atlas NESDIS 84, edited by: Mishonov, A., NOAA, 35 pp., https://doi.org/10.25923/ng6j-ey81, 2018a.

Garcia, H. E., Weathers, K. W., Paver, C. R., Smolyar, I. V., Boyer, T. P., Locarnini, R. A., Zweng, M. M., Mishonov, A. V., Baranova, O. K., and Reagan, J. R.: World Ocean Atlas 2018, in: Volume 3: Dissolved Oxygen, Apparent Oxygen Utilization, and Oxygen Saturation, NOAA Atlas NESDIS 83, edited by: Mishonov, A., NOAA, https://doi.org/10.25923/qspr-pn52, 2018b.

Garcia, H. E., Boyer, T. P., Locarnini, R. A., Reagan, J. R., Mishonov, A. V., Baranova, O. K., Paver, C. R., Wang, Z., Bouchard, C. N., Cross, S. L., Seidov, D., and Dukhovskoy, D.: World Ocean Database 2023: User's Manual, in: NOAA Atlas NESDIS 98, edited by: Mishonov, A. V., NOAA, 129 pp., https://doi.org/10.25923/j8gq-eee82, 2024.

Gattuso, J.-P. and Hansson, L.: Ocean acidification, Oxford University Press, 326 pp., https://doi.org/10.1093/oso/9780199591091.001.0001, 2011.

Gattuso, J.-P., Epitalon, J.-M., Lavigne, H., and Orr, J.: seacarb: Seawater Carbonate Chemistry, R Package, Version 3.2.16, https://CRAN.R-project.org/package=seacarb (last access: 7 January 2026), 2021a.

Gattuso, J.-P., Alliouane, S., and Mousseau, L.: Seawater carbonate chemistry in the Bay of Villefranche, Point B (France), January 2007–June 2023, PANGAEA [data set], https://doi.org/10.1594/PANGAEA.727120, 2021b.

Gattuso, J.-P., Alliouane, S., and Fischer, P.: High-frequency, year-round time series of the carbonate chemistry in a high-Arctic fjord (Svalbard), Earth Syst. Sci. Data, 15, 2809–2825, https://doi.org/10.5194/essd-15-2809-2023, 2023a.

Gattuso, J.-P., Alliouane, S., and Fischer, P.: High-frequency, year-round time series of the carbonate chemistry in a high-Arctic fjord (Svalbard), PANGAEA [data set], https://doi.org/10.1594/PANGAEA.957028, 2023b.

Ghoshal, P. K., Joshi, A. P., and Chakraborty, K.: An improved long-term high-resolution surface pCO_2 data product for the Indian Ocean using machine learning, Sci. Data, 12, https://doi.org/10.1038/s41597-025-04914-z, 2025a.

Ghoshal, P. K., Joshi, A. P., and Chakraborty, K.: An improved long-term high-resolution surface pCO_2 data product for the Indian Ocean using machine learning from 1980-01-01 to 2020-12-31 (NCEI Accession 0307788), NOAA National Centers for Environmental Information [data set], https://doi.org/10.25921/r2q9-d197, 2025b.

Gibb, O., Cyr, F., Azetsu-Scott, K., Chassé, J., Childs, D., Gabriel, C.-E., Galbraith, P. S., Maillet, G., Pepin, P., Punshon, S., and Starr, M.: Spatiotemporal variability in pH and carbonate parameters on the Canadian Atlantic continental shelf between 2014 and 2022, Earth Syst. Sci. Data, 15, 4127–4162, https://doi.org/10.5194/essd-15-4127-2023, 2023.

Gloege, L., Yan, M., Zheng, T., and McKinley, G. A.: LDEO-HPD: Lamont-Doherty Earth Observatory Hybrid Physics

Data pCO_2 Product (Version 20210425), Zenodo [data set], https://doi.org/10.5281/zenodo.4760205, 2021.

Gloege, L., Yan, M., Zheng, T., and McKinley, G. A.: Improved quantification of ocean carbon uptake by using machine learning to merge global models and pCO_2 data, J. Adv. Model. Earth Syst., 14, https://doi.org/10.1029/2021ms002620, 2022.

González-Dávila, M.: Physical oceanography measured on water bottle samples at site ESTOC in 1994, Faculty of Marine Sciences, University of Las Palmas, Gran Canaria, PANGAEA [data set], https://doi.org/10.1594/PANGAEA.856590, 2016a.

González-Dávila, M.: Physical oceanography measured on water bottle samples at site ESTOC in 2009, Faculty of Marine Sciences, University of Las Palmas, Gran Canaria, PANGAEA [data set], https://doi.org/10.1594/PANGAEA.856615, 2016b.

González-Dávila, M.: Physical oceanography measured on water bottle samples at site ESTOC in 2003, Faculty of Marine Sciences, University of Las Palmas, Gran Canaria, PANGAEA [data set], https://doi.org/10.1594/PANGAEA.856608, 2016c.

González-Dávila, M.: Physical oceanography measured on water bottle samples at site ESTOC in 2010, Faculty of Marine Sciences, University of Las Palmas, Gran Canaria, PANGAEA [data set], https://doi.org/10.1594/PANGAEA.856616, 2016d.

González-Dávila, M.: Physical oceanography measured on water bottle samples at site ESTOC in 1995, Faculty of Marine Sciences, University of Las Palmas, Gran Canaria, PANGAEA [data set], https://doi.org/10.1594/PANGAEA.856593, 2016e.

González-Dávila, M.: Physical oceanography measured on water bottle samples at site ESTOC in 2007, Faculty of Marine Sciences, University of Las Palmas, Gran Canaria, PANGAEA [data set], https://doi.org/10.1594/PANGAEA.856612, 2016f.

González-Dávila, M.: Physical oceanography measured on water bottle samples at site ESTOC in 2008, Faculty of Marine Sciences, University of Las Palmas, Gran Canaria, PANGAEA [data set], https://doi.org/10.1594/PANGAEA.856614, 2016g.

González-Dávila, M.: Physical oceanography measured on water bottle samples at site ESTOC in 2002, Faculty of Marine Sciences, University of Las Palmas, Gran Canaria, PANGAEA, [data set], https://doi.org/10.1594/PANGAEA.856607, 2016h.

González-Dávila, M. and Santana-Casiano, J. M.: Long-term trends of pH and inorganic carbon in the Eastern North Atlantic: the ESTOC site, Front. Mar. Sci., 10, 1236214, https://doi.org/10.3389/fmars.2023.1236214, 2023a.

González-Dávila, M. and Santana-Casiano, J. M.: European Carbonate system Time Series (November 2011–April 2023) in the North East Atlantic, ESTOC site, PANGAEA [data set], https://doi.org/10.1594/PANGAEA.959856, 2023b.

González-Dávila, M., Santana-Casiano, J. M., and Curbelo-Hernández, D.: Surface-to-bottom total alkalinity, inorganic carbon and CTD data in coastal areas leeward of the Macaronesia archipelagos during POS533, PANGAEA [data set], https://doi.org/10.1594/PANGAEA.956272, 2023.

Gregor, L.: luke-gregor/OceanSODA-ETHZ: code, Zenodo [code], https://doi.org/10.5281/zenodo.4455354, 2021.

Gregor, L. and Fay, A.: SeaFlux: harmonised sea-air CO_2 fluxes from surface pCO_2 data products using a standardised approach, Zenodo [data set], https://doi.org/10.5281/zenodo.5482547, 2021.

Gregor, L. and Gruber, N.: OceanSODA-ETHZ: A global gridded dataset of the surface ocean carbonate system for seasonal to decadal studies of ocean acidification (v2023) (NCEI Accession 0220059), NOAA National Centers for Environmental Information [data set], https://doi.org/10.25921/m5wx-ja34, 2020.

Gregor, L. and Gruber, N.: Oceansoda-ETHZ: A global gridded data set of the surface ocean carbonate system for seasonal to decadal studies of ocean acidification, Earth Syst. Sci. Data, 13, 777–808, https://doi.org/10.5194/essd-13-777-2021, 2021.

Gregor, L. and Gruber, N.: OceanSODA-ETHZ: A global gridded dataset of the surface ocean carbonate system for seasonal to decadal studies of ocean acidification (v2023) (NCEI accession 0220059), NOAA National Centers for Environmental Information [data set], https://doi.org/10.25921/m5wx-ja34, 2023.

Gregor, L. and Jiang, L.: Ocean CO_2 products web page (Version 0.3), GitHub [data set], https://oceanco2.github.io/co2-products/ (last access: 10 February 2026), 2026.

Gregor, L., Lebehot, A. D., Kok, S., and Monteiro, P. M. S.: A comparative assessment of the uncertainties of Global Surface Ocean CO_2 Estimates using a machine-learning ensemble (CSIR-ML6 version 2019a) – have we hit the wall?, Geosci. Model Dev., 12, 5113–5136, https://doi.org/10.5194/gmd-12-5113-2019, 2019a.

Gregor, L., Lebehot, A. D., Kok, S., and Monteiro, P. M. S.: Global surface-ocean partial pressure of carbon dioxide (pCO_2) estimates from a machine learning ensemble: CSIR-ML6 v2019a (NCEI Accession 0206205), NOAA National Centers for Environmental Information [data set], https://doi.org/10.25921/z682-mn47, 2019b.

Gregor, L., Shutler, J., and Gruber, N.: High-resolution variability of the Ocean Carbon Sink, Global Biogeochem. Cy., 38, https://doi.org/10.1029/2024gb008127, 2024a.

Gregor, L., Shutler, J., and Gruber, N.: OceanSODA-ETHZ-v2: Surface ocean sea-air CO_2 fluxes from 1982 to 2022 (8-day by $0.25° \times 0.25°$) (v2.2024r01), Zenodo [data set], https://doi.org/10.5281/zenodo.11206366, 2024b.

Gruber, N., Clement, D., Carter, B. R., Feely, R. A., van Heuven, S., Hoppema, M., Ishii, M., Key, R. M., Kozyr, A., Lauvset, S. K., Lo Monaco, C., Mathis, J. T., Murata, A., Olsen, A., Perez, F. F., Sabine, C. L., Tanhua, T., and Wanninkhof, R.: The oceanic sink for anthropogenic CO_2 from 1994 to 2007, Science, 363, 1193–1199, https://doi.org/10.1126/science.aau5153, 2019a.

Gruber, N., Clement, D., Carter, B. R., Feely, R. A., van Heuven, S., Hoppema, M., Ishii, M., Key, R. M., Kozyr, A., Lauvset, S. K., Lo Monaco, C., Mathis, J. T., Murata, A., Olsen, A., Perez, F. F., Sabine, C. L., Tanhua, T., and Wanninkhof, R.: The oceanic sink for anthropogenic CO_2 from 1994 to 2007 – the data (NCEI Accession 0186034), NOAA National Centers for Environmental Information [data set], https://doi.org/10.25921/wdn2-pt10, 2019b.

Gruber, N., Bakker, D. C. E., DeVries, T., Gregor, L., Hauck, J., Landschützer, P., McKinley, G. A., and Müller, J. D.: Trends and variability in the ocean carbon sink, Nat. Rev. Earth Environ., 4, 119–134, https://doi.org/10.1038/s43017-022-00381-x, 2023.

Hauck, J., Mayot, N., Landschützer, P., and Jersild, A.: Global Carbon Budget 2024, surface ocean fugacity of CO_2 (fCO_2) and air–sea CO_2 flux of individual global ocean biogeochemical models and surface ocean fCO_2-based data-products, Zenodo [data set], https://doi.org/10.5281/zenodo.14639761, 2025.

Holding, T., Ashton, I. G. C., and Shutler, J. D.: Reanalysed (depth and temperature consistent) surface ocean

CO_2 atlas (SOCAT) version 2019 PANGAEA [data set], https://doi.org/10.1594/PANGAEA.905316, 2019.

Hollitzer, H. A. L., Patara, L., Terhaar, J., and Oschlies, A.: Competing effects of wind and buoyancy forcing on ocean oxygen trends in recent decades, Nat. Commun., 15, 9264, https://doi.org/10.1038/s41467-024-53557-y, 2024.

Holzer, M., DeVries, T., and de Lavergne, C.: Diffusion controls the ventilation of a Pacific Shadow Zone above abyssal overturning, Nat. Commun., 12, 4348, https://doi.org/10.1038/s41467-021-24648-x, 2021.

Huguenin, M. F., Holmes, R. M., and England, M. H.: Drivers and distribution of global ocean heat uptake over the last half century, Nat. Commun., 13, 4921, https://doi.org/10.1038/s41467-022-32540-5, 2022.

Humphreys, M. P., Lewis, E. R., Sharp, J. D., and Pierrot, D.: PyCO2SYS v1.8: Marine carbonate system calculations in Python, Geosci. Model Dev., 15, 15–43, https://doi.org/10.5194/gmd-15-15-2022, 2022.

Iida, Y., Takatani, Y., Kojima, A., and Ishii, M.: Global trends of ocean CO_2 sink and ocean acidification: An observation-based reconstruction of surface ocean inorganic carbon variables, J. Oceanogr., 77, 323–358, https://doi.org/10.1007/s10872-020-00571-5, 2021.

IPCC: Climate Change 2023: Synthesis Report, Contribution of Working Groups I, II and III to the Sixth Assessment Report of the Intergovernmental Panel on Climate Change, edited by: Core Writing Team, Lee, H., and Romero, J., IPCC, Geneva, Switzerland, 35–115, https://doi.org/10.59327/IPCC/AR6-9789291691647, 2023.

Ishii, M., Kosugi, N., Sasano, D., Saito, S., Midorikawa, T., and Inoue, H. Y.: Ocean acidification off the south coast of Japan: A result from time series observations of CO_2 Parameters from 1994 to 2008, . Geophys. Res., 116, https://doi.org/10.1029/2010jc006831, 2011a.

Ishii, M., Suzuki, T., and Key, R.: Pacific Ocean Interior Carbon Data Synthesis, PACIFICA, in Progress, PICES Press, 20–23, https://www.pices.int/publications/pices_press/volume19/v19_n1/pp_20-23_PACIFICA_f.pdf (last access: 7 January 2026)), 2011b.

Jersild, A., Landschützer, P., Gruber, N., and Bakker, D. C. E.: An observation-based global monthly gridded sea surface pCO_2 and air–sea CO_2 flux product from 1982 onward and its monthly climatology (NCEI Accession 0160558), NOAA National Centers for Environmental Information [data set], https://doi.org/10.7289/v5z899n6, 2017.

Jiang, L., Dunne, J., Carter, B. R., Tjiputra, J. F., Terhaar, J., Sharp, J. D., Olsen, A., Alin, S., Bakker, D. C., Feely, R. A., Gattuso, J., Hogan, P., Ilyina, T., Lange, N., Lauvset, S. K., Lewis, E. R., Lovato, T., Palmieri, J., Santana-Falcón, Y., Schwinger, J., Séférian, R., Strand, G., Swart, N., Tanhua, T., Tsujino, H., Wanninkhof, R., Watanabe, M., Yamamoto, A., and Ziehn, T.: Global surface ocean acidification indicators from 1750 to 2100 (NCEI Accession 0259391), NOAA National Centers for Environmental Information [data set], https://doi.org/10.25921/9ker-bc48, 2022c.

Jiang, L., Dunne, J., Carter, B. R., Tjiputra, J. F., Terhaar, J., Sharp, J. D., Olsen, A., Alin, S., Bakker, D. C., Feely, R. A., Gattuso, J., Hogan, P., Ilyina, T., Lange, N., Lauvset, S. K., Lewis, E. R., Lovato, T., Palmieri, J., Santana-Falcón, Y., Schwinger, J., Séférian, R., Strand, G., Swart, N., Tanhua, T., Tsujino, H., Wanninkhof, R., Watanabe, M., Yamamoto, A., and Ziehn, T.: Global surface ocean acidification indicators from 1750 to 2100, J. Adv. Model. Earth Syst., 15, https://doi.org/10.1029/2022ms003563, 2023b.

Jiang, L.-Q. and Feely, R. A.: Aragonite saturation state gridded to 1×1 degree latitude and longitude at depth levels of 0, 50, 100, 200, 500, 1000, 2000, 3000, and 4000 meters in the global oceans (NCEI Accession 0139360), NOAA National Centers for Environmental Information [data set], https://doi.org/10.7289/v5q81b4p, 2015.

Jiang, L.-Q., Feely, R. A., Carter, B. R., Greeley, D. J., Gledhill, D. K., and Arzayus, K. M.: Climatological distribution of aragonite saturation state in the global oceans, Global Biogeochem. Cy., 29, 1656–1673, https://doi.org/10.1002/2015GB005198, 2015.

Jiang, L.-Q., Carter, B. R., Feely, R. A., Lauvset, S., and Olsen, A.: Surface ocean pH and buffer capacity: Past, present and future, Sci. Rep., 9, 18624, https://doi.org/10.1038/s41598-019-55039-4, 2019a.

Jiang, L.-Q., Carter, B. R., Feely, R. A., Lauvset, S., and Olsen, A.: Global surface ocean pH, acidity, and Revelle Factor on a 1×1 degree global grid from 1770 to 2100 (NCEI Accession 0206289), NOAA National Centers for Environmental Information [data set], https://doi.org/10.25921/kgqr-9h49, 2019b.

Jiang, L.-Q., Feely, R. A., Wanninkhof, R., Greeley, D., Barbero, L., Alin, S., Carter, B. R., Pierrot, D., Featherstone, C., Hooper, J., Melrose, C., Monacci, N., Sharp, J. D., Shellito, S., Xu, Y.-Y., Kozyr, A., Byrne, R. H., Cai, W.-J., Cross, J., Johnson, G. C., Hales, B., Langdon, C., Mathis, J., Salisbury, J., and Townsend, D. W.: Coastal Ocean Data Analysis Product in North America (CODAP-NA, Version 2021) (NCEI Accession 0219960), NOAA National Centers for Environmental Information [data set], https://doi.org/10.25921/531n-c230, 2020.

Jiang, L.-Q., Feely, R. A., Wanninkhof, R., Greeley, D., Barbero, L., Alin, S., Carter, B. R., Pierrot, D., Featherstone, C., Hooper, J., Melrose, C., Monacci, N., Sharp, J. D., Shellito, S., Xu, Y.-Y., Kozyr, A., Byrne, R. H., Cai, W.-J., Cross, J., Johnson, G. C., Hales, B., Langdon, C., Mathis, J., Salisbury, J., and Townsend, D. W.: Coastal Ocean Data Analysis Product in North America (CODAP-NA) – an internally consistent data product for discrete inorganic carbon, oxygen, and nutrients on the North American ocean margins, Earth Syst. Sci. Data, 13, 2777–2799, https://doi.org/10.5194/essd-13-2777-2021, 2021.

Jiang, L.-Q., Pierrot, D., Wanninkhof, R., Feely, R. A., Tilbrook, B., Alin, S., Barbero, L., Byrne, R. H., Carter, B. R., Dickson, A. G., Gattuso, J.-P., Greeley, D., Hoppema, M., Humphreys, M. P., Karstensen, J., Lange, N., Lauvset, S. K., Lewis, E. R., Olsen, A., Perez, F. F., Sabine, C., Sharp, J. D., Tanhua, T., Trull, T. W., Velo, A., Allegra, A. J., Barker, P., Burger, E., Cai, W.-J., Chen, C.-T. A., Cross, J., Garcia, H., Hernandez-Ayon, J. M., Hu, X., Kozyr, A., Langdon, C., Lee, K., Salisbury, J., Wang, Z. A., and Xue, L.: Best practice data standards for discrete chemical oceanographic observations, Front. Mar. Sci., 8, https://doi.org/10.3389/fmars.2021.705638, 2022a.

Jiang, L.-Q., Boyer, T. P., Paver, C. R., Yoo, H., Reagan, J. R., Alin, S. R., Barbero, L., Carter, B. R., Feely, R. A., and Wanninkhof, R.: Climatological distribution of ocean acidification indicators from surface to 500 meters water depth on the North American ocean margins from 2003-12-06 to 2018-11-22 (NCEI Accession 0270962), NOAA National Centers for Environmental Information [data set], https://doi.org/10.25921/g8pb-zy76, 2022b.

Jiang, L.-Q., Kozyr, A., Relph, J., Ronje, E., Kamb, L., Burger, E., Myer, J., Nguyen, L., Arzayus, K. M., Boyer, T., Cross, S., Garcia, H., Hogan, P., Larsen, K., and Parsons, A. R.: The ocean carbon and acidification data system, Nature – Sci. Data, 10, https://doi.org/10.1038/s41597-023-02042-0, 2023a.

Jiang, L.-Q., Boyer, T. P., Paver, C. R., Yoo, H., Reagan, J. R., Alin, S. R., Barbero, L., Carter, B. R., Feely, R. A., and Wanninkhof, R.: Climatological distribution of ocean acidification variables along the North American ocean margins, Earth Syst. Sci. Data, 16, 3383–3390, https://doi.org/10.5194/essd-16-3383-2024, 2024.

John, S. G., Liang, H., Weber, T., DeVries, T., Primeau, F., Moore, K., Holzer, M., Mahowald, N., Gardner, W., Mishonov, A., Richardson, M. J., Faugere, Y., and Taburet, G.: Awesome OCIM: A simple, flexible, and powerful tool for modeling elemental cycling in the oceans, Chem. Geol., 533, 119403, https://doi.org/10.1016/j.chemgeo.2019.119403, 2020.

Johnson, G. C., Robbins, P. E., and Hufford, G. E.: Systematic adjustments of hydrographic sections for internal consistency, J. Atmos. Ocean. Tech., 18, 1234–1244, 2001.

Johnson, R. J., Bates, N., Lethaby, P. J., Smith, D., and Chambers, E.: Two decibar averaged CTD profiles collected during BATS Validation (BVAL) cruises from April 1991 through July 2024, (Version 9) Version Date 2025-02-25, Biological and Chemical Oceanography Data Management Office (BCO-DMO) [data set], https://doi.org/10.26008/1912/bco-dmo.939210.9, 2025a.

Johnson, R. J., Bates, N., Lethaby, P. J., Smith, D., and Chambers, E.: Two decibar averaged CTD profiles collected at the Bermuda Atlantic Time-series Study (BATS) site from October 1988 through December 2024, (Version 10) Version Date 2025-05-28, Biological and Chemical Oceanography Data Management Office (BCO-DMO) [data set], https://doi.org/10.26008/1912/bco-dmo.3918.10, 2025b.

Joshi, A. P., Ghoshal, P. K., Chakraborty, K., and Sarma, V. V. S. S.: Sea-surface pCO_2 maps for the Bay of Bengal based on Advanced Machine Learning Algorithms, Sci. Data, 11, https://doi.org/10.1038/s41597-024-03236-w, 2024.

Joshi, A. P., Ghoshal, P. K., Chakraborty, K., and Sarma, V. V. S. S.: Sea-surface pCO_2 maps for the Bay of Bengal based on advanced machine learning algorithms from 2015-01-01 to 2015-12-31 (NCEI Accession 0307627), NOAA National Centers for Environmental Information [data set], https://doi.org/10.25921/2sjr-pg16, 2025a.

Joshi, A. P., Ghoshal, P. K., Chakraborty, K., Roy, R., Jayaram, C., Sridevi, B., and Sarma, V. V. S. S.: Long-term changes of surface total alkalinity and its driving mechanisms in the north Indian Ocean, Global Biogeochem. Cy., 39, e2024GB008344, https://doi.org/10.1029/2024GB008344, 2025b.

Joshi, A. P., Ghoshal, P. K., Chakraborty, K., Roy, R., Jayaram, C, Sridevi, B., and Sarma, V. V. S. S.: Long-term changes of surface total alkalinity and its driving mechanisms in the Northern Indian Ocean from 1993-01-01 to 2020-12-31 (NCEI Accession 0307789), NOAA National Centers for Environmental Information [data set], https://doi.org/10.25921/7as7-et15, 2025c.

Kapsenberg, L., Alliouane, S., Gazeau, F., Mousseau, L., and Gattuso, J.-P.: Coastal ocean acidification and increasing total alkalinity in the northwestern Mediterranean Sea, Ocean Sci., 13, 411–426, https://doi.org/10.5194/os-13-411-2017, 2017.

Karl, D., Dore, J., Lukas, R., Michaels, A., Bates, N., and Knap, A.: Building the long-term picture: The U.S. JGOFS Time-series programs, Oceanography, 14, 6–17, https://doi.org/10.5670/oceanog.2001.02, 2001.

Karl, D. M. and Lukas, R.: The Hawaii Ocean Time-series (HOT) program: Background, rationale and field implementation, Deep-Sea Res. Pt. II, 43, 129–156, https://doi.org/10.1016/0967-0645(96)00005-7, 1996.

Kennedy, E. G., Zulian, M., Hamilton, S. L., Hill, T. M., Delgado, M., Fish, C. R., Gaylord, B., Kroeker, K. J., Palmer, H. M., Ricart, A. M., Sanford, E., Spalding, A. K., Ward, M., Carrasco, G., Elliott, M., Grisby, G. V., Harris, E., Jahncke, J., Rocheleau, C. N., Westerink, S., and Wilmot, M. I.: Multistressor Observations of Coastal Hypoxia and Acidification (MOCHA) Synthesis (NCEI Accession 0277984), NOAA National Centers for Environmental Information [data set], https://doi.org/10.25921/2vve-fh39, 2023.

Kennedy, E. G., Zulian, M., Hamilton, S. L., Hill, T. M., Delgado, M., Fish, C. R., Gaylord, B., Kroeker, K. J., Palmer, H. M., Ricart, A. M., Sanford, E., Spalding, A. K., Ward, M., Carrasco, G., Elliott, M., Grisby, G. V., Harris, E., Jahncke, J., Rocheleau, C. N., Westerink, S., and Wilmot, M. I.: A high-resolution synthesis dataset for multistressor analyses along the US West Coast, Earth Syst. Sci. Data, 16, 219–243, https://doi.org/10.5194/essd-16-219-2024, 2024.

Keppler, L., Landschützer, P., Gruber, N., Lauvset, S. K., and Stemmler, I.: Seasonal carbon dynamics in the near-global ocean, Global Biogeochem. Cy., 34, e2020GB006571, https://doi.org/10.1029/2020GB006571, 2020a.

Keppler, L., Landschützer, P., Gruber, N., Lauvset, S. K., and Stemmler, I.: Mapped Observation-Based Oceanic Dissolved Inorganic Carbon (DIC), monthly climatology from January to December (based on observations between 2004 and 2017), from the Max-Planck-Institute for Meteorology (MOBO-DIC_MPIM) (NCEI Accession 0221526), NOAA National Centers for Environmental Information [data set], https://doi.org/10.25921/yvzj-zx46, 2020b.

Keppler, L., Landschützer, P., Lauvset, S. K., and Gruber, N.: Recent trends and variability in the oceanic storage of dissolved inorganic carbon, Global Biogeochem. Cy., 37, https://doi.org/10.1029/2022gb007677, 2023a.

Keppler, L., Landschützer, P., Lauvset, S. K., and Gruber, N.: Mapped Observation-Based Oceanic Dissolved Inorganic Carbon Monthly fields from 2004 through 2019 (MOBO-DIC2004-2019) (NCEI Accession 0277099), NOAA National Centers for Environmental Information [data set], https://doi.org/10.25921/z31n-3m26, 2023b.

Key, R. M., Kozyr, A., Sabine, C. L., Lee, K., Wanninkhof, R., Bullister, J. L., Feely, R. A., Millero, F. J., Mordy, C., and Peng, T. -H.: A global ocean carbon climatology: Results from Global Data Analysis Project (GLODAP), Global Biogeochem. Cy., 18, https://doi.org/10.1029/2004gb002247, 2004.

Key, R. M., Tanhua, T., Olsen, A., Hoppema, M., Jutterström, S., Schirnick, C., van Heuven, S., Kozyr, A., Lin, X., Velo, A., Wallace, D. W. R., and Mintrop, L.: The CARINA data synthesis project: introduction and overview, Earth Syst. Sci. Data, 2, 105–121, https://doi.org/10.5194/essd-2-105-2010, 2010.

Key, R. M., Olsen, A., van Heuven, S., Lauvset, S. K., Velo, A., Lin, X., Schirnick, C., Kozyr, A., Tanhua, T., Hoppema, M.,

Jutterström, S., Steinfeldt, R., Jeansson, E., Ishi, M., Perez, F. F., and Suzuki, T.: Global Ocean Data Analysis Project, Version 2 (GLODAPv2), ORNL/CDIAC-162, ND-P093, Ocean Carbon and Acidification Data System, National Centers for Environmental Information, Silver Spring, Maryland, https://www.ncei.noaa.gov/access/ocean-carbon-acidification-data-system/oceans/GLODAPv2/NDP_093.pdf (last access: 7 January 2026), 2015.

Kheshgi, H. S.: Sequestering atmospheric carbon dioxide by increasing ocean alkalinity, Energy, 20, 915–922, https://doi.org/10.1016/0360-5442(95)00035-f, 1995.

Knor, L. A. C. M., Sabine, C. L., Sutton, A. J., White, A. E., Potemra, J., and Weller, R. A.: Quantifying net community production and calcification at Station ALOHA near Hawai?i: Insights and limitations from a dual tracer carbon budget approach, Global Biogeochem. Cy., 37, e2022GB007672, https://doi.org/10.1029/2022GB007672, 2023.

Knor, L. A. C. M., Sabine, C. L., Dore, J. E., White, A. E., and Potemra, J.: Drivers and variability of intensified subsurface ocean acidification trends at Station ALOHA, J. Geophys. Res.-Oceans, 130, e2024JC022251, https://doi.org/10.1029/2024JC022251, 2025.

Kwiatkowski, L., Torres, O., Bopp, L., Aumont, O., Chamberlain, M., Christian, J. R., Dunne, J. P., Gehlen, M., Ilyina, T., John, J. G., Lenton, A., Li, H., Lovenduski, N. S., Orr, J. C., Palmieri, J., Santana-Falcón, Y., Schwinger, J., Séférian, R., Stock, C. A., Tagliabue, A., Takano, Y., Tjiputra, J., Toyama, K., Tsujino, H., Watanabe, M., Yamamoto, A., Yool, A., and Ziehn, T.: Twenty-first century ocean warming, acidification, deoxygenation, and upper-ocean nutrient and primary production decline from CMIP6 model projections, Biogeosciences, 17, 3439–3470, https://doi.org/10.5194/bg-17-3439-2020, 2020.

Landschützer, P., Gruber, N., Bakker, D. C. E., Schuster, U., Nakaoka, S., Payne, M. R., Sasse, T., and Zeng, J.: A neural network-based estimate of the seasonal to inter-annual variability of the Atlantic Ocean carbon sink, Biogeosciences, 10, 7793–7815, https://doi.org/10.5194/bg-10-7793-2013, 2013.

Landschützer, P., Gruber, N., Bakker, D. C. E., and Schuster, U.: Recent variability of the Global Ocean Carbon Sink, Global Biogeochem. Cy., 28, 927–949, https://doi.org/10.1002/2014gb004853, 2014.

Landschützer, P., Gruber, N., and Bakker, D. C. E.: Decadal variations and trends of the Global Ocean Carbon Sink, Global Biogeochem. Cy., 30, 1396–1417, https://doi.org/10.1002/2015gb005359, 2016.

Landschützer, P., Laruelle, G. G., Roobaert, A., and Regnier, P.: A uniform pCO_2 climatology combining open and coastal oceans, Earth Syst. Sci. Data, 12, 2537–2553, https://doi.org/10.5194/essd-12-2537-2020, 2020a.

Landschützer, P., Laruelle, G. G., Roobaert, A., and Regnier, P.: A combined global ocean pCO_2 climatology combining open ocean and coastal areas (NCEI Accession 0209633), NOAA National Centers for Environmental Information [data set], https://doi.org/10.25921/qb25-f418, 2020b.

Lange, N., Tanhua, T., Pfeil, B., Bange, H. W., Lauvset, S. K., Grégoire, M., Bakker, D. C., Jones, S. D., Fiedler, B., O'Brien, K. M., and Körtzinger, A.: A status assessment of selected data synthesis products for ocean biogeochemistry, Front. Mar. Sci., 10, https://doi.org/10.3389/fmars.2023.1078908, 2023.

Lange, N., Fiedler, B., Álvarez, M., Benoit-Cattin, A., Benway, H., Buttigieg, P. L., Coppola, L., Currie, K., Flecha, S., Gerlach, D. S., Honda, M., Huertas, I. E., Lauvset, S. K., Muller-Karger, F., Körtzinger, A., O'Brien, K. M., Ólafsdóttir, S. R., Pacheco, F. C., Rueda-Roa, D., Skjelvan, I., Wakita, M., White, A., and Tanhua, T.: Synthesis product for ocean time series (spots) – a ship-based biogeochemical pilot, Earth Syst. Sci. Data, 16, 1901–1931, https://doi.org/10.5194/essd-16-1901-2024, 2024a.

Lange, N., Fiedler, B., Álvarez, M., Benoit-Cattin, A., Benway, H., Buttigieg, P. L., Coppola, L., Currie, K. I., Flecha, S., Gerlach, D. S., Honda, M. C., Huertas, E. I., Kinkade, D., Muller-Karger, F., Lauvset, S. K., Körtzinger, A., O'Brien, K. M., Ólafsdóttir, S., Pacheco, F. C., Rueda-Roa, D., Skjelvan, I., Wakita, M., White, A. E., and Tanhua, T.: Synthesis Product for Ocean Time Series (SPOTS), Biological and Chemical Oceanography Data Management Office (BCO-DMO), (Version 2) Version Date 2024-02-22, BCO-DMO – Biological and Chemical Oceanography Data Management Office [data set], https://doi.org/10.26008/1912/bco-dmo.896862.2, 2024b.

Laruelle, G. G., Landschützer, P., Gruber, N., Tison, J.-L., Delille, B., and Regnier, P.: Global high-resolution monthly pCO_2 climatology for the coastal ocean derived from neural network interpolation, Biogeosciences, 14, 4545–4561, https://doi.org/10.5194/bg-14-4545-2017, 2017.

Lauvset, S. K. and Tanhua, T.: A toolbox for secondary quality control on ocean chemistry and Hydrographic Data, Limnol. Oceanogr.: Meth., 13, 601–608, https://doi.org/10.1002/lom3.10050, 2015.

Lauvset, S. K., Key, R. M., Olsen, A., van Heuven, S., Velo, A., Lin, X., Schirnick, C., Kozyr, A., Tanhua, T., Hoppema, M., Jutterström, S., Steinfeldt, R., Jeansson, E., Ishii, M., Perez, F. F., Suzuki, T., and Watelet, S.: A new global interior ocean mapped climatology: The $1^\circ \times 1^\circ$ GLODAP version 2, Earth Syst. Sci. Data, 8, 325–340, https://doi.org/10.5194/essd-8-325-2016, 2016.

Lauvset, S. K., Lange, N., Tanhua, T., Bittig, H. C., Olsen, A., Kozyr, A., Álvarez, M., Becker, S., Brown, P. J., Carter, B. R., Cotrim da Cunha, L., Feely, R. A., van Heuven, S., Hoppema, M., Ishii, M., Jeansson, E., Jutterström, S., Jones, S. D., Karlsen, M. K., Lo Monaco, C., Michaelis, P., Murata, A., Pérez, F. F., Pfeil, B., Schirnick, C., Steinfeldt, R., Suzuki, T., Tilbrook, B., Velo, A., Wanninkhof, R., Woosley, R. J., and Key, R. M.: An updated version of the global interior ocean biogeochemical data product, GLODAPv2.2021, Earth Syst. Sci. Data, 13, 5565–5589, https://doi.org/10.5194/essd-13-5565-2021, 2021.

Lauvset, S. K., Lange, N., Tanhua, T., Bittig, H. C., Olsen, A., Kozyr, A., Alin, S., Álvarez, M., Azetsu-Scott, K., Barbero, L., Becker, S., Brown, P. J., Carter, B. R., da Cunha, L. C., Feely, R. A., Hoppema, M., Humphreys, M. P., Ishii, M., Jeansson, E., Jiang, L.-Q., Jones, S. D., Lo Monaco, C., Murata, A., Müller, J. D., Pérez, F. F., Pfeil, B., Schirnick, C., Steinfeldt, R., Suzuki, T., Tilbrook, B., Ulfsbo, A., Velo, A., Woosley, R. J., and Key, R. M.: GLODAPv2.2022: the latest version of the global interior ocean biogeochemical data product, Earth Syst. Sci. Data, 14, 5543–5572, https://doi.org/10.5194/essd-14-5543-2022, 2022.

Lauvset, S. K., Key, R. M., Olsen, A., van Heuven, S. M. A. C., Velo, A., Lin, X., Schirnick, C., Kozyr, A., Tanhua, T., Hoppema, M., Jutterström, S., Steinfeldt, R., Jeansson, E., Ishii, M., Pérez, F. F., Suzuki, T., and Watelet, S.: A new global inte-

rior ocean mapped climatology: the 1° × 1° GLODAP version 2 from 1972-01-01 to 2013-12-31 (NCEI Accession 0286118), NOAA National Centers for Environmental Information [data set], https://doi.org/10.3334/cdiac/otg.ndp093_glodapv2, 2023a.

Lauvset, S. K., Lange, N., Tanhua, T., Bittig, H. C., Olsen, A., Kozyr, A., Álvarez, M., Azetsu-Scott, K., Becker, S., Brown, P. J., Carter, B. R., Cotrim da Cunha, L., Feely, R. A., Hoppema, M., Humphreys, M. P., Ishii, M., Jeansson, E., Jones, S. D., Lo Monaco, C. Murata, A., Müller, J. D., Pérez, F. F., Schirnick, C., Steinfeldt, R., Suzuki, T., Tilbrook, B., Ulfsbo, A., Velo, A., Woosley, R. J., and Key, R. M.: Global Ocean Data Analysis Project version 2.2023 (GLODAPv2.2023) (NCEI Accession 0283442), NOAA National Centers for Environmental Information [data set], https://doi.org/10.25921/zyrq-ht66, 2023b.

Lauvset, S. K., Lange, N., Tanhua, T., Bittig, H. C., Olsen, A., Kozyr, A., Álvarez, M., Azetsu-Scott, K., Brown, P. J., Carter, B. R., Cotrim da Cunha, L., Hoppema, M., Humphreys, M. P., Ishii, M., Jeansson, E., Murata, A., Müller, J. D., Pérez, F. F., Schirnick, C., Steinfeldt, R., Suzuki, T., Ulfsbo, A., Velo, A., Woosley, R. J., and Key, R. M.: The annual update GLODAPv2.2023: the global interior ocean biogeochemical data product, Earth Syst. Sci. Data, 16, 2047–2072, https://doi.org/10.5194/essd-16-2047-2024, 2024.

Lee, C.-H., Subhas, A. V., Kim, J.-H., and Lee, K.: Ocean carbon dioxide removal and storage, Chem. Rev., https://doi.org/10.1021/acs.chemrev.5c00433, in press, 2026.

Lee, K., Tong, L. T., Millero, F. J., Sabine, C. L., Dickson, A. G., Goyet, C., Park, G., Wanninkhof, R., Feely, R. A., and Key, R. M.: Global relationships of total alkalinity with salinity and temperature in surface waters of the world's oceans, Geophys. Res. Lett., 33, https://doi.org/10.1029/2006gl027207, 2006.

Lewis, E. and Wallace, D. W. R.: Program Developed for CO_2 System Calculations, ORNL/CDIAC-105, Carbon Dioxide Information Analysis Center, Oak Ridge National Laboratory, Oak Ridge, TN, https://www.ncei.noaa.gov/access/ocean-carbon-acidification-data-system/oceans/CO2SYS/co2rprt.html (last access: 7 January 2026), 1998.

Locarnini, R. A., Mishonov, A. V., Antonov, J. I., Boyer, T. P., Garcia, H. E., Baranova, O. K., Zweng, M. M., Paver, C. R., Reagan, J. R., Johnson, D. R., Hamilton, M., and Seidov, D.: World Ocean Atlas 2013, in: Volume 1: Temperature, NOAA Atlas NESDIS 73, edited by: Levitus, S. and Mishonov, A., NOAA, 40 pp., https://doi.org/10.7289/V55X26VD, 2013.

Locarnini, R. A., Mishonov, A. V., Baranova, O. K., Boyer, T., P., Zweng, M. M., Garcia, H. E., Reagan, J. R., Seidov, D., Weathers, K. W., Paver, C. R., and Smolyar, I. V.: World Ocean Atlas 2018, in: Volume 1: Temperature, NOAA Atlas NESDIS 81, edited by: Mishonov, A., NOAA, https://doi.org/10.25923/e5rn-9711, 2019.

Ma, D., Gregor, L., and Gruber, N.: Four decades of trends and drivers of global surface ocean acidification, Global Biogeochem. Cy., 37, https://doi.org/10.1029/2023gb007765, 2023.

Manzello, D. P., Enochs, I. C., and Hendee, J. C.: National Coral Reef Monitoring Program: Carbonate chemistry data collected in the Atlantic Ocean, NOAA National Centers for Environmental Information [data set], https://doi.org/10.25921/vfz0-dg77, 2018.

Mercier, H., Desbruyères, D., Lherminier, P., Velo, A., Carracedo, L., Fontela, M., and Pérez, F. F.: New insights into the eastern subpolar North Atlantic Meridional overturning circulation from OVIDE, Ocean Sci., 20, 779–797, https://doi.org/10.5194/os-20-779-2024, 2024.

Metzl, N., Tilbrook, B., Bakker, D., le Quéré, C., Doney, S., Feely, R., Hood, M., and Dargaville, R.: Surface Ocean CO_2 variability and Vulnerability Workshop, Paris, France, 11–14 April 2007, Eos Trans. Am. Geophys. Union, 88, 287–287, https://doi.org/10.1029/2007eo280005, 2007.

Metzl, N., Fin, J., Lo Monaco, C., Mignon, C., Alliouane, S., Antoine, D., Bourdin, G., Boutin, J., Bozec, Y., Conan, P., Coppola, L., Diaz, F., Douville, E., Durrieu de Madron, X., Gattuso, J.-P., Gazeau, F., Golbol, M., Lansard, B., Lefèvre, D., Lefèvre, N., Lombard, F., Louanchi, F., Merlivat, L., Olivier, L., Petrenko, A., Petton, S., Pujo-Pay, M., Rabouille, C., Reverdin, G., Ridame, C., Tribollet, A., Vellucci, V., Wagener, T., and Wimart-Rousseau, C.: A synthesis of ocean total alkalinity and dissolved inorganic carbon measurements from 1993 to 2022: the SNAPO-CO_2-v1 dataset, SEANOE [data set], https://doi.org/10.17882/95414, 2023.

Metzl, N., Fin, J., Lo Monaco, C., Mignon, C., Alliouane, S., Antoine, D., Bourdin, G., Boutin, J., Bozec, Y., Conan, P., Coppola, L., Diaz, F., Douville, E., Durrieu de Madron, X., Gattuso, J.-P., Gazeau, F., Golbol, M., Lansard, B., Lefèvre, D., Lefèvre, N., Lombard, F., Louanchi, F., Merlivat, L., Olivier, L., Petrenko, A., Petton, S., Pujo-Pay, M., Rabouille, C., Reverdin, G., Ridame, C., Tribollet, A., Vellucci, V., Wagener, T., and Wimart-Rousseau, C.: A synthesis of ocean total alkalinity and dissolved inorganic carbon measurements from 1993 to 2022: the SNAPO-CO2-v1 dataset, Earth Syst. Sci. Data, 16, 89–120, https://doi.org/10.5194/essd-16-89-2024, 2024.

Mishonov, A. V., Boyer, T. P., Baranova, O. K., Bouchard, C. N., Cross, S. L., Garcia H. E., Locarnini, R. A., Paver, C. R., Wang, Z., Seidov, D., Grodsky, A. I., and Beauchamp, J. G.: World Ocean Database 2023, in: NOAA Atlas NESDIS 97, edited by: Bouchard, C., NOAA, 20 pp., https://doi.org/10.25923/z885-h264, 2024.

Monacci, N. M., Cross, J. N., Danielson, S. L., Evans, W., Hopcroft, R. R., Mathis, J. T., Mordy, C. W., Naber, D. D., Shake, K. L., Trahanovsky, K., Wang, H., Weingartner, T. J., and Whitledge, T. E.: Marine carbonate system discrete profile data from the Gulf of Alaska (GAK) Seward Line cruises between 2008 and 2017 (NCEI Accession 0277034), NOAA National Centers for Environmental Information [data set], https://doi.org/10.25921/x9sg-9b08, 2023.

Monacci, N. M., Cross, J. N., Evans, W., Mathis, J. T., and Wang, H.: A decade of marine inorganic carbon chemistry observations in the northern Gulf of Alaska – insights into an environment in transition, Earth Syst. Sci. Data, 16, 647–665, https://doi.org/10.5194/essd-16-647-2024, 2024.

Müller, J. D.: RECCAP2-ocean data collection, Zenodo [data set], https://doi.org/10.5281/zenodo.7990823, 2023.

Müller, J. D. and Gruber, N.: Progression of ocean interior acidification over the industrial era, Sci. Adv., 10, https://doi.org/10.1126/sciadv.ado3103, 2024a.

Müller, J. D. and Gruber, N.: Progression of Ocean Interior Acidification over the Industrial Era from 1800-07-01 to 2014-06-30 (NCEI Accession 0298993), NOAA National Centers for Environmental Information [data set], https://doi.org/10.25921/tefm-x802, 2024b.

Müller, J. D., Gruber, N., Carter, B., Feely, R., Ishii, M., Lange, N., Lauvset, S. K., Murata, A., Olsen, A., Pérez, F. F., Sabine, C., Tanhua, T., Wanninkhof, R., and Zhu, D.: Decadal trends in the oceanic storage of anthropogenic carbon from 1994 to 2014, AGU Adv., 4, https://doi.org/10.1029/2023av000875, 2023a.

Müller, J. D., Gruber, N., Carter, B. R., Feely, R. A., Ishii, M., Lange, N., Lauvset, S. K., Murata, A., Olsen, A., Pérez, F. F., Sabine, C. L., Tanhua, T., Wanninkhof, R., and Zhu, D.: Decadal Trends in the Oceanic Storage of Anthropogenic Carbon from 1994 to 2014 (NCEI Accession 0279447), NOAA National Centers for Environmental Information [data set], https://doi.org/10.25921/ppcf-w020, 2023b.

Olsen, A., Key, R. M., van Heuven, S., Lauvset, S. K., Velo, A., Lin, X., Schirnick, C., Kozyr, A., Tanhua, T., Hoppema, M., Jutterström, S., Steinfeldt, R., Jeansson, E., Ishii, M., Pérez, F. F., and Suzuki, T.: The Global Ocean Data Analysis Project version 2 (GLODAPv2) – an internally consistent data product for the world ocean, Earth Syst. Sci. Data, 8, 297–323, https://doi.org/10.5194/essd-8-297-2016, 2016.

Olsen, A., Lange, N., Key, R. M., Tanhua, T., Álvarez, M., Becker, S., Bittig, H. C., Carter, B. R., Cotrim da Cunha, L., Feely, R. A., van Heuven, S., Hoppema, M., Ishii, M., Jeansson, E., Jones, S. D., Jutterström, S., Karlsen, M. K., Kozyr, A., Lauvset, S. K., Lo Monaco, C., Murata, A., Pérez, F. F., Pfeil, B., Schirnick, C., Steinfeldt, R., Suzuki, T., Telszewski, M., Tilbrook, B., Velo, A., and Wanninkhof, R.: GLODAPv2.2019 – an update of GLODAPv2, Earth Syst. Sci. Data, 11, 1437–1461, https://doi.org/10.5194/essd-11-1437-2019, 2019.

Olsen, A., Lange, N., Key, R. M., Tanhua, T., Bittig, H. C., Kozyr, A., Álvarez, M., Azetsu-Scott, K., Becker, S., Brown, P. J., Carter, B. R., Cotrim da Cunha, L., Feely, R. A., van Heuven, S., Hoppema, M., Ishii, M., Jeansson, E., Jutterström, S., Landa, C. S., Lauvset, S. K., Michaelis, P., Murata, A., Pérez, F. F., Pfeil, B., Schirnick, C., Steinfeldt, R., Suzuki, T., Tilbrook, B., Velo, A., Wanninkhof, R., and Woosley, R. J.: An updated version of the global interior ocean biogeochemical data product, GLODAPv2.2020, Earth Syst. Sci. Data, 12, 3653–3678, https://doi.org/10.5194/essd-12-3653-2020, 2020.

Orr, J. C., Fabry, V. J., Aumont, O., Bopp, L., Doney, S. C., Feely, R. A., Gnanadesikan, A., Gruber, N., Ishida, A., Joos, F., Key, R. M., Lindsay, K., Maier-Reimer, E., Matear, R., Monfray, P., Mouchet, A., Najjar, R. G., Plattner, G.-K., Rodgers, K. B., Sabine, C. L., Sarmiento, J. L., Schlitzer, R., Slater, R. D., Totterdell, I. J., Weirig, M.-F., Yamanaka, Y., and Yool, A.: Anthropogenic ocean acidification over the twenty-first century and its impact on calcifying organisms, Nature, 437, 681–686, https://doi.org/10.1038/nature04095, 2005.

Orr, J. C., Epitalon, J.-M., and Gattuso, J.-P.: Comparison of ten packages that compute ocean carbonate chemistry, Biogeosciences, 12, 1483–1510, https://doi.org/10.5194/bg-12-1483-2015, 2015.

Orr, J. C., Epitalon, J.-M., Dickson, A. G., and Gattuso, J.-P.: Routine uncertainty propagation for the Marine Carbon Dioxide System, Mar. Chem., 207, 84–107, https://doi.org/10.1016/j.marchem.2018.10.006, 2018.

Oschlies, A., Bach, L. T., Fennel, K., Gattuso, J.-P., and Mengis, N.: Perspectives and challenges of marine carbon dioxide removal, Front. Clim., 6, https://doi.org/10.3389/fclim.2024.1506181, 2025.

Padin, X. A., Velo, A., and Pérez, F. F.: Arios: A database for ocean acidification assessment in the Iberian Upwelling System (1976–2018), Earth Syst. Sci. Data, 12, 2647–2663, https://doi.org/10.5194/essd-12-2647-2020, 2020.

Palacio-Castro, A. M., Enochs, I. C., Besemer, N., Boyd, A., Jankulak, M., Kolodziej, G., Hirsh, H. K., Webb, A. E., Towle, E. K., Kelble, C., Smith, I., and Manzello, D. P.: Coral Reef carbonate chemistry reveals interannual, seasonal, and spatial impacts on ocean acidification off Florida, Global Biogeochemi. Cy., 37, https://doi.org/10.1029/2023gb007789, 2023.

Pérez, F. F., Fontela, M., García-Ibáñez, M. I., Mercier, H., Velo, A., Lherminier, P., Zunino, P., de la Paz, M., Alonso-Pérez, F., Guallart, E. F., and Padin, X. A.: Meridional overturning circulation conveys fast acidification to the deep Atlantic Ocean, Nature, 554, 515–518, https://doi.org/10.1038/nature25493, 2018.

Pérez, F. F., Velo, A., Padin, X. A., Doval, M. D., and Prego, R.: ARIOS Database: An Acidification Ocean Database for the Galician Upwelling Ecosystem, Instituto de Investigacións Marinas, CSIC – Consejo Superior de Investigaciones Cientificas, https://doi.org/10.20350/digitalCSIC/12498, 2020.

Pérez, F. F., Olafsson, J., Ólafsdóttir, S. R., Fontela, M., and Takahashi, T.: Contrasting drivers and trends of ocean acidification in the Subarctic Atlantic, Sci. Rep., 11, https://doi.org/10.1038/s41598-021-93324-3, 2021.

Pfeil, B., Olsen, A., Bakker, D. C. E., Hankin, S., Koyuk, H., Kozyr, A., Malczyk, J., Manke, A., Metzl, N., Sabine, C. L., Akl, J., Alin, S. R., Bates, N., Bellerby, R. G. J., Borges, A., Boutin, J., Brown, P. J., Cai, W.-J., Chavez, F. P., Chen, A., Cosca, C., Fassbender, A. J., Feely, R. A., González-Dávila, M., Goyet, C., Hales, B., Hardman-Mountford, N., Heinze, C., Hood, M., Hoppema, M., Hunt, C. W., Hydes, D., Ishii, M., Johannessen, T., Jones, S. D., Key, R. M., Körtzinger, A., Landschützer, P., Lauvset, S. K., Lefèvre, N., Lenton, A., Lourantou, A., Merlivat, L., Midorikawa, T., Mintrop, L., Miyazaki, C., Murata, A., Nakadate, A., Nakano, Y., Nakaoka, S., Nojiri, Y., Omar, A. M., Padin, X. A., Park, G.-H., Paterson, K., Perez, F. F., Pierrot, D., Poisson, A., Ríos, A. F., Santana-Casiano, J. M., Salisbury, J., Sarma, V. V. S. S., Schlitzer, R., Schneider, B., Schuster, U., Sieger, R., Skjelvan, I., Steinhoff, T., Suzuki, T., Takahashi, T., Tedesco, K., Telszewski, M., Thomas, H., Tilbrook, B., Tjiputra, J., Vandemark, D., Veness, T., Wanninkhof, R., Watson, A. J., Weiss, R., Wong, C. S., and Yoshikawa-Inoue, H.: A uniform, quality controlled Surface Ocean CO_2 Atlas (SOCAT), Earth Syst. Sci. Data, 5, 125–143, https://doi.org/10.5194/essd-5-125-2013, 2013.

Qi, D., Chen, L., Chen, B., Gao, Z., Zhong, W., Feely, R. A., Anderson, L. G., Sun, H., Chen, J., Chen, M., Zhan, L., Zhang, Y., and Cai, W.-J.: Increase in acidifying water in the Western Arctic ocean, Nat. Clim. Change, 7, 195–199, https://doi.org/10.1038/nclimate3228, 2017.

Qi, D., Ouyang, Z., Chen, L., Wu, Y., Lei, R., Chen, B., Feely, R. A., Anderson, L. G., Zhong, W., Lin, H., Polukhin, A., Zhang, Y., Zhang, Y., Bi, H., Lin, X., Luo, Y., Zhuang, Y., He, J., Chen, J., and Cai, W.-J.: Climate change drives rapid decadal acidification in the Arctic Ocean from 1994 to 2020, Science, 377, 1544–1550, https://doi.org/10.1126/science.abo0383, 2022.

Resplandy, L., Hogikyan, A., Müller, J. D., Najjar, R. G., Bange, H. W., Bianchi, D., Weber, T., Cai, W. -J., Doney, S. C., Fennel, K., Gehlen, M., Hauck, J., Lacroix, F., Landschützer, P., Le Quéré, C., Roobaert, A., Schwinger, J., Berthet, S., Bopp,

L., Chau, T. T. T., Dai, M., Gruber, N., Ilyina, T., Kock, A., Manizza, M., Lachkar, Z., Laruelle, G. G., Liao, E., Lima, I. D., Nissen, C., Rödenbeck, C., Séférian, R., Toyama, K., Tsujino, H., and Regnier, P.: A synthesis of global coastal Ocean Greenhouse Gas Fluxes, Global Biogeochem. Cy., 38, https://doi.org/10.1029/2023gb007803, 2024.

Revelle, R. and Suess, H. E.: Carbon dioxide exchange between atmosphere and ocean and the question of an increase of atmospheric CO_2 during the past decades, Tellus, 9, 18–27, https://doi.org/10.1111/j.2153-3490.1957.tb01849.x, 1957.

Rödenbeck, C.: Jena CarboScope: pCO_2-based ocean mixed-layer scheme, Max Planck Institute for Biogeochemistry [data set], https://doi.org/10.17871/CarboScope-oc_v2024E, 2024.

Rödenbeck, C., Keeling, R. F., Bakker, D. C., Metzl, N., Olsen, A., Sabine, C., and Heimann, M.: Global surface-ocean pCO_2 and sea-air CO_2 flux variability from an observation-driven ocean mixed-layer scheme, Ocean Sci., 9, 193–216, https://doi.org/10.5194/os-9-193-2013, 2013.

Rödenbeck, C., DeVries, T., Hauck, J., Le Quéré, C., and Keeling, R. F.: Data-based estimates of interannual sea-air CO_2 flux variations 1957–2020 and their relation to environmental drivers, Biogeosciences, 19, 2627–2652, https://doi.org/10.5194/bg-19-2627-2022, 2022.

Roobaert, A., Regnier, P., Landschützer, P., and Laruelle, G. G.: A novel sea surface partial pressure of carbon dioxide (pCO_2) data product for the global coastal ocean resolving trends over the 1982–2020 period (NCEI Accession 0279118), NOAA National Centers for Environmental Information [data set], https://doi.org/10.25921/4sde-p068, 2023.

Roobaert, A., Regnier, P., Landschützer, P., and Laruelle, G. G.: A novel sea surface pCO_2-product for the global coastal ocean resolving trends over 1982–2020, Earth Syst. Sci. Data, 16, 421–441, https://doi.org/10.5194/essd-16-421-2024, 2024.

Sabine, C. L., Feely, R. A., Gruber, N., Key, R. M., Lee, K., Bullister, J. L., Wanninkhof, R., Wong, C. S., Wallace, D. W., Tilbrook, B., Millero, F. J., Peng, T.-H., Kozyr, A., Ono, T., and Rios, A. F.: The oceanic sink for anthropogenic CO_2, Science, 305, 367–371, https://doi.org/10.1126/science.1097403, 2004.

Sabine, C. L., Feely, R. A., Key, R. M., Wanninkhof, R., Millero, F. J., and Kozyr, A.: GLobal Ocean Data Analysis Project (GLODAP) version 1.1 (NCEI Accession 0001644), NOAA National Centers for Environmental Information [data set], https://doi.org/10.25921/pkjs-5w29, 2005.

Sabine, C. L., Feely, R. A., Millero, F. J., Dickson, A. G., Langdon, C., Mecking, S., and Greeley, D.: Decadal changes in Pacific Carbon, J. Geophys. Res.-Oceans, 113, https://doi.org/10.1029/2007jc004577, 2008.

Sabine, C. L., Hankin, S., Koyuk, H., Bakker, D. C. E., Pfeil, B., Olsen, A., Metzl, N., Kozyr, A., Fassbender, A., Manke, A., Malczyk, J., Akl, J., Alin, S. R., Bellerby, R. G. J., Borges, A., Boutin, J., Brown, P. J., Cai, W.-J., Chavez, F. P., Chen, A., Cosca, C., Feely, R. A., González-Dávila, M., Goyet, C., Hardman-Mountford, N., Heinze, C., Hoppema, M., Hunt, C. W., Hydes, D., Ishii, M., Johannessen, T., Key, R. M., Körtzinger, A., Landschützer, P., Lauvset, S. K., Lefèvre, N., Lenton, A., Lourantou, A., Merlivat, L., Midorikawa, T., Mintrop, L., Miyazaki, C., Murata, A., Nakadate, A., Nakano, Y., Nakaoka, S., Nojiri, Y., Omar, A. M., Padin, X. A., Park, G.-H., Paterson, K., Perez, F. F., Pierrot, D., Poisson, A., Ríos, A. F., Salisbury, J., Santana-Casiano, J. M., Sarma, V. V. S. S., Schlitzer, R., Schneider, B., Schuster, U., Sieger, R., Skjelvan, I., Steinhoff, T., Suzuki, T., Takahashi, T., Tedesco, K., Telszewski, M., Thomas, H., Tilbrook, B., Vandemark, D., Veness, T., Watson, A. J., Weiss, R., Wong, C. S., and Yoshikawa-Inoue, H.: Surface Ocean CO_2 Atlas (SOCAT) gridded data products, Earth Syst. Sci. Data, 5, 145–153, https://doi.org/10.5194/essd-5-145-2013, 2013.

Sarma, V. V. S. S., Krishna, M. S., Paul, Y. S., and Murty, V. S. N.: Observed changes in ocean acidity and carbon dioxide exchange in the coastal bay of Bengal – A link to air pollution, Tellus B, 67, 24638, https://doi.org/10.3402/tellusb.v67.24638, 2015.

Schimel, D. S. and Carroll, D.: Carbon cycle–climate feedbacks in the post-paris world, Annu. Rev. Earth Planet. Sci., 52, https://doi.org/10.1146/annurev-earth-031621-081700, 2024.

Schoderer, M., Bittig, H., Klein, B., Hägele, R., Steinhoff, T., Castro-Morales, K., Cotrim da Cunha, L., Hornidge, A., and Körtzinger, A.: From individual observations to global assessments: Tracing the Marine Carbon Knowledge Value Chain, Ocean Soc., 2, https://doi.org/10.17645/oas.8891, 2024.

Sharp, J. D., Pierrot, D., Humphreys, M. P., Epitalon, J.-M., Orr, J. C., Lewis, E. R., and Wallace, D. W. R.: CO2SYSv3 for MATLAB (Version v3.2.1), Zenodo [code], https://doi.org/10.5281/zenodo.3950562, 2023.

Sharp, J. D., Jiang, L.-Q., Carter, B. R., Lavin, P. D., Yoo, H., and Cross, S. L.: A mapped dataset of surface ocean acidification indicators in large marine ecosystems of the United States, Sci. Data, 11, 715, https://doi.org/10.1038/s41597-024-03530-7, 2024a.

Sharp, J. D., Jiang, L-Q., Carter, B. R., Lavin, P. D., Yoo, H., and Cross, S. L.: RFR-LME Ocean Acidification Indicators from 1998 to 2023 (NCEI Accession 0287551), NOAA National Centers for Environmental Information [data set], https://doi.org/10.25921/h8vw-e872, 2024b.

Sridevi, B. and Sarma, V. V. S. S.: Role of river discharge and warming on ocean acidification and pCO_2 levels in the Bay of Bengal, Tellus B, 73, 1–20, https://doi.org/10.1080/16000889.2021.1971924, 2021.

Steinberg, D. K. and Cope, J.: Zooplankton biomass measured from net tows conducted during ongoing monthly cruises, from April 1994 to December 2024, at the Bermuda Atlantic Time-series Study (BATS) site in the Sargasso Sea, (Version 6) Version Date 2025-07-16, Biological and Chemical Oceanography Data Management Office (BCO-DMO) [data set], https://doi.org/10.26008/1912/bco-dmo.881861.6, 2025.

Sutton, A. J., Feely, R. A., Maenner-Jones, S., Musielwicz, S., Osborne, J., Dietrich, C., Monacci, N., Cross, J., Bott, R., and Kozyr, A.: Autonomous seawater partial pressure of carbon dioxide (pCO_2) and pH time series from 40 surface buoys between 2004 and 2017 (NCEI Accession 0173932), NOAA National Centers for Environmental Information [data set], https://doi.org/10.7289/v5db8043, 2018.

Sutton, A. J., Feely, R. A., Maenner-Jones, S., Musielwicz, S., Osborne, J., Dietrich, C., Monacci, N., Cross, J., Bott, R., Kozyr, A., Andersson, A. J., Bates, N. R., Cai, W.-J., Cronin, M. F., De Carlo, E. H., Hales, B., Howden, S. D., Lee, C. M., Manzello, D. P., McPhaden, M. J., Meléndez, M., Mickett, J. B., Newton, J. A., Noakes, S. E., Noh, J. H., Olafsdottir, S. R., Salisbury, J. E., Send, U., Trull, T. W., Vandemark, D. C., and Weller, R. A.:

Autonomous seawater pCO_2 and pH time series from 40 surface buoys and the emergence of anthropogenic trends, Earth Syst. Sci. Data, 11, 421–439, https://doi.org/10.5194/essd-11-421-2019, 2019.

Suzuki, T., Ishii, M., Aoyama, M., Christian, J. R., Enyo, K., Kawano, T., Key, R. M., Kosugi, N., Kozyr, A., Miller, L. A., Murata, A., Nakano, T., Ono, T., Saino, T., Sasaki, K., Sasano, D., Takatani, Y., Wakita, M., and Sabine, C. L. The Pac:ific Ocean Interior Carbon (PACIFICA) Database (NCEI Accession 0110865), NOAA National Centers for Environmental Information [data set], https://doi.org/10.25921/n9nn-8324, 2013.

Swift, J. and Osborne, J.: The Java OceanAtlas Suite, https://joa.ucsd.edu (last access: 8 February 2025), 2025.

Takahashi, T., Feely, R. A., Weiss, R. F., Wanninkhof, R. H., Chipman, D. W., Sutherland, S. C., and Takahashi, T. T.: Global Air–sea Flux of CO_2: An estimate based on measurements of sea–air pCO_2 difference, P. Natl. Acad. Sci. USA, 94, 8292–8299, https://doi.org/10.1073/pnas.94.16.8292, 1997.

Takahashi, T., Sutherland, S. C., Sweeney, C., Poisson, A., Metzl, N., Tilbrook, B., Bates, N., Wanninkhof, R., Feely, R. A., Sabine, C., Olafsson, J., and Nojiri, Y.: Global sea–air CO_2 flux based on climatological surface ocean pCO_2, and seasonal biological and temperature effects, Deep-Sea Res. Pt. II, 49, 1601–1622, https://doi.org/10.1016/s0967-0645(02)00003-6, 2002.

Takahashi, T., Sutherland, S. C., Wanninkhof, R., Sweeney, C., Feely, R. A., Chipman, D. W., Hales, B., Friederich, G., Chavez, F., Sabine, C., Watson, A., Bakker, D. C. E., Schuster, U., Metzl, N., Yoshikawa-Inoue, H., Ishii, M., Midorikawa, T., Nojiri, Y., Körtzinger, A., Steinhoff, T., and de Baar, H. J. W.: Climatological mean and decadal change in Surface Ocean pCO_2, and net sea–air CO_2 flux over the Global Oceans, Deep-Sea Res. Pt. II, 56, 554–577, https://doi.org/10.1016/j.dsr2.2008.12.009, 2009.

Takahashi, T., Sutherland, S. C., and Kozyr, A.: LDEO Database (Version 2019): Global Ocean Surface Water Partial Pressure of CO_2 Database: Measurements Performed During 1957–2019 (NCEI Accession 0160492), NOAA National Centers for Environmental Information [data set], https://doi.org/10.3334/cdiac/otg.ndp088(v2015), 2017.

Takano, Y., Ilyina, T., Tjiputra, J., Eddebbar, Y. A., Berthet, S., Bopp, L., Buitenhuis, E., Butenschön, M., Christian, J. R., Dunne, J. P., Gröger, M., Hayashida, H., Hieronymus, J., Koenigk, T., Krasting, J. P., Long, M. C., Lovato, T., Nakano, H., Palmieri, J., Schwinger, J., Séférian, R., Suntharalingam, P., Tatebe, H., Tsujino, H., Urakawa, S., Watanabe, M., and Yool, A.: Simulations of ocean deoxygenation in the historical era: insights from forced and coupled models, Front. Mar. Sci., 10, 1139917, https://doi.org/10.3389/fmars.2023.1139917, 2023.

Tanhua, T., Jones, E. P., Jeansson, E., Jutterström, S., Smethie, W. M., Wallace, D. W., and Anderson, L. G.: Ventilation of the Arctic Ocean: Mean ages and inventories of Anthropogenic CO_2 and CFC-11, J. Geophys. Res.-Oceans, 114, https://doi.org/10.1029/2008jc004868, 2009.

Tanhua, T., van Heuven, S., Key, R. M., Velo, A., Olsen, A., and Schirnick, C.: Quality control procedures and methods of the CARINA database, Earth Syst. Sci. Data, 2, 35–49, https://doi.org/10.5194/essd-2-35-2010, 2010.

Tanhua, T., Olsen, A., Hoppema, M., Jutterström, S., Schirnick, C., van Heuven, S. M. A. C., Velo, A., Lin, X., Kozyr, A., Álvarez, M., Bakker, D. C. E., Brown, P. J., Falck, E., Jeansson, E., Lo Monaco, C., Ólafsson, J., Pérez, F. F., Pierrot, D., Ríos, A. F., Sabine, C. L., Schuster, U., Steinfeldt, R., Stendardo, I., Anderson, L. G., Bates, N., Bellerby, R. G. J., Blindheim, J., Bullister, J. L., Gruber, N., Ishii, M., Johannessen, T., Jones, E. P., Köhler, J., Körtzinger, A., Metzl, N., Murata, A., Musielewicz, S., Omar, A. M., Olsson, K. A., de la Paz, M., Pfeil, B., Rey, F., Rhein, M., Skjelvan, I., Tilbrook, B., Wanninkhof, R., Mintrop, L. J., Wallace, D. W. R., and Key, R. M.: The CARbon dioxide IN the Atlantic Ocean (CARINA) Database V1.1 2010 (NCEI Accession 0113899). NOAA National Centers for Environmental Information [data set], https://doi.org/10.3334/cdiac/otg.ndp091, 2013.

Tans, P. and Keeling, R.: Trends in atmospheric carbon dioxide, NOAA Global Monitoring Laboratory, Boulder, Colorado, USA and Scripps Institution of Oceanography, LaJolla, California, USA, https://gml.noaa.gov/ccgg/trends/ (last access: 7 January 2025), 2026.

Terhaar, J.: Composite model-based estimate of the ocean carbon sink from 1959 to 2022, Biogeosciences, 22, 1631–1649, https://doi.org/10.5194/bg-22-1631-2025, 2025.

Terhaar, J., Orr, J. C., Ethé, C., Regnier, P., and Bopp, L.: Simulated Arctic Ocean response to doubling of riverine carbon and nutrient delivery, Global Biogeochem. Cy., 33, 1048–1070, https://doi.org/10.1029/2019GB006200, 2019.

Terhaar, J., Tanhua, T., Stöven, T., Orr, J. C., and Bopp, L.: Evaluation of data-based estimates of anthropogenic carbon in the Arctic Ocean, J. Geophys. Res.-Oceans, 125, https://doi.org/10.1029/2020jc016124, 2020.

Terhaar, J., Torres, O., Bourgeois, T., and Kwiatkowski, L.: Arctic Ocean acidification over the 21st century co-driven by anthropogenic carbon increases and freshening in the CMIP6 model ensemble, Biogeosciences, 18, 2221–2240, https://doi.org/10.5194/bg-18-2221-2021, 2021a.

Terhaar, J., Frölicher, T. L., and Joos, F.: Southern Ocean anthropogenic carbon sink constrained by sea surface salinity, Sci. Adv., 7, https://doi.org/10.1126/sciadv.abd5964, 2021b.

Terhaar, J., Frölicher, T. L., Joos, F.: Simulated and constrained Southern Ocean carbon sink from 1850 to 2100 based on CMIP5 and CMIP6 models, SEANOE [data set], https://doi.org/10.17882/103938, 2021c.

Terhaar, J., Frölicher, T. L., and Joos, F.: Observation-constrained estimates of the Global Ocean Carbon Sink from earth system models, Biogeosciences, 19, 4431–4457, https://doi.org/10.5194/bg-19-4431-2022, 2022a.

Terhaar, J., Frölicher, T. L., and Joos, F.: Simulated and constrained ocean carbon sink from 1850 to 2100 based on CMIP6 models, SEANOE [data set], https://doi.org/10.17882/103934, 2022b.

Terhaar, J., Frölicher, T. L., and Joos, F.: Ocean acidification in emission-driven temperature stabilization scenarios: The role of TCRE and non-CO_2 greenhouse gases, Environ. Res. Lett., 18, 02403, https://doi.org/10.1088/1748-9326/acaf91, 2023.

Terhaar, J., Tanhua, T., Stöven, T., Orr, J. C., and Bopp, L.: Observation-based anthropogenic carbon estimates in the Arctic Ocean, SEANOE [data set], https://doi.org/10.17882/103920, 2024a.

Terhaar, J., Goris, N., Müller, J. D., DeVries, T., Gruber, N., Hauck, J., Perez, F. F., and Séférian, R.: Assessment of global ocean biogeochemistry models for ocean carbon sink estimates in Reccap2

and recommendations for future studies, J. Adv. Model. Earth Syst., 16, https://doi.org/10.1029/2023ms003840, 2024b.

van Hooidonk, R.: Modeled ocean acidification data in the Gulf of Mexico and wider Caribbean using satellites and climate model data for the Ocean Acidification Products for the Gulf of Mexico and East Coast project from 2014-01-01 to 2020-12-31 (NCEI Accession 0245950), NOAA National Centers for Environmental Information [data set], https://doi.org/10.25921/tt1c-dx53, 2022.

Velo, A., Pérez, F. F., Tanhua, T., Gilcoto, M., Ríos, A. F., and Key, R. M.: Total alkalinity estimation using MLR and neural network techniques, J. Mar. Syst., 111–112, 11–18, https://doi.org/10.1016/j.jmarsys.2012.09.002, 2013.

Wanninkhof, R., Pierrot, D., Sullivan, K., Barbero, L., and Triñanes, J.: Gridded surface water fugacity of CO_2 observations, and calculated pH, aragonite saturation state and air–sea CO_2 fluxes in the northern Caribbean Sea from 2002 through 2019 (NCEI Accession 0207749), NOAA National Centers for Environmental Information [data set], https://doi.org/10.25921/2swk-9w56, 2019.

Wanninkhof, R., Pierrot, D., Sullivan, K., Barbero, L., and Triñanes, J.: A 17-year dataset of surface water fugacity of CO_2 along with calculated pH, aragonite saturation state and air–sea CO_2 fluxes in the northern Caribbean Sea, Earth Syst. Sci. Data, 12, 1489–1509, https://doi.org/10.5194/essd-12-1489-2020, 2020.

Wanninkhof, R., Triñanes, J., Pierrot, D., Munro, D. R., Sweeney, C., and Fay, A. R.: AOML_ET: Partial pressure of CO_2 (pCO_2) and air–sea CO_2 fluxes for the global ocean, along with the predictor variables from 1998-01-01 to 2023-12-30, using an Extra Trees (extremely randomized trees) machine learning (NCEI Accession 0298989), NOAA National Centers for Environmental Information [data set], https://doi.org/10.25921/0s8y-q287, 2024.

Wanninkhof, R., Triñanes, J., Pierrot, D., Munro, D. R., Sweeney, C., and Fay, A. R.: Trends in sea-air CO_2 fluxes and sensitivities to atmospheric forcing using an extremely randomized trees machine learning approach, Global Biogeochem. Cy., 39, https://doi.org/10.1029/2024GB008315, 2025.

Watson, A. J., Schuster, U., Shutler, J. D., Holding, T., Ashton, I. G., Landschützer, P., Woolf, D., and Goddijn-Murphy, L.: Revised estimates of ocean-atmosphere CO_2 flux are consistent with ocean carbon inventory, Nat. Commun., 11, 1–6, https://doi.org/10.1038/s41467-020-18203-3, 2020.

Watson, A. J., Schuster, U., Shutler, J. D., Holding, T., Ashton, I. G., Landschützer, P., Woolf, D., and Goddijn-Murphy, L.: Revised estimates of ocean-atmosphere CO_2 flux accounting for near-surface temperature and salinity deviations from 1985-01-01 to 2019-12-31 (NCEI Accession 0301544), NOAA National Centers for Environmental Information [data set], https://doi.org/10.25921/2dp5-xm29, 2025.

White, A. E., Karl, D. M., and Fujieki, L. A.: Niskin bottle water samples and associated CTD measurements from the Hawaii Ocean Time-Series cruises from 1988–2023, (Version 3) Version Date 2025-04-22, Biological and Chemical Oceanography Data Management Office (BCO-DMO) [data set], https://doi.org/10.26008/1912/bco-dmo.3773.3, 2025.

Wilkinson, M. D., Dumontier, M., Aalbersberg, I. J., Appleton, G., Axton, M., Baak, A., Blomberg, N., Boiten, J.-W., da Silva Santos, L. B., Bourne, P. E., Bouwman, J., Brookes, A. J., Clark, T., Crosas, M., Dillo, I., Dumon, O., Edmunds, S., Evelo, C. T., Finkers, R., Gonzalez-Beltran, A., Gray, A. J. G., Groth, P., Goble, C., Grethe, J. S., Heringa, J., Hoen, P., Hooft, R., Kuhn, T., Kok, R., Kok, J., Scott J. Lusher, S. J., Martone, M. E., Mons, A., Packer, A. L., Persson, B., Rocca-Serra, P., Roos, M., van Schaik, R., Sansone, S.-A., Schultes, E., Sengstag, T., Slater, T., Strawn, G., Swertz, M. A., Thompson, M., van der Lei, J., van Mulligen, E., Velterop, J., Waagmeester, A., Wittenburg, P., Wolstencroft, K., Zhao, J., and Mons, B.: The Fair Guiding Principles for Scientific Data Management and Stewardship, Sci. Data, 3, https://doi.org/10.1038/sdata.2016.18, 2016.

Winn, C. D., MacKenzie, F. T., Carrillo, C. J., Sabine, C. L., and Karl, D. M.: Air–sea carbon dioxide exchange in the North Pacific Subtropical Gyre: Implications for the global carbon budget, Global Biogeochem. Cy., 8, 157–163, https://doi.org/10.1029/94GB00387, 1994.

Winn, C. D., Li, Y.-H., Mackenzie, F. T., and Karl, D. M.: Rising surface ocean dissolved inorganic carbon at the Hawaii Ocean Time-series site, Mar. Chem., 60, 33–47, https://doi.org/10.1016/S0304-4203(97)00085-6, 1998.

Wu, Z., Lu, W., Roobaert, A., Song, L., Yan, X.-H., and Cai, W.-J.: A Reconstructed Coastal Acidification Database (ReCAD) pCO_2 data product for the North American Atlantic Coastal Ocean Margins, Zenodo [data set], https://doi.org/10.5281/zenodo.11500974, 2024.

Wu, Z., Lu, W., Roobaert, A., Song, L., Yan, X.-H., and Cai, W.-J.: A machine-learning reconstruction of sea surface pCO_2 in the North American Atlantic Coastal Ocean Margin from 1993 to 2021, Earth Syst. Sci. Data, 17, 43–63, https://doi.org/10.5194/essd-17-43-2025, 2025.

Zeng, J.: NIES-ML3 ensemble product of surface ocean CO_2 concentrations and air–sea CO_2 fluxes reconstructed by using three machine learning models with new CO_2 trends, NIES – National Institute for Environmental Studies, Japan, https://doi.org/10.17595/20220311.001, 2022.

Zeng, J., Iida, Y., Matsunaga, T., and Shirai, T.: Surface ocean CO_2 concentration and air–sea flux estimate by machine learning with modelled variable trends, Front. Mar. Sci., 9, 989233, https://doi.org/10.3389/fmars.2022.989233, 2022.

Zhang, H., Menemenlis, D., and Fenty, I. G.: ECCO LLC270 ocean-ice state estimate, Tech. Rep., Jet Propulsion Laboratory, California Institute of Technology, http://hdl.handle.net/1721.1/119821 (last access: 7 January 2026), 2018.

Zhong, G.: IOCAS global ocean gridded pCO_2 version 2025, Marine Science Data Center Chinese Academy of Sciences [data set], https://doi.org/10.12157/IOCAS.20250814.001 2025.

Zhong, G., Li, X., Song, J., Qu, B., Wang, F., Wang, Y., Zhang, B., Sun, X., Zhang, W., Wang, Z., Ma, J., Yuan, H., and Duan, L.: Reconstruction of global surface ocean pCO_2 using region-specific predictors based on a stepwise FFNN regression algorithm, Biogeosciences, 19, 845–859, https://doi.org/10.5194/bg-19-845-2022, 2022.

Zhong, G., Li, X., and Song, J.: Global ocean gridded seawater pH during 1992–2020 at 0–2000 m depth based on Stepwise FFNN algorithm 2023 version, Marine Science Data Center of the Chinese Academy of Sciences [data set], https://doi.org/10.12157/IOCAS.20230720.001, 2023.

Zhong, G., Li, X., Song, J., Qu, B., Wang, F., Wang, Y., Zhang, B., Cheng, L., Ma, J., Yuan, H., Duan, L., Li, N., Wang, Q., Xing, J., and Dai, J.: A global monthly 3D field of seawater pH over

3 decades: a machine learning approach, Earth Syst. Sci. Data, 17, 719–740, https://doi.org/10.5194/essd-17-719-2025, 2025.

Zweng, M. M, Reagan, J. R., Antonov, J. I., Locarnini, R. A., Mishonov, A. V., Boyer, T. P., Garcia, H. E., Baranova, O. K., Johnson, D. R., Seidov, D., and Biddle, M. M.: World Ocean Atlas 2013, in: Volume 2: Salinity, NOAA Atlas NESDIS 74, edited by: Levitus, S. and Mishonov, A., NOAA, 39 pp., https://doi.org/10.7289/V5251G4D, 2013.

Zweng, M. M, Reagan, J. R., Seidov, D., Boyer, T. P., Locarnini, R. A., Garcia, H. E., Mishonov, A. V., Baranova, O. K., Weathers, K. W., Paver, C. R., and Smolyar, I. V.: World Ocean Atlas 2018, in: Volume 2: Salinity, NOAA Atlas NESDIS 82, edited by: Mishonov, A., NOAA, https://doi.org/10.25923/9pgv-1224, 2019.